This is to certify that the

thesis entitled

Characterization of Cationic Photopolymerizations of Divinyl Ether Systems Involving a Diaryliodonium Salt Initiator and Photosensitized by Anthracene

presented by

Jeffry L. Jacobs

has been accepted towards fulfillment
of the requirements for

M.S. degree in ChE

Alec Scranton
Major professor

Date 5/16/95

CHARACTERIZATION OF CATIONIC PHOTOPOLYMERIZATIONS OF DIVINYL ETHER SYSTEMS INVOLVING A DIARYLIODONIUM SALT INITIATOR AND PHOTOSENSITIZED BY ANTHRACENE

By

Jeffry L. Jacobs

A THESIS

Submitted to
Michigan State University
in partial fulfillment of the requirements
for the degree of

MASTER OF SCIENCE

Department of Chemical Engineering

May 1995

ABSTRACT

CHARACTERIZATION OF CATIONIC PHOTOPOLYMERIZATIONS OF DIVINYL ETHER SYSTEMS INVOLVING A DIARYLIODONIUM SALT INITIATOR AND PHOTOSENSITIZED BY ANTHRACENE

By

Jeffry L. Jacobs

Cationic photopolymerizations of divinyl ethers have tremendous potential for the development of solvent-free films and coatings. These polymerizations rapidly form highly crosslinked polymer films which exhibit excellent adhesion, chemical and abrasion resistance, and are not inhibited by oxygen. Cationic photopolymerizations have not been well characterized. Photo-differential scanning calorimetry was used to obtain previously unavailable polymerization kinetics. Fluorescence monitoring and isothermal photo-differential scanning calorimetry were used to investigate the effect of water on the polymerization kinetics. It was found that increasing the water content in the monomer slows the reaction due to a heat effect. An *in situ* fluorescence method for monitoring reaction temperature based upon lanthanide chelates is also reported. Finally, transmission electron microscopy and an osmium tetroxide stain were used to identify areas of heterogeneity and degrees of crosslinking in the divinyl ether polymer. These micrographs indicated that depending on cure rate there is a significant degree of heterogeneity present due to incomplete crosslinking of the pendant double bonds.

ACKNOWLEDGMENTS

This work was supported by National Science Foundation Grant No. CTS 9216939. The fluorescence monitoring measurements were carried out in the Michigan State University *LASER* Laboratory, Department of Chemistry and in Dr. Scranton's laboratory in the Chemical Engineering department. The transmission electron microscopy work was performed in the Michigan State University Center for Electron Optics, Department of Natural Sciences. The photo-differential scanning calorimetry experiments were carried out in Dr. Christopher N. Bowman's laboratory in the Department of Chemical Engineering at the University of Colorado, Boulder.

In addition to the ever essential monetary support, I would like to especially thank my thesis advisor, Dr. Alec B. Scranton for his guidance, and inspiration. I also want to thank Dr. Tom Carter for his expert help in a number of areas.

Furthermore I want to thank Dr. Chris Bowman for the generous use of his laboratory at the University of Colorado. Both Dr. Bowman's and Kristi Anseth's help and encouragement with the photo-DSC work was invaluable.

In the area of transmission electron microscopy and also for moral support, I would be remise if I did not thank Dr. Karen Klomparens. I would also like to thank her for taking the time to be on my thesis committee.

For their tireless efforts in the lab helping to develop the temperature-sensitive probes and providing comic relief, I thank both Czarena Crofcheck and Brenda Becker.

A special thanks to Roger Chen for all his excellent help in tracking down literature articles from all over the world.

I can't thank Eric Nelson enough for the endless hours of discussions we have had both in and out of the lab, especially the ones that had nothing to do with cationic photopolymerizations. His help, collaboration, and suggestions were more often than not beneficial.

Finally I'd like to thank Dr. Martin Hawley for his interest in this work and for taking the time to be on my thesis committee.

TABLE OF CONTENTS

LIST OF TABLES

LIST OF FIGURES

page

Chapter 5

CHAPTER 1. INTRODUCTION AND OBJECTIVES

1.1. Issues for the Development of Pollution-Free Films, Coatings, and Inks

Throughout the past several decades the U.S. government has spent more and more time and money in the form of research grants, laws and regulations on developing technology and enforcing its use to reduce environmental pollution. The Environmental Protection Agency (EPA) was formed specifically to aid in finding ways to reduce the levels of pollution produced each year in the United States. One of the areas specifically targeted by the EPA for regulation and reduction of pollution is the air. Increasing levels of smog and air pollution in large cities and industrial areas has made the protection of a certain level of air quality an important issue. The emission of volatile organic components (VOCs) from the curing of inks, paints, films, and coatings is a major cause of the decreasing air quality. Traditionally, volatile organic solvents are added to such things as ink and coating formulations in order to give them the desired viscosity and cure rate properties required for the quick and easy application necessary in many industrial processes. These solvents result in a formulation that is fluid enough to be easily applied and yet still volatile enough to allow rapid curing by evaporation of the solvent. However, numerous studies have shown that once these solvents evaporate and enter the atmosphere they result in the formation of smog and air pollution. For this reason the EPA has been continually tightening its restrictions on the annual allowable levels of VOCs that can be emitted into the atmosphere. Consequently, there is a significant need for the development of inks and coatings that do not result in the emission of VOCs.

In order for a pollution-free formulation for inks or coatings to be acceptable it must be more than just environmentally friendly. The cured ink or coating must meet a number of additional requirements such as good abrasion and chemical resistance, flexibility, and superior adhesion to the substrate. Many industrial application processes

such as a continuous web system also require that the formulation is stable and to be realistic should have a shelf life of six months or more.[1] Safety considerations also require a substance that is non-toxic and reasonably safe to handle. Economically, the cost of the formulation should not be too far out of line with existing costs. However, economic incentives such as fines and penalties could be used by the EPA to make up for a certain amount of price discrepancies.

Currently many formulations consist of pigments and multifunctional oligomers dispersed in a volatile solvent. This system forms a highly crosslinked polymer network upon curing which easily provides the required abrasion and chemical resistance. This system could be greatly improved if highly reactive low viscosity monomers were used instead in order to alleviate the need for organic solvents. An ideal system would consist of a low vapor pressure monomer in a 100% reactive system. This would emit essentially no organic vapors before, during, or after curing.

There are a number of different possibilities for initiating the curing of this type of system which include heat, electromagnetic radiation, electron beam irradiation, and light waves. Heat-initiated thermal systems, however, generally have the disadvantage of requiring high temperatures to attain reasonably fast cure rates. Such temperatures result in high energy costs as well as often producing significant distortions in the substrate dimensions.[1] High-energy irradiation such as γ-radiation and electron beam radiation, while they may have rapid cure rates in a variety of systems,[2,3,4,5] are likely to be very limited in their usefulness because they often result in degradation of the substrate. The use of light to initiate photopolymerizations, however, promises to have many advantages for ink and coating formulations such as very fast reaction rates at room temperature, low energy requirements, and applicability to a wide range of monomers. One area of concern is whether or not degradation of the substrate can be avoided, possibly by proper selection of the wavelength of the initiating light source.

1.2. UV-Initiated Photopolymerizations

Recently, the use of ultraviolet (UV) light has shown a great deal of promise as a rapid, pollution-free initiating source for the photopolymerization of polymer films (for reviews see references 6,7,8,9). Ultraviolet light has the advantage of being relatively low energy compared to thermally cured systems, and easy to use to cure films. In addition, a number of convenient compounds will initiate chain polymerizations upon absorption of UV light.[6,7,8,9,10,11,12] These photoinitiators, which are available for both free-radical and cationic polymerizations, are generally effective at a number of different wavelengths.[6,7,8,9,10,11,12] It is important to be able to use different wavelengths in the curing of inks and coatings in order to avoid regions where commonly used pigments are strong absorbers.

There is nothing new about free-radical photopolymerizations, they were first reported in the literature almost fifty years ago.[13] The classes of monomers currently receiving attention for UV-initiated free-radical photopolymerizations are multifunctional acrylates and methacrylates (for reviews see references 6,7,8,13). The interest in these monomers is largely due to their rapid polymerization and the ease with which the ester group can be modified to provide a variety of different properties.[6] The major disadvantages of the acrylate monomers are their relative volatility and unpleasant odor.[6] Moreover, there has been increasing concern over the potential health hazards associated with acrylates.[7,8,14] An additional concern involving free-radical polymerizations of multifunctional acrylates and methacrylates is their unusual kinetic behavior such as the immediate onset of autoacceleration, the formation of heterogeneous polymers,[6,19,20,21,22,-23,24] and the attainment of a maximum conversion significantly less than unity.[6,25,26,27,28] A final disadvantage to free-radical photopolymerizations is that they are inhibited by oxygen which requires that they be carried out under an inert atmosphere.[6,7,13]

In contrast, UV-initiated cationic photopolymerizations exhibit a number of advantages over these free-radical systems. One advantage of significant practical importance for industrial processes is that cationic photopolymerizations are not inhibited by oxygen.[7,13,14,30] This removes the need to provide an inert atmosphere in order to achieve rapid cure rates. Furthermore, cationic polymerizations continue to react long after the light source is removed resulting in the consumption of most of the monomer.[13,33] Free-radical polymerizations, on the other hand, experience a rapid decrease in the rate of reaction once the light source is removed due to radical-radical terminations. Finally, cationic photopolymerizations open the door to the use of several important classes of monomers including vinyl ethers and epoxides,[14,30,31,32,33,34,35] which cannot be cured by a free-radical process.[36] Much of the importance in these monomers lies in their desirable properties both as a monomer and as a cured polymer. The monomers exhibit desirable properties such as low volatility, low viscosity, and negligible toxicity.[7] The cured polymer films formed from these monomers exhibit such properties as excellent clarity, adhesion, abrasion resistance, and chemical resistance.[13,14,34,35]

1.3. Recent Developments in the Area of Cationic Photopolymerizations

Despite the various advantages of UV-initiated photopolymerizations , the technique has received considerably less attention than the analogous free-radical reactions. This may very well be due to the lack of suitable UV-sensitive cationic photoinitiators until only recently.[31,33] In fact, applicable photoinitiators for cationic polymerizations were not developed until the late 1970s, over thirty years after free-radical initiators had been first reported. Early photoinitiators for cationic polymerizations, first introduced in 1965, were aryldiazonium salts of complex metal halide anions.[31] Upon photolysis, these species produce an aryl halide, molecular nitrogen, and a strong Lewis acid capable of

initiating cationic polymerization.[13,31] While the aryldiazonium salts were highly photoactive, they were also thermally unstable, which resulted in unacceptably short shelf lives for fully formulated systems.

In 1976 and 1979, Crivello and Lam reported two classes of thermally stable photoinitiators for cationic polymerizations: diaryliodonium and triarylsulfonium salts, respectively (for a review of the development of these initiators, see reference 10). Upon photolysis, these compounds undergo irreversible photofragmentation in which the carbon-iodine or carbon-sulfur bond is cleaved to produce an aryliodonium or an arylsulfonium cation-radical capable of initiating cationic polymerization.[12] While the diaryliodonium and triarylsulfonium salts actively initiate cationic polymerization in the presence of UV light, they are remarkably latent in the absence of light. In fact, fully formulated solutions of some salts in epoxide monomers have shelf lives of several years.[12]

The wavelength at which the diaryliodonium and triarylsulfonium salts exhibit their maximum UV absorbance depends somewhat upon the substituents attached to the ring, but typically falls between 225 and 275 nm [9,33] (some sulfonium salts absorb near 300 nm [9]). Although the initiators absorb strongly at wavelengths near 250 nm, their absorption diminishes at longer wavelengths.[9,32] This fact could limit the efficiency of the initiators for photopolymerizations driven by mercury lamps which provide most of their emission at wavelengths above 300 nm.[9,33] However, the spectral region over which the initiators are effective may be expanded by the addition of one of a variety of different photosensitizers, including hydrocarbons, ketones and heterocyclic compounds.[9] These compounds actively sensitize the iodonium and sulfonium initiators by an electron transfer process, rendering them effective in the long UV and visible wavelengths of light.[9,32,33]

1.4. Need for Characterization Research on Cationic Photopolymers

Due to the substantial potential that UV-initiated cationic photopolymerizations present for the development of improved, pollution-free inks and coatings there is a strong demand for more detailed information on these systems. It is clear that these reactions have the potential to rapidly form highly crosslinked polymer films that exhibit excellent adhesion, abrasion resistance, and chemical resistance without the emission of VOC's and require only a fraction of the energy of thermal systems. In addition, cationic reactions are not inhibited by oxygen, which is a drawback to free-radical systems, and may be used to polymerize epoxides and vinyl ethers. The ability to use these types of monomers is important because they exhibit a number of desirable properties such as low volatility, good rheological characteristics, and negligible toxicity.[7,33] Furthermore, fully formulated systems containing monomer, pigment, initiator, and photosensitizer exhibit shelf lives of more than a year,[12] and initiators or photosensitizers can be chosen to be effective for wavelengths at which the pigments have low extinction coefficients. Finally, the UV irradiation is less likely to significantly degrade the substrate than electron beam curing.[13,33]

Regardless of the fact that UV-initiated cationic photopolymerizations appear to have a lot to offer, they have received only limited attention. This is probably primarily due to the lack of suitable initiators until recently. Most of the work done on cationic photopolymerizations that has been reported in the literature deals mainly with the initiation step of the reaction (for reviews see references 8,9,10,11,12,30,31,32,33,34). Since the development of thermally stable UV-sensitive cationic photoinitiators there has been an increased interest in the cationic photopolymerization of epoxides and vinyl ethers,[31,32,33,34,35,36] but the field is still not nearly as well characterized as that of free-radical photopolymerizations.

1.5. Research Objectives

There are a number of major objectives for the research presented in this thesis. Due to the largely uncharacterized nature of the cationic photopolymerizations of divinyl ethers in terms of both reaction kinetics and the properties of the resulting polymer this work was aimed at several aspects of these two areas. More specifically, the first objective was to look at the polymerization kinetics this cationic photopolymerization using photo-differential scanning calorimetry.

The second major objective was to identify and characterize the effect of humidity (water) on the reaction rate. In order to maintain uniform high quality films and coatings it is essential to establish how changes in humidity or water content in the monomer will effect the reaction. This area of research involved identifying what, if any, effects increasing concentrations of water in the reaction system have on the overall rate of reaction. In addition, it was desirable to establish what are the underlying reasons for any observed effects.

A third objective was to look at the morphology of the divinyl ether polymer in order to identify the nature (homogeneous or heterogeneous) of the cured film with respect to degree of cure. This objective was aimed at establishing the effect of different cure conditions on the resulting polymer morphology.

A fourth objective was to characterize the chemical resistance of various common polymers in two vinyl ether monomers. This involved identifying both the solubility and the swellability of these polymer in these monomers.

A fifth objective was to both gain familiarity with a variety of existing instrumental techniques as well as help develop new techniques necessary to meeting the objectives mentioned above. These techniques encountered throughout this research include: photo-differential scanning calorimetry, transmission electron microscopy,

Fourier transform infrared spectroscopy, fluorescence spectroscopy, UV-vis spectroscopy, and gel permeation chromatography.

1.6. References

1. Graminski, E. L., in "Fundamental Chemical and Engineering Issues in Paper Currency Production," *National Science Foundation*, Washington D.C., 1, 1991.
2. Sundell, P.E.; Jonsson, S.; Hult, A., in "Radiation Curing of Polymeric Materials," edited by C.E. Hoyle and J.F. Kinstle, *ACS Symposium Series*, Vol. 417, American Chemical Society, Washington D.C., 459, 1989.
3. Kim, H.C.; El-Naggar, A.M.; Wilkes, G.L.; Yoo, Y.; McGrath, J.E., in "Radiation Curing of Polymeric Materials," edited by C.E. Hoyle and J.F. Kinstle, *ACS Symposium Series*, Vol. 417, American Chemical Society, Washington D.C., 474, 1989.
4. Stannett, V.; Deffieux, A., in "Cationic Polymerization and Related Processes," edited by E.J. Goethals, International Union of Pure and Applied Chemistry, Oxford, UK, 307, 1984.
5. Pacansky, J.; Waltman, R.J., in "Radiation Curing of Polymeric Materials," edited by C.E. Hoyle and J.F. Kinstle, *ACS Symposium Series*, Vol. 417, American Chemical Society, Washington D.C., 498, 1989.
6. Kloosterboer, J.G., "Network Formation by Chain Crosslinking Photopolymerization and Its Applications in Electronics", *Adv. Polym. Sci.*, **84**, 1 (1988).
7. Roffey, C.G., *Photopolymerization of Surface Coatings*, Wiley, New York, 1981.
8. Pappas,S.P., *UV Curing, Science and Technology*, Vol. 2, Technology Marketing Corporation, Norwalk, CT, 1985.
9. Crivello, J.V. ,"Cationic Polymerization-Iodonium and Sulfonium Salt Photoinitiators," *Adv. Polym. Sci.*, **62,** 1 (1984).
10. Crivello, J.V.; Lee, J.L., "Alkoxy-Substituted Diaryliodonium Salt Cationic Photoinitiators," *J. Polym. Sci., Polym. Chem.*, , **27**, 3951 (1989).
11. Ledwith, A.; Al-Kass, S.; Hulme-Lowe, A., in "Cationic Polymerization and Related Processes," edited by E.J. Goethals, International Union of Pure and Applied Chemistry, Oxford, UK, 275, 1984.
12. Crivello, J.V., in "Cationic Polymerization and Related Processes," edited by E.J. Goethals, International Union of Pure and Applied Chemistry, Oxford, UK, 289, 1984.
13. Reiser, A., "Photoreactive Polymers," Wiley, New York, NY, 1989.
14. Lapin, S.P., in "Radiation Curing of Polymeric Materials," edited by C.E. Hoyle and J.F. Kinstle, *ACS Symposium Series*, Vol. 417, American Chemical Society, Washington D.C., 363, 1989.

15. Allen, P.E.M.; Simon, G.P.; Williams, D.R.G.; Williams, E.H., *Macromolecules*, **22**, 809 (1989).

16. Miyazaki, K.; Horibe, T., *J. Biomedical Mater. Res.*, **22**, 1011 (1988).

17. Hubca, G.H.; Oprescu, C.R.; Dragan, G.H.; Dimonie, M., *Rev. Roum. Chem.*, **27**, 435 (1982).

18. Kloosterboer, J.G.; Litjen, C.F.C.M., in "Cross-linked Polymer Chemistry," edited by R. Dickie, S. Labana and R. Bauer, *ACS Symposium Series*, Vol. 367, American Chemical Society, Washington D.C., 409 (1988).

19. Boots, H.M.J.; Kloosterboer, J.G.; van de Hei, G., *Brit. Polym. J.*, **17**, 219 (1985).

20. Galina, H.; Kolarz, B.; Wieczorek, P.; Wojczynska, M., *Brit. Polym. J.*, **17**, 215 (1985).

21. Funke, W., *Brit. Polym. J.*, **21**, 107 (1989).

22. Bastide, J.; Leibler, L., *Macromolecules*, **21**, 2649 (1988).

23. Matsumoto, A.; Matsuo, H.; Ando, H.; Oiwa, M., *Eur. Polym. J.*, **25**, 237 (1989).

24. Baselga, J.; Llorente, M.; Hernandez-Ruentes, I.; Pierola, I., *Eur. Polym. J.*, **25**, 471 (1989).

25. Turner, D.; Haque, Z.; Kalachandra, S.; Wilson, T., *Polym. Mater. Sci. Eng. Proceed,* **56**, 769 (1987).

26. Simon, G.P.; Allen, P.E.M.; Bennett, D.J.; Williams, D.R.G.; Williams, E.H., *Macromolecules*, **22**, 3555 (1989).

27. Kloosterboer, J.G.; Lijten, G.F.C.M.; Zegers, C.P.G., *Polym. Mater. Sci. Eng. Proceed.*, **60**, 122 (1989).

28. Allen, P.E.M.; Bennett, D.J.; Hagias, S.; Hounslow, A.; Ross, G.; Simon, G.P.; Williams, D.G.R.; Williams, E.H., *Eur. Polym. J.*, **25**, 785 (1989).

29. Kloosterboer, J.G.; Lijten, G.F.C.M.; Boots, H.M.J., *Makromol. Chem., Macromol. Symp.*,**24**, 223 (1989).

30. Crivello, J.V.; Lam, J.H.W., in "Epoxy Resin Chemistry," edited by R.S. Bauer, *ACS Symposium Series*, Vol. 114, American Chemical Society, Washington D.C., 1, 1979.

31. Pappas, S.P., *Prog. Org. Coat.*, **13**, 35 (1985).

32. Crivello, J.V., in "Organic Coatings, Science and Technology," Vol. 5 edited by G.D. Parfitt and A.V. Patsis, Marcel Dekker, Inc., New York, NY, 35, 1983.

33. Watt,W.R., in "Epoxy Resin Chemistry," edited by R.S. Bauer, *ACS Symposium Series*, Vol. 114, American Chemical Society, Washington D.C., 17, 1979.

34. Loshe, F.; Zweifel, H., *Adv. Polym. Sci.*, **78**, 61 (1986).

35. Crivello, J.V.; Conlon, D.A., "Aromatic Bisvinyl Ethers: A New Class of Highly Reactive Thermosetting Monomers", *J. Polym. Sci., Polym. Chem.*, **21,** 1785 (1983).

36. Odian, G., "Principles of Polymerization," 2nd Edition, Wiley, New York, NY, 1981.

CHAPTER 2. GENERAL BACKGROUND

2.1. Step Polymerizations

There are two general types of polymerization mechanisms by which monomer reacts to form polymer, step and chain.[1] The step polymerization mechanism is based on a stepwise reaction between the functional groups of the monomer and the growing polymer. Monomer reacts with another monomer to form a dimer, which reacts with another monomer to form a trimer and so on. The size of the polymer molecules grows at a relatively slow rate. Therefore high molecular weight polymer is obtained only near the end of the reaction.[1] As a result both the size and amount of polymer in a step polymerization reaction are dependent on the degree of conversion.[1]

Step polymerizations can be further broken down into two different categories depending the types of monomer used. The first group involves reaction between two different multifunctional monomers in which each monomer contains only one type of functionality. The second group consists of those monomers that contain at least two different types of functionalities.[1]

The major disadvantage of step polymerizations is that in order to synthesize polymers of high molecular weight, very high conversions are required. This means that the desired reaction needs to have a very favorable equilibrium, and no side reactions.[1] This restriction greatly reduces the number of step reactions that will lead to useful polymers. However, step polymerizations do have the advantage of being very versatile in allowing customization of a polymer's chemical structure in order to obtain specific physical properties. Step polymerizations are commonly used to produce a number of important different polymers such as polyesters [example: poly(ethylene terephthalate), PET], polycarbonates, polyamides, (example: nylon), and crosslinked polymers such as epoxy resins and polyurethanes.[1]

2.2. Chain Polymerizations

The second general type of classification of polymers based on the reaction mechanism is chain polymerization. Chain polymerizations proceed in a much different manner from step polymerizations. In a chain polymerization reaction large polymer molecules are formed almost immediately after initiation of the reaction. An initiator is required to start the chain reaction. The initiator is used to create a reactive center, $R^{\bullet}$, R^{+}, or R^{-}, depending on whether the reactive center is a free radical, a cation, or an anion. Initiation is followed by propagation of the reactive center to large numbers of monomer molecules in a rapid chain reaction. In contrast to step polymerizations where large polymer molecules aren't formed until very near the end of the reaction, chain polymerizations result in full-sized polymer molecules near the start of the action at low conversions.[1] This is a result of monomer reacting only with the propagating reactive center on the growing polymer chain and not with other monomer molecules as in step polymerizations.

The active center in a chain reaction polymerization continues to react until it is destroyed by a termination reaction or becomes trapped in the polymer matrix. Growth of the polymer chain can also be terminated by the transfer of a species such as a hydrogen atom to it from some compound present in the reaction system. The active center is then transferred to this other compound which can be initiator, monomer, solvent, or foreign materials such as water and alcohols (referred to as a chain transfer agents) present in the system.[1] In this case, the active center is not destroyed and can continue to react by starting a new polymer chain, however, the old polymer chain's growth is terminated. The overall effect of chain transfer reactions is a decrease in the molecular weight of the polymer since chain growth is prematurely ended.[1] Therefore, chain transfer agents are

often intentionally added to reaction systems in order to obtain a specific molecular weight.[1]

Finally, there are certain substances that can be used to temporarily suppress the polymerization reaction by reacting with the active centers to create either a nonreactive species or one with very low reactivity.[1] There are two classes of suppressers, inhibitors and retarders. The difference between these two is based on their effectiveness in suppressing the reaction. Inhibitors completely stop the reaction until consumed, while retarders prevent only a portion of the active centers from reacting.[1] Inhibitors are often used in radical systems to prevent premature polymerization during storage. To initiate a polymerization, the inhibitor is generally removed or excess initiator is added to overcome the inhibitor.[1]

Chain polymerization reactions are commonly used in the production of commercially important polymers such as polyethylene, polystyrene, poly (vinyl chloride) (PVC), and poly (methyl methacrylate) (PMMA).[1]

2.2a. Radical Chain Polymerization

Free radical chain polymerizations are currently the most important type of polymerization method.[2] The first step in a free radical polymerization is the initiation step in which the free radical species is formed. There are a number of different types if initiators available depending on the initiating system. In general, the initiator is decomposed by exposure to heat, radiation, or redox reaction. When the initiator decomposes it forms free radicals, $R^{\bullet}$, which react rapidly with the monomer. The free radical is transferred to the monomer during this reaction allowing this new active center to react with additional monomer. Each time the free radical reacts with a monomer molecule the radical is transferred to the chain end resulting in propagation of the active center (free radical). The free radical can be terminated by combination, where two free

radicals react with each other to result in a dead site, or by disproportionation which involves the transfer of a hydrogen from one chain to another.[2]

Photochemical initiation of free radical polymerizations has received considerable interest for use in environmental applications that require solvent-free systems.[1] The disadvantage of this system is that reaction only occurs in the areas that are exposed to the light. Therefore, thickness of the resulting material is severely limited.[1] Photopolymerizations have also found significant use in the photoimaging industry as photoresists for the production of printed circuitry.[1]

The photoinitiation occurs as a result of the absorption of ultraviolet or visible light which ultimately causes the decomposition of the initiator species into free radicals.[3,4] Radicals can be produced by either of two pathways. The pathway involves direct excitation of the initiator by energy absorption from the light resulting in decomposition into radicals. The second path involves a photosensitizer which absorbs the light and becomes excited. This excited state species then interacts with the initiator causing it to decompose into radicals.[1]

2.2b. Cationic Chain Polymerization

Although free-radical systems are currently more widely used, cationic chain polymerization systems offer a number of advantages as mentioned in the previous section. The wide-spread use of free-radical systems is largely due to the fact that ionic polymerizations are much more selective. This selectivity is a result of the need to have substituents present that can stabilize the ionic propagating species. For a cationic polymerization, monomers are limited to those containing electron-releasing groups (vinyl, phenyl, alkoxy, and 1,1-dialkyl).[1] An understanding of how the cationic chain mechanism differs from the free-radical mechanism is essential to the investigation of the bisvinyl systems since these systems are extremely favorable to cationic polymerization.

However, due to experimental difficulties, such as obtaining reproducible kinetic data on polymerizations that are completed within 1-2 seconds and sensitive to the presence of low levels of impurities, cationic polymerizations are not nearly as well understood as free-radical.[1]

In a cationic system the propagating species is not a free-radical but a positively charged ion (cation). Due to its charge, the cationic species requires the stabilization of an electron-donating substituents to produce ions with lifetimes long enough to produce high molecular weight polymers. In contrast the radical species is neutral and doesn't have strict requirements for stabilization in order to form polymers.[1]

2.2c. Cationic Photopolymerization

In the specific system investigated in this work, the cationic initiator was a diaryliodonium salt (Ar_2I^+) with a hexafluoroantimonate (SbF_6^-) anion. The anion is nonnucleophilic and also photostable since this initiator is cleaved photolytically. This type of initiator which also includes aryldiazonium and triarylsulfoniuim salts with anions such as tetrafluoroborate (BF_4^-) and hexafluorophosphate (PF_6^-), where originally identified as thermally stable photoinitiators for cationic systems by Crivello in the mid 1970's.[5] These initiators are photolytically fragmented at the Ar-I or Ar-S bond to give a radical-cation that then undergoes an oxidation-reduction reaction with an acidic hydrogen (HY) to produce an initiator-coinitiator species. This complex then acts as a proton donor to initiate polymerization (see *Equation 2-1*).[1,5]

$$Ar_2I^+(SbF_6^-) \xrightarrow{h\upsilon} [Ar_2I^+(SbF_6^-)]^* \rightarrow ArI^{+}\bullet(SbF_6^-) + Ar\bullet \xrightarrow{R-H} ArI + R\bullet + H^+(SbF_6^-)$$

Equation 2-1.

The onium salt initially absorbs light at specific wavelengths depending on the particular salt used elevating the salt to an electronically excited state. This is followed by cleavage

of the carbon-iodine bond as a result of the rapid decay from the excited state.[5] The triarylsulfonium initiator has been shown to follow a similar mechanism.[5]

2.3. Photosensitization

Since most diaryliodonium and triarylsulfonium salts absorb strongly only in the UV region, around 250 nm, considerable effort has been directed towards providing a means for improving their sensitivity to longer wavelengths. It is far more useful to be able to excite the initiators using light in the visible region such as the 300 - 450 nm region since common, and relatively inexpensive, light sources such and mercury arc lamps can then be used. Furthermore, the 250 nm region has the added disadvantage of coinciding with the absorption bands of the aromatic products of the photolysis and any aromatic substituents that may be present on the monomer.[5] This results in suppression of the initiation process since the aromatic products absorb increasing quantities of the excitation light as the reaction proceeds.[5]

One of the easiest and most successful ways of increasing the size of the wavelength region over which polymerization will occur is to add a photosensitizer. A photosensitizer is generally used to refer to any substance that either increases or shifts the wavelength region to which the initiator is sensitive or increases the rate of a photopolymerization.[1] More specifically, in the sense referred to here, the photosensitizer expands the region of sensitivity of the initiator by undergoing excitation at the desired wavelength to form an excited state species. This excited state then interacts with the initiator to form cations as described previously. Photosensitization of diaryliodonium and triarylsulfonium was independently discovered by Smith[6] at 3M and by Crivello and Lam[7, 8] at GE.

The most effective wavelengths for initiating diaryliodonium and triarylsulfonium salts are between 255 and 275 nm.[9,10] Therefore, one disadvantage of the onium salt

initiators is their poor absorption at wavelengths above 300 nm,[11] where medium and high-pressure mercury lamps emit much of their radiation. Photosensitizers overcome this limitation, making it possible to initiate polymerization in the near-UV or visible wavelengths as a result of a direct interaction between an excited state of a photosensitizer and the initiator. Anthracene, which absorbs between 320 and 390 nm (see *Figure 2-1*), was chosen to expand the initiating window to the near-visible region of the spectrum.[12]

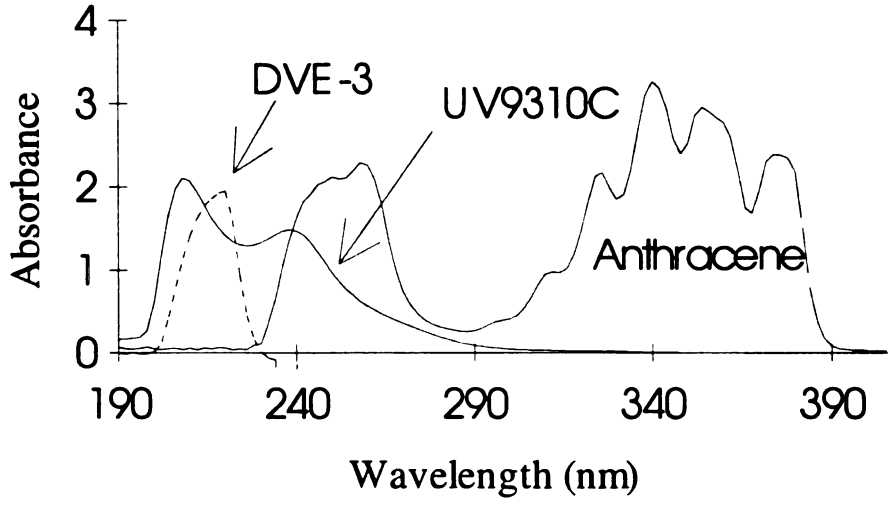

Figure 2-1 *Absorption Spectrum of Monomer (DVE-3), Initiator (UV9310C) and Photo-sensitizer (Anthracene).*

2.4. References

1. Odian, G., "Principles of Polymerization," 2nd Edition, Wiley, New York, NY, 1981.
2. Sperling, L.H., "Introduction to Physical Polymer Science," 2nd Edition, Wiley, New York, NY, 1992.
3. Oster, G.; Yang, N.-L.; *Chem. Rev.*, **68**, 125 (1968).
4. Pappas, S.P., in "Photopolymerization," *Encylcopedia of Polymer Science and Engineering*, Vol. 11, edited by H.F. Mark, N.M. Bikales, C.G. Overberger, and G. Menges, Wiley-Interscience, New York, 186, 1988.
5. Crivello, J.V., "Cationic Polymerization-Iodonium and Sulfonium Salt Photoinitiators," *Adv. Polym. Sci.*, **62,** 1 (1984).
6. Smith, G.H., U.S. Patent 4,069,054, Jan. 17, 1978; Chem. Abstr. **94**, 112539e (1981).
7. Crivello, J.V.; Lam, J.H.W., "Dye-Sensitized Photoinitiated Cationic Polymerization," *J. Polym. Sci., Polym. Chem. Ed.*, **16,** 2441 (1978).
8. Crivello, J.V.; Lam, J.H.W., "Dye-Sensitized PhotoinitiatedCationic Polymerization. The System: Perylene-Triarylsulfonium Salts," *J. Polym. Sci., Polym. Chem. Ed.*, **17**, 1059 (1979).
9. Sager, W.F.; Filipescu, N.; Serafin, F.A., "Substituent Effects on Intramolecular Energy Transfer," *J. of Phys. Chem*, **69**, 4 (1965).
10. Sundell, P.E.; Jonsson, S.; Hult, A., in "Radiation Curing of Polymeric Materials," edited by C.E. Hoyle and J.F. Kinstle, *ACS Symposium Series*, Vol. 417, American Chemical Society, Washington D.C., 459, 1989.
11. Nelson, E.W.; Carter, T.P.; Scranton, A.B., "Fluorescence Monitoring of Cationic Photopolymerizations of Divinyl Ethers Photosensitized by Anthracene Derivatives," *Macromolecules*, **27**, 1013 (1994).
12. Jacobs, J.L.; Nelson, E.W.; Scranton, A.B., "Use of Fluorescence to Monitor Temperature and Observe Water Effects in Cationic Photopolymerizations of Divinyl Ethers," *ACS Polym. Mat. Sci. and Eng.*, **70**, 74 (1994).

CHAPTER 3. PHOTO-DIFFERENTIAL SCANNING CALORIMETRY KINETIC STUDIES

3.1. Photo-Differential Scanning Calorimetry Studies of Cationic Polymerizations of Divinyl Ethers

Introduction. In general carbocationic polymerization kinetics are complex and vary from system to system. Therefore a simple, coherent, kinetic expression of general validity is not available for cationic polymerizations.[1] There are several difficulties that contribute to this deficiency. First, the reactivity of the carbocationic center depends strongly on the proximity of the counterion, and a number of propagating species may be identified, including ion pairs, solvated ions, or aggregates. The reactivities of the separated or solvated cations are greatly increased over ion pairs and have different chemical characteristics.[1] Second, the pseudo steady-state active center concentration assumption is invalid for cationic polymerizations. In contrast to free radical polymerizations, combination of active centers does not occur, and termination is generally suppressed in cationic polymerizations. Therefore, in most cases, the rates of initiation and termination are not equal, and non-steady state calculations are required.[1] In addition, transfer reactions are typically important in cationic polymerizations, and the polymerization rate constants are affected by the nature of the counter-ion and solvent. Kinetic analysis of cationic polymerizations is not impossible, but requires careful individual consideration for each system under investigation.

Photo-differential scanning calorimetry (PDSC) offers a simple method to characterize the kinetics of photopolymerization reactions. Because the polymerizations are highly exothermic, the reaction rate may be measured by monitoring the rate at which

heat is released from the polymerizing sample. Therefore, the profiles of reaction heat versus time provided by PDSC may be used to characterize the reaction kinetics and evaluate polymerization rate constants.[2] Several authors have used PDSC to characterize free radical photopolymerizations[3,2-6] however application of the technique to cationic photopolymerizations of divinyl ethers is more problematic. First, the polymerizations of divinyl ethers proceed very rapidly, and care must be taken to ensure that the reaction rate does not exceed the time resolution of the instrument. Since the DSC response time is on the order of 2-3 seconds,[7,8] relatively low light intensities must be used to increase the reaction time for the divinyl ether photopolymerizations.[12] Second, photopolymerizations of divinyl ethers are highly exothermic, therefore to maintain isothermal conditions during the reactions very small sample sizes must be used (0.5 - 1.5 mg). If larger sample sizes are used, the heat evolved during the reaction generally cannot be removed on the time scale of the reaction.

In this contribution, PDSC was used to study the photosensitized cationic homopolymerization of a model divinyl ether monomer. Divinyl ethers have received increased attention in recent years because they generally exhibit very low vapor pressures, relatively low viscosities and low toxicity.[9] Divinyl ethers also polymerize very rapidly to form films that exhibit excellent clarity, adhesion, and solvent resistance. There are now a number of commercially available divinyl ether monomers, however, relatively few detailed kinetic studies have been reported. Understanding the kinetics of these cationic photopolymerizations is important due to the increasing number of applications for rapid, solvent-free curing of polymer films. This recent surge in applications of UV-initiated photopolymerizations has been motivated by at least two

factors: environmental concerns about the production of volatile organic emissions, and the need for high-speed reactions to enhance production rates (see refs 3, 9, 10, 11).

A series of PDSC experiments were performed on cationic photopolymerizations of a divinyl ether initiated with a diaryliodonium hexafluoroantimonate salt photosensitized by anthracene. The photosensitizer allowed the initiating wavelength to be shifted from the deep UV region of the spectrum to the near UV region at approximately 350 nm.[13] Isothermal PDSC experiments were performed for a series of reaction temperatures and light intensities. The profiles were used in conjunction with previously determined photosensitization rate constants[13] to determine the kinetic constant for propagation. The kinetic constant for termination was determined from a series of unsteady-state "dark-cure" reactions at different temperatures and light exposure times. The resulting profiles for the propagation and termination rate constants as functions of conversion provide important insight into the nature of the cationic photopolymerizations.

3.1a. Experimental

Materials. In these studies, 3,6,9,12-tetraoxatetradeca-1,13-diene (DVE-3) (ISP) was used as the monomer. The monomer was dried over molecular sieves to remove any traces of water. As in previous spectroscopic studies,[14,13] a commercially available initiator (UV9310C - GE Silicones) was used. The initiator formulation includes 5-10 wt % linear alkylate dodecylbenzene, ~50 wt % 2-ethyl-1,3-hexanediol, and ~50 wt % bis(4-dodecylphenyl) iodoniumhexafluoroantimonate. Initiator concentrations specified

in the remainder of this paper correspond to the total UV9310C concentration. The photosensitizer, anthracene, was purchased from Aldrich Chemical Company and was used as received. A representative reaction sample contained 10^{-2} wt % anthracene and 1 wt % initiator in DVE-3.

PDSC Experiments. The PDSC experiments were conducted using a differential scanning calorimeter equipped with a photocalorimetric accessory (Perkin Elmer, DSC-DPA 7). The photocalorimeter accessory included transfer optics to produce full beam ultraviolet light with a desired intensity and a monochromator to produce light of a given wavelength. The initiation light source was a 100 watt mercury arc lamp used in conjunction with neutral density filters (Melles Griot) to control the intensity of the incident light. The strong mercury line at 365 nm was used to excite the anthracene photosensitizer. The polymerization reactions were run isothermally by means of a refrigerated recirculating chiller (NESLAB, CFT-25) maintained at 5 °C. Small sample sizes (0.5 - 1.5 mg) were required in order to limit the total heat released during the polymerization reaction so that isothermal conditions could be maintained. The samples were placed in uncovered aluminum DSC pans and cured with a UV light intensity of 1.6 mW/cm^2 and maintained isothermal at 30°C.

3.1b. Results and Discussion

Effect of Light Intensity. Experiments were performed at several different excitation intensities in order to determine the effect of light intensity on the reaction profiles. The light intensity at 365 nm was adjusted by placing a neutral density filter

after the excitation monochromator. A range of relative optical densities from 0.5 to 2.0 were needed to adjust the light intensity. At optical densities less than 0.5, the reaction proceeded very rapidly and did not remain isothermal. Optical densities greater than 2.0 resulted in very slow reactions limiting the number of reactions that could be completed in a reasonable time.

Figure 3-1 shows the relationship of reaction rate and light intensity. As expected, an increase in the initiating light intensity resulted in an increased reaction rate as indicated by the exotherm reaching its maximum more rapidly. For example, at 0.56 mW/cm^2 the heat flux reached the maximum at 2.5 ± 0.7 min. and had an average peak area of 660 ± 59 J/g, while for initiating intensities of 0.19 mW/cm^2 the maximum was reached at 5.4 ± 0.7 min. and had an average area of 553 ± 14 J/g. Each of the curves in *Figure 3-1* is an average of several profiles obtained at each light intensity, therefore the average curves are slightly shorter and wider than the original data, however the average curves represent the general shape and provide the correct average time at the peak maximum and the average area.

Effect of Temperature. Reactions were performed at a series of temperatures between 20 and 50°C in order to determine an overall activation energy for the polymerization reaction. A maximum temperature of 50°C was used to ensure that no thermal initiation occurred. An average initial reaction rate was determined for each temperature by measuring the time required to reach 20 % conversion. This conversion was chosen since it represents the maximum conversion for the lowest temperature experiment. The activation energy was determined from an Arrhenius fit to the data.

Figure 3-2 shows PDSC exotherms for the cationic polymerization of DVE-3 photosensitized with 1.0 x 10^{-2} wt % anthracene and 1 wt % initiator controlled at temperatures from 20 to 50°C. As expected, the reaction rate and total conversion increased with increasing temperature as illustrated by the fact that the exotherms reach the maximum in a shorter time and exhibit larger integrated heat as the temperature is increased. Based upon an Arrhenius fit, the overall activation energy for the cationic polymerization was determined to be 26.5 ± 3.2 kJ/mol. Since the PDSC measures the total heat of reaction, this value represents an overall activation energy including initiation, propagation, and termination.

$$E_R = E_P + E_I - E_T \qquad \text{Eq. 3-1.}$$

For Equation 3-1 to be valid, the active center production must continue throughout the reaction. Based upon previous measurements of the kinetic constants for photosensitization,[13] the photosensitizer is not completely consumed until well after the time for the peak maximum, therefore the active center concentration continues to increase at the peak maximum (the point where the reaction rate was measured). Therefore, Equation 3-1 can be used to represent the overall activation energy for the photopolymerization reaction.

Termination Rate Constant. To determine the termination rate constant, k_t, for the polymerization of DVE-3, dark cure experiments were performed. In these studies the polymerization samples were exposed to the initiating light for a short period of time, after which the light source was removed. The remaining cure was monitored with no

exposure to the light source, and the reaction rate was found to decay exponentially. Samples that were exposed for 2 minutes or less had total double bond conversions of less than 5 percent. Since the change in the vinyl bond concentration during the dark cure was small, it was assumed that the reduction in the polymerization rate was caused by the decline in the number of active centers due to termination and not due to depletion of monomer.

The PDSC exotherms were fit with an exponential decay curve from the point at which the excitation source was removed with an average exponential time constant of 17.3 ± 0.4 minutes. Therefore, the termination rate constant, k_t, was calculated to be 0.0010 ± 0.0002 s^{-1}. These results illustrate that the cationic centers exhibit a relatively long lifetime and relatively small termination rate constants compared to free radical systems. This arises from the fact that, in contrast to free radicals, cationic centers do not terminate with one another. Termination in cationic systems typically occurs due to combination with the counterion or other nucleophilic species. As will be shown later, the termination rate constant for the polymerization reaction was determined to be approximately 5 times lower than the initiation rate constant.

Initiation Rate Constants. In these photopolymerizations active cationic centers are produced through a photosensitization reaction in which an electron is transferred from an excited state anthracene molecule to the initiator.[13] Although the reaction proceeds by a multi-step photochemical mechanism,[13] the rate of generation of active centers may be described by the following simple expression:

$$\text{Rate of active center generation} = k_i[A][I] \qquad \text{Eq. 3-2}$$

where [*A*] is the anthracene concentration, [*I*] is the initiator concentration, and k_i is an initiation rate constant which accounts for a number of photophysical steps including excitation, intersystem crossing, exciplex formation, and electron transfer.[13] According to this convention, k_i is dependent on the incident light intensity. In our reactions the initiator (diaryliodonium salt) concentration greatly exceeds the anthracene concentration and can be assumed to be constant.[13] Therefore a pseudo-first-order kinetic constant, $k_i^* = k_i[I]$, may be used to describe the rate of generation of active centers. The above analysis is based upon the assumptions that one active center is produced per photosensitizer and initiator molecules and that all reactive centers are capable of propagating, as indicated by previous fluorescence measurements.[14]

The overall rate of change of the active center concentration, [M^+], may be derived by combining the rate of generation by photosensitization with the rate of consumption by termination:

$$\frac{d[M^+]}{dt} = k_i^*[A] - k_t[M^+] \qquad \text{Eq. 3-3.}$$

This equation may be integrated (with the initial condition [M_0^+] = 0 and the exponentially decreasing anthracene concentration) to yield the following equation:

$$[M^+] = [A_0]\frac{k_i^*}{k_t - k_i^*}(e^{-k_i^* t} - e^{-k_t t}) \qquad \text{Eq. 3-4.}$$

In this equation, the termination rate constant, k_t was evaluated above while the initiation rate constant, k_i may be determined from solving the photophysical rate expressions as described in earlier work.[13] For the PDSC experiments the incident light intensity used in this calculation was determined by measuring the energy absorbed by graphite discs

placed in the sample and reference cells. Using the incident light intensity value, k_i^* was determined to be 4.03 x 10^{-3} s^{-1} at 25 °C by solving the corresponding set of rate expressions.[13]

The activation energy for the photosensitization reaction was determined from fluorescence measurements of the photosensitization reaction between anthracene and the diaryliodonium salt. The rate constant, k_i, was determined for several different temperatures and fit to an Arrhenius equation to yield an activation energy, E_I, of 28.5 ±1.6 kJ/mol. Using this activation energy, the temperature-dependence of k_i^* was described. Based upon the values of k_t, k_i^*, E_I, and A_0, Equation 3-4 was used to obtain profiles of the active center ($[M^+]$) concentration as a function of time for each of the PDSC reactions.

Propagation Rate Constant. As previously mentioned, the rate of polymerization (R_p) is directly proportional to the rate at which heat is released from the polymerizing sample and is therefore proportional to the height of the DSC exotherm measured in W/g. For a polymerization rate in units of mol(double bonds)/(l sec), the proportionality constant is the density (ρ - the density of the reaction mixture) divided by the heat of polymerization, ΔH_p, and the instantaneous rate of polymerization may be calculated from the following relationship:

$$R_p = \frac{d[M]}{dt} = \frac{\text{height of exotherm (W / g)} * \rho}{\Delta H_p} \qquad \text{Eq. 3-5.}$$

According to kinetic analysis, the rate of propagation is given by a propagation rate constant multiplied by the active center concentration, $[M^+]$, and the vinyl bond concentration, [M], as shown below:

$$R_p = \frac{d[M]}{dt} = k_p[M][M^+] = [A_0]\frac{k_p k_i^*}{k_t - k_i^*}(e^{-k_i^* t} - e^{-k_t t})[M] \qquad \text{Eq. 3-6.}$$

If a number of propagating centers with different reactivities exist, this equation may be used to fit the polymerization data to yield an apparent propagation constant that comprises all types of propagating centers (e.g. ion pairs, separated ions, etc.). In this paper we will use this approach to interpret changes in the value of the apparent propagation constant, k_p.

The vinyl bond concentration ([*M*]) and the conversion may be calculated from the integral of the reaction rate profile (Equation 3-5). Therefore, the instantaneous double bond concentration may be calculated form the PDSC profile using the following equations:

$$[M] = [M_0] - \left(\frac{\text{exotherm area (J / g)} * \rho}{\Delta H_p}\right) \qquad \text{Eq. 3-7.}$$

$$\text{Conversion} = \left(\frac{\text{exotherm area (J / g)} * \rho}{\Delta H_p [M_0]}\right) \qquad \text{Eq. 3-8.}$$

Equation 3-7 gives the vinyl bond concentration in mol/l when ρ is the density of the reaction mixture. The heat of reaction for the vinyl bond was determined to be 75 kJ/mol by reacting a monovinyl ether to high conversion. A complete profile of the double bond concentration or conversion may be obtained by determining the area under the DSC curve as a function of time and applying Equation 3-7 or 3-8.

For each PDSC exotherm, a profile of the quantity $k_p[M^+]$ may be obtained using the empirical profiles of R_p and [M]. Based only on the PDSC data, this product may be determined using the following version of Equation 3-6.

$$k_p[M^+] = \frac{R_p}{[M]} \qquad \text{Eq. 3-9.}$$

Profiles of the rate of polymerization (propagation) obtained by applying Equations 3-5 and 3-6 to a set of PDSC exotherms are shown in *Figure 3-3*. The figure illustrates that as the temperature is increased the maximum value of R_p increases accordingly. Furthermore, the conversion at the peak maximum is shifted to higher values as the temperature increases. Therefore *Figure 3-3* verifies the importance of temperature during the cationic photopolymerization of DVE-3, as characterized by the increase in conversion and rate of the reaction with temperature.

Profiles of $k_p[M^+]$ obtained in this manner are shown in *Figure 3-4*. As shown in the figure, $k_p[M^+]$ initially increases sharply and then levels off at a plateau value between 0.001 and 0.01 s^{-1} depending upon the reaction temperature (as temperature is increased a higher value of $k_p[M^+]$ is observed). Finally, the value of $k_p[M^+]$ decreases as a limiting conversion is reached. The shape of the profiles in *Figure 3-4* indicates that the apparent propagation rate constant k_p changes as the reaction proceeds. If k_p remained constant throughout the reaction, this change in $k_p[M^+]$ would be governed by the active center concentration. Therefore, the $k_p[M^+]$ value would increase monotonically until it reached a maximum when all of the photosensitizer is consumed.

More information about the behavior of k_p may be obtained by coupling the PDSC data with the k_i^* and k_t values discussed previously. Profiles of the apparent propagation rate constant, k_p were obtained by substituting the values of $[A_0]$, k_i^*, and k_t along with the empirically determined profiles of $[M]$ and R_p into Equation 3-6. *Figure 3-5* shows k_p as

a function of vinyl bond conversion. The curves exhibit a similar characteristic shape as the $k_p[M^+]$ profiles of *Figure 3-4*, although the plateau value is much higher due to the small active center concentration. The similarity in shape indicates that relative changes in k_p are much larger than those for $[M^+]$. The final magnitude obtained for k_p values were between 5 and 30 l/mol*s, which compare satisfactorily with values from the literature.[15]

One possible explanation for the initial large increase in the apparent rate constant for propagation is a change in the reactivity of the carbocation species due to the proximity of the counterion. In the early stage of the reaction, polymerization leads to a large local increase in viscosity which reduces diffusional mobility. The active carbocation retains considerable mobility through propagation since the cation effectively moves through the reaction mixture by reacting with new monomers. This type of mobility has been termed "reaction diffusion" and may become the dominant mechanism for mobility of the active center in highly crosslinked polymerizations.[5,16] However, the large hexafluoroantimonate counterion experiences a decrease in mobility as the viscosity increases since it cannot diffuse through the reaction mixture in a similar manor. During this process, the counterion and carbocation become separated, and since separated ions are orders of magnitude more reactive than ion pairs,[1] this would lead to a large increase in the apparent propagation rate constant, k_p. This type of "reaction diffusion" is well known for highly crosslinked free radical systems[5,16] and may aid in explaining the shape of the curves in *Figures 3-4* and *3-5*. The final decrease in k_p arises from active center trapping during these highly crosslinked polymerizations. Therefore a limiting conversion at which the reaction ceases is observed despite the presence of active centers.

As previously mentioned, the above analysis is based upon the assumptions that one active center is produced for each photosensitizer molecule consumed and that all reactive centers are capable of propagating.[13]

3.2. Conclusions

In this contribution photo-differential scanning calorimetry (PDSC) was used to monitor cationic photopolymerizations of a divinyl ether. The PDSC method offers a direct method for evaluating the heat generated during a polymerization reaction. The heat of reaction profiles provided by PDSC were used to characterize the reaction kinetics and evaluate polymerization rate constants. However, the reaction system was extremely rapid and highly exothermic, making DSC measurements particularly challenging. To maintain isothermal reaction conditions, low light intensities and very small sample sizes (0.5 - 1.5 mg) were used to increase the reaction time for the divinyl ether photopolymerizations.

The PDSC experiments were used to determine kinetic constants for a series of unsteady-state divinyl ether polymerizations at different temperatures and light exposure times. Kinetic constants for propagation and termination were obtained from the PDSC experiments in conjunction with previously determined photosensitization rate constants. As expected, an increase in the initiating light intensity or an increase in the reaction temperature resulted in an increased reaction rate. This increase in reaction rate was found to result in higher final conversions as determined from the total heat of reaction.

To determine the termination rate constant, k_t, PDSC dark cure exotherms were fit with an exponential decay from the point at which the excitation source was removed (the exponential time constant was 17.3 ± 0.4 minutes). These results illustrate that the cationic centers exhibit a relatively long lifetime and relatively small termination rate constants compared to free radical systems, arising from the fact that cationic centers do not terminate by combination with themselves.

An apparent propagation rate constant that comprises all types of propagating centers (e.g. ion pairs, separated ions, etc.) with different reactivities was determined from the PDSC reaction profiles. The apparent propagation constant, k_p, initially increases sharply and then levels off at a plateau value (as temperature is increased a higher value of k_p is observed). Finally, the value of k_p decreases as a limiting conversion is reached. This profile shape indicates that the apparent propagation rate constant k_p changes greatly as the reaction proceeds. The initial large increase in the apparent rate constant for propagation may be explained by a change in the reactivity of the carbocation species due to the proximity of the counterion. During the polymerization, the counterion experiences a decrease in the mobility of the large hexafluoroantimonate counterion as the viscosity of the system increases. However, the active carbocation retains diffusional mobility by reacting with vinyl bonds and may lead to separation of the two species. Since separated ions are orders of magnitude more reactive than ion pairs,[1] the apparent value of k_p increases dramatically during the early stages of the reaction. The final decrease in k_p arises from active center trapping during these highly crosslinked polymerizations. Therefore, a limiting conversion at which the reaction ceases is observed despite the presence of active centers.

The PDSC profiles for the propagation and termination rate constants as functions of conversion provide important insight into the nature of these high-speed cationic photopolymerizations. Understanding the kinetics of these cationic photopolymerizations is important due to the increasing number of applications for rapid, solvent-free curing of polymer films.

Acknowledgments This work was supported by National Science Foundation Grants CTS 9216939 and CTS 9209899. The PDSC experiments were performed at the University of Colorado, Boulder.

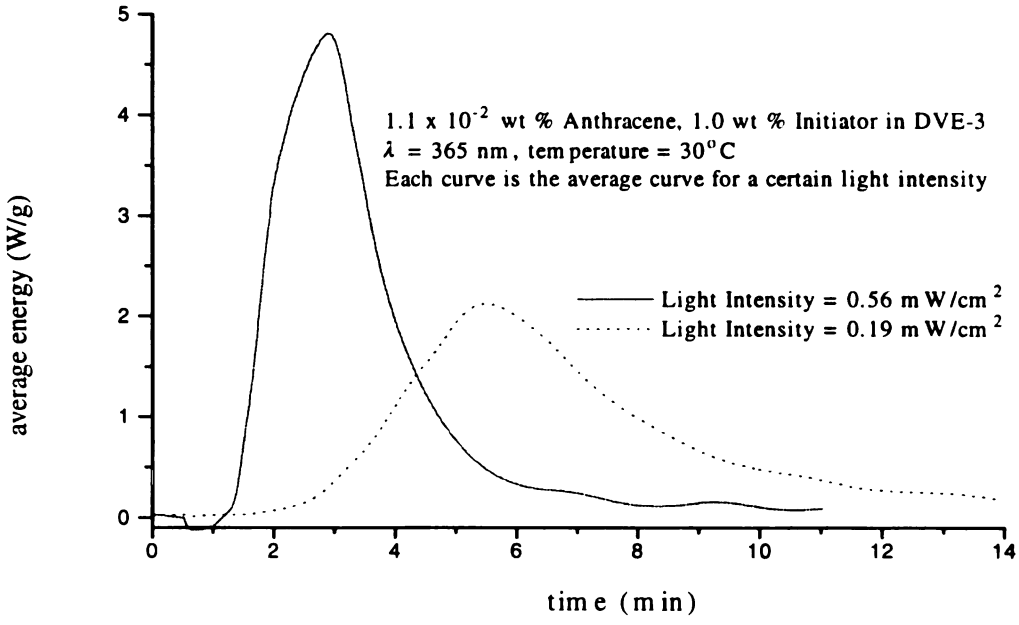

Figure 3-1 *PDSC exotherms for the cationic polymerization of DVE-3 at different light intensity values.*

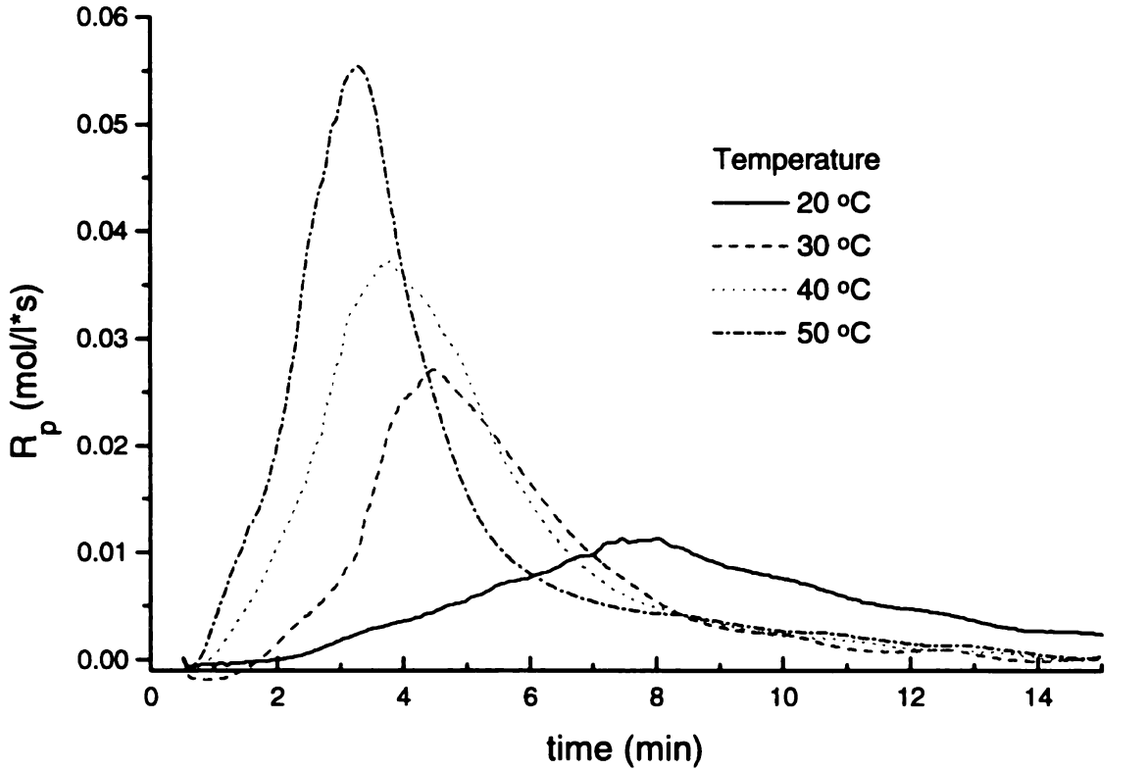

Figure 3-2. *PDSC exotherms for the cationic polymerization of DVE-3 at temperatures ranging from 20 to 50 °C.*

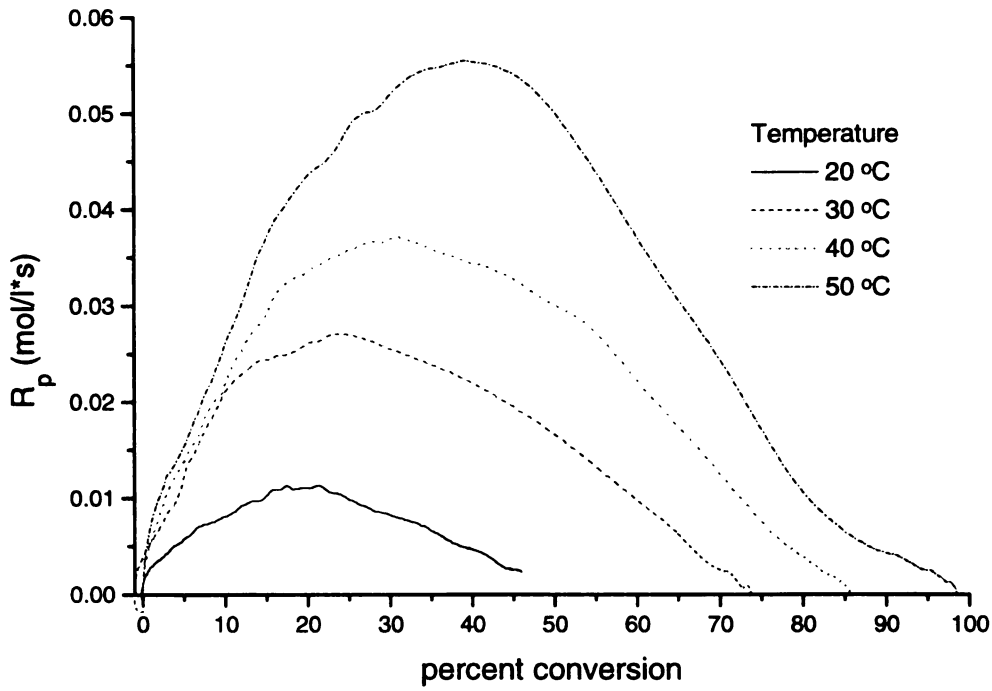

Figure 3-3. *Overall rate of propagation versus conversion for DVE-3 photosensitized with 1.0 x 10^{-2} wt % anthracene and 1 wt % initiator.*

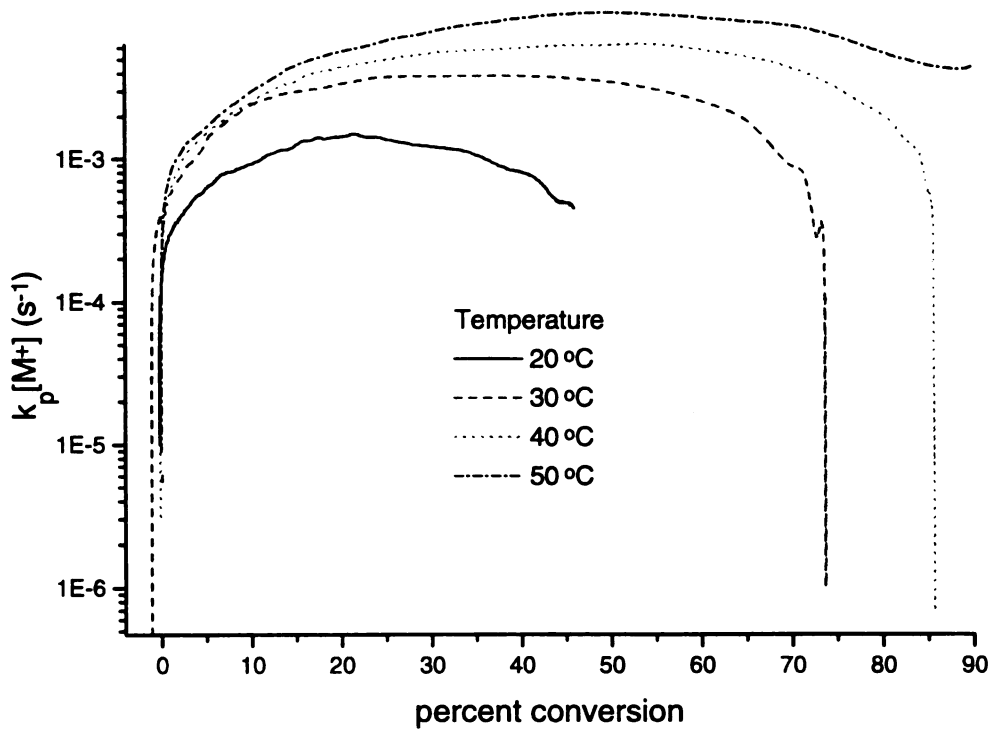

Figure 3-4. *k_p [M^+] versus conversion for the cationic photopolymerization of DVE-3 at temperatures ranging from 20 to 50 °C.*

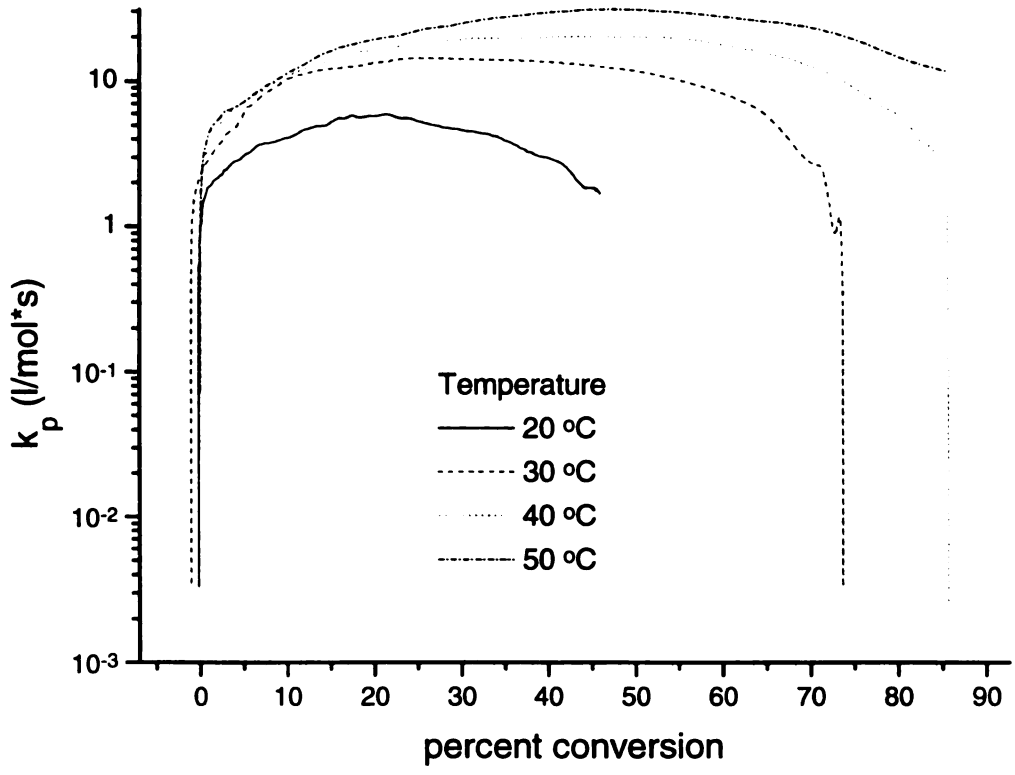

Figure 3-5. *k_p versus conversion for the photopolymerization of DVE-3 at various temperatures.*

3.3. References

1 Kennedy, J. P.; Marechal, E., "Carbocationic Polymerization," John Wiley & Son, New York, 1982.

2 Doornkamp, T., and Tan, Y. Y. *Polymer Commun.* 1990, **31**, 362.

3. Kloosterboer, J. G., "Network Formation by Chain Crosslinking Photopolymerization and its Applications in Electronics," *Adv. Polym. Sci.*, **84**, 1 (1988).

4 Kloosterboer, J. G.; Lijten, G.F.C.M., *Polymer,* **28**, 1149 (1987).

5 Anseth, K. S.; Wang, C. M.; Bowman, C. N., "Kinetic Evidence of Reaction Diffusion during the Polymerization of Multi(meth)acrylate Monomers," *Macromolecules,* **27**, 650 (1994).

6 Anseth, K. S.; Wang, C. M.; Bowman, C. N., "Reaction Behavior and Kinetic Constants for Photopolymerizations of Multi(meth)acrylate Monomers," *Polymer,* **35**, 3243 (1994).

7 Decker, C.; Moussa, K., "Real-Time Monitoring at Ultrafast Curing By UV-Radiation and Laser Beams," *J. Coatings Tech.*, **62**, 55 (1990).

8 Kloosterboer, J.G.; Lijten, G.F.C.M., *Cross-Linked Polymers;* Dickie, R.A.; Labana, S.S.; Bauer, R.S., Ed.; ACS Symposium Series 367; ACS: Washington DC, 1987.

9. Roffey, C. G., *Photopolymerization of Surface Coatings*, Wiley, New York, 1981.

10. Pappas, S. P., "Photoinitiators", *UV Curing, Science and Technology*, Technology Marketing Corp., Norwalk, CT, **2**, 1985.

11. Crivello, J. V., "Cationic Polymerization ---- Iodonium and Sulfonium Salt Photoinitiators," *Adv. Polym. Sci.*, **62**, 1 (1984).

12 Crivello, J.V.; Lee, J.L.; Conlon, D., "Photoinitiated Cationic Polymerization with Multifunctional Vinyl Ether," *J. Rad. Curing*, **6** (1983).

13 Nelson, E.W.; Carter, T.P.; Scranton, A.B., "The Role of the Triplet State in the Photosensitization of Cationic Polymerizations by Anthracene," *J. Polym. Sci., Polym. Chem.*, **33**, 247 - 256 (1995).

14. Nelson, E.W.; Carter, T.P.; Scranton, A.B., "Fluorescence Monitoring of Cationic Photopolymerizations: Divinyl Ethers Photosensitized by Anthracene Derivatives," *Macromolecules,* **27**, 1013-1019 (1994).

15 Odian, G., "Principles of Polymerization," 2nd Ed., Wiley, NY, 22, 1981.

16 Anseth, K. S.; Bowman, C. N., "Reaction Diffusion Enhanced Termination in Polymerizations of Multifunctional Monomers," *Polymer Reaction Engineering*, **1(4)**, 499-520 (1992-93).

CHAPTER 4. EFFECTS OF WATER ON THE REACTION RATE

In this chapter, a time-resolved fluorescence monitoring scheme is used to investigate the effect of small concentrations of water on the polymerization kinetics. These studies are important because monomers will often absorb water in humid environments, which may adversely affect cationic polymerizations. In addition, a photo-differential scanning calorimeter is used to verify how water causes the effects observed in the fluorescence monitoring experiments.

4.1. Fluorescence Measurements: Use of Fluorescence to Observe Water Effects

4.1a. Background

Despite the advantages of cationic photopolymerizations discussed in Chapter 1, nearly all the research in UV-initiated polymerizations has focused on free radical reactions. This fact may be largely attributed to the lack of suitable UV-sensitive cationic photoinitiators until recently.[4,7,8] In the late 1970s, Crivello and Lam reported the development of two novel classes of photoinitiators for cationic polymerizations: diaryliodonium and triarylsulfonium salts (for reviews of the development of these initiators see references 4 and 13). Upon photolysis, these compounds undergo irreversible photofragmentation to produce aryliodonium or arylsulfonium cation-radicals capable of initiating cationic polymerization.[14] However, it was the thermal stability of the initiators that greatly improved their utility over previous photoinitiators. Although the diaryliodonium and triarylsulfonium salts actively initiate cationic polymerization in

the presence of light, they are also remarkably latent in the absence of light, eliminating the necessity of mixing immediately before use.

Diaryliodonium and triarylsulfonium salts are most effective for initiating wavelengths between 225 and 275 nm.[4,9] Therefore, one disadvantage of the onium salt initiators is their poor absorption at wavelengths above 300 nm,[15] where medium and high pressure mercury lamps emit much of their radiation. One method of overcoming this limitation is to use photosensitizers to expand the spectral region over which onium salts are effective. Through a direct interaction between an excited state of the photosensitizer and the initiator, photosensitizers make it possible to initiate polymerization in the near UV or visible wavelengths of light. Aromatic compounds with heterocyclic or fused rings often show activity as photosensitizers. Anthracene has been used to photosensitize both free radical[16] and cationic[17,38] polymerizations. Anthracene absorbs strongly at wavelengths between 320-390 nm, and therefore expands the initiating window to the near visible region of the spectrum.

To date, most of the work on cationic photopolymerizations reported in the literature focuses on the initiation step of the reaction, and the polymerization step as well as the resulting polymers are not well characterized. It is clear that cationic photopolymerizations of vinyl ethers proceed very rapidly, however few detailed kinetic studies have been performed for these reactions. For example, except for recent work by Nelson *et al.*,[18,38,41] the kinetics of these photopolymerizations have been characterized in only a cursory manner by measuring the tack-free time of a curing polymer film. Nelson *et al.* have reported detailed profiles of conversion versus time for the DVE-3 photopolymerization.[18, 39] The results presented here expand the work done by Nelson *et al.* by

characterizing the effects of small concentrations of water on this reaction profile for an otherwise identical reaction system.

A major reason for the lack of kinetic studies is the extremely rapid reaction rates exhibited by cationic photopolymerizations of divinyl ethers. Because these reactions may proceed to completion in a matter of seconds, there are few experimental techniques with sufficient time resolution to characterize these polymerizations. Differential scanning calorimetry (DSC) has been used extensively to study free radical photopolymerizations of acrylates[1] as well as cationic photopolymerizations of epoxides,[19,20] however the technique's relatively slow response-time limits its applicability for vinyl ether photopolymerizations. Because the DSC response time is on the order of 2-3 seconds,[21,22] the technique is only applicable for vinyl ether photopolymerizations that are initiated with relatively low intensity light[23, 39] where the cure time is relatively long (tens of seconds), and small sample sizes where the total heat released is low.[39] Real-time infrared spectroscopy has recently been used to monitor high-speed, laser-induced radical photopolymerizations.[21,24] This technique has a response time of 0.02 seconds[21] and could therefore be useful for characterizing cationic photopolymerizations. The advantages and limitations of this technique have recently been addressed.[21]

In the studies presented in this chapter, the effects of small concentrations of water on the reaction rate of cationic photopolymerizations of vinyl ethers were investigated using *in situ* laser-induced fluorescence spectroscopy. The fluorescence intensity of the photosensitizer was monitored during the reaction to obtain a direct measure of the rate of initiation in samples with varying concentrations of water. Fluor-

escence spectroscopy is particularly attractive as an *in situ,* time-resolved technique for monitoring these high speed polymerizations because it has an extremely short intrinsic timescale (typically 10^{-9} seconds). The response time for the monitoring technique is invariably determined by the speed of the detection system. In these studies, a high-speed diode array detection system was employed, and fluorescence spectra were collected in intervals as short as 2 milliseconds. Therefore, the fluorescence monitoring method has a considerably faster response time than DSC and real-time IR methods, and provides ample time-resolution needed to characterize this cationic photopolymerization.

In recent years, several authors[25,26,27,28] have reported the use of fluorescence techniques for monitoring polymerizations. Most of these fluorescence techniques monitor polymerization indirectly through the corresponding increase in viscosity. For example, several fluorescence monitoring schemes make use of an increase in the fluorescence intensity of a fluorescent probe with increasing viscosity.[25,26] A distinct limitation of this viscosity-sensitive technique is in its poor ability to continue to monitor a cross-linking polymerization above the gel point, where the viscosity changes relatively little with time. The fluorescence monitoring scheme used here was largely developed by Nelson *et al.*[38] This technique is considerably different than the viscosity-sensitive methods reported in the literature. The fundamental difference between this fluorescence monitoring scheme and the viscosity-sensitive probe approach arises from the fact that this technique monitors the fluorescence of one of the reactants (the photosensitizer), not that of an inert probe. Therefore, this technique provides a more direct measurement of the reaction itself, and does not lose sensitivity at the gel point.

4.1b. General Experimental Setup

Fluorescence Measurements. The laser-induced fluorescence studies were performed in the *LASER* Laboratory at Michigan State University. The fluorescence and photosensitization were both excited with a Coherent Innova 200 Argon ion laser operating at 363.8 nm. A Newport 845HP-01 Digital Shutter system was opened with an electric pulse from the detector controller, ensuring that the initiation and fluorescence acquisition were started simultaneously. Fifteen milliwatts of unfocused laser radiation (measured with a Scientech 362 Power/Energy meter) in an approximately 3 mm diameter beam was directed on to the quartz capillary tube containing the sample, whose longitudinal axis was perpendicular to the laser beam direction. The quartz capillary was approximately 2.5 cm in length with an inner diameter of 1 mm and an outer diameter of 2 mm. A typical reaction system contained ~1 wt% initiator (UV9310C) and ~10^{-2} wt% of photosensitizer in monomer (DVE-3). The fluorescent light was collected at an angle of 90° from the incident beam and 90° from the long axis of the quartz tube (see *Figure 4-1*). The fluorescence signal was collected using a Spex 1877 Triplemate spectrometer with a subtractive dispersion filter stage and a spectrograph stage. An EG&G Princeton Applied Research Model 1421 intensified diode array, cooled to -20 °C to minimize dark charge levels, was used to detect the signal. The data was analyzed with an EG&G Princeton Applied Research Model OMA III detector controller. To simulate typical process conditions for coating, ink, adhesive and electronic applications,

all reactions, unless specifically noted, were initiated at room temperature and were performed without external heating or cooling.

In previous work[38], Nelson *et al.* used this setup with 150 groove/mm gratings in both the filter and spectrograph stages to obtain a full anthracene fluorescence spectrum spanning 300 nm centered around 450 nm. The OMA III detection system has the capability of collecting this entire spectrum in 16.67 ms. However, if smaller regions of the spectrum are collected, less time is required per acquisition. For example, spectral regions from 50 to 100 nm wide were collected in intervals as short as 2 milliseconds per spectrum.

4.2. Time Resolved Fluorescence

4.2.a. Experimental

Materials. In these studies, 3,6,9,12-tetraoxatetradeca-1,13-diene (DVE-3) (GAF Chemicals Corp.) was used as the monomer. The monomer was initially dried over molecular sieves to remove any traces of water. The initiator (UV9310C - GE Silicones) had a composition of 5-10 wt% linear alkylate dodecylbenzene, ~50 wt% 2-ethyl-1,3-hexanediol, and ~50 wt% bis(4-dodecylphenyl)iodoniumhexafluoroantimonate. Initiator concentrations specified in the remainder of this paper correspond to the total UV9310C concentration. The anthracene photosensitizer (Aldrich Chemical Company) was used as purchased.

Fluorescence Monitoring of Cationic Photopolymerizations. The photo-polymerization kinetics were investigated by monitoring the photosensitizer fluorescence

as a function of time as described above in the previous section. A series of samples containing DVE-3, 1.03 wt% UV9310C, and 1.25×10^{-2} wt% anthracene with water varying from 0.0 wt% to 3.21 wt% were investigated. These samples were all prepared from the same dry solution of monomer, initiator, and anthracene. This solution was checked for zero water content by adding a fine powder of $MgSO_4$ to a sample. A 30 nm wide spectrum centered around the maximum anthracene fluorescence peak was then collected. The spectral range was narrowed to this region in order to increase the time resolution.

4.2b. Results and Discussion

Figure 4-2 contains a series of fluorescence spectra obtained during the cationic photopolymerization of DVE-3. This time dependent plot consists of twenty anthracene spectra with time as the depth axis. The spectra follow a general trend in which the anthracene fluorescence decreases slowly for several hundred milliseconds, then drops dramatically as the anthracene is consumed.[18,39,40,41] This rapid fluorescence decrease has been attributed to a temperature increase arising from the heat of polymerization in these nearly adiabatic reactions. Under the reaction conditions shown in *Figure 4-2*, the entire reaction is complete in 1.5 seconds, however times as short as 0.4 seconds were observed for other initiator and photosensitizer concentrations.[18,39,40,41] Since some photosensitizer molecules may remain unreacted, the fluorescence levels off and reaches a steady state value greater than zero.

Water Effects. To investigate the effect of water on the polymerization kinetics, fluorescence reaction profiles were obtained for 14 different water concentrations between 0 and 3.21 wt%. *Figure 4-3* is a representative plot of the maximum fluorescence intensity versus time obtained in these experiments. All of these profiles exhibited a long exponential decay period followed by a rapid decrease in fluorescence intensity. The slight increase in fluorescence intensity just before the break in the curve may be a result of vitrification, where the intensity increases due to an increase in viscosity. *Figure 4-4* illustrates how the point of rapid decrease is delayed as water content is increased. The time required before the sudden decrease in fluorescence intensity (63 seconds in *Figure 4-3*) showed a marked dependence on the water content. The experimental relationship between the time of the sudden decrease in fluorescence and water concentration is summarized in *Figure 4-5*.

Figure 4-6 illustrates the effect of anthracene concentration on the reaction time, with curves for 10^{-1}, 10^{-2}, 10^{-3} wt% anthracene. An order of magnitude increase in anthracene concentration results in a downward shift of the time curve, while the same decrease shifts the curve upward. This indicates that increasing the anthracene concentration partially offsets the effect of the water by photosensitizing a larger number of initiator molecules. This has the effect of increasing the initiator concentration by providing a larger number of reactive sites which increases the reaction rate.

A couple of possible explanations for the observed increase in time with increasing water content at constant initiator and photosensitizer concentration were theorized. The first was that the water is inhibiting or retarding the propagation reaction by consuming the reactive cations. The second possibility was that the water is acting as

a heat sink and therefore increasing the time required for the heat of polymerization to raise the reaction temperature. In order to determine which, if either, of these theories was correct a couple different approaches were considered.

4.3. Temperature-Dependent Luminescence

The first approach was to use an *in situ* luminescent temperature-sensitive probe based on a lanthanide salt. The selection of a probe and development of the experimental technique is described in detail in chapter 5. *Figure 4-7* illustrates the time-resolved temperature-dependent luminescence emission that was collected *in situ* during polymerization of DVE-3. Notice that the peaks at 618 nm and 622nm decrease in intensity as the exothermic reaction proceeds. While this temperature-sensitive luminescence technique has significant potential as a non-intrusive, *in situ*, high-speed method for monitoring reaction temperature profiles, it was found to be unsatisfactory for systems containing varying amounts of water. It is believed that the water in the reaction system "solvates" the lanthanide salt causing water concentration dependent shifts in the luminescence intensity of the lanthanide probe. The europium center of the chelate is elevated to an excited state by an electronic energy transfer through the ligands.[42] Water may inhibit efficiency by which the ligands are able to absorb energy and transfer it to the metal center. *Figure 4-8* illustrates the non-linear reduction in luminescence of the lanthanide compound, tris(1,1,1,5,5,5,-hexafluoroacetylacetone) europium ($Eu(hfa)_3$), as the water content is increased. This work was done using an Aminco Bowman Luminescence Spectrophotometer.

An attempt was made to find a relationship between water concentration and luminescence intensity in order to establish a three dimensional calibration curve accounting for weight percent water. *Figure 4-9* and *Figure 4-10* show the results of varying water concentration at different temperatures. As these figures illustrate the relationship between water concentration and luminescence intensity changes with sample temperature. The data was approximated using an exponential fit, however, the exponential decay constants are dependent on the sample temperature. This is likely due to increased solubility of the europium chelate in water at higher temperatures. The combined difficulty of both water concentration and its changing relationship to luminescence intensity based on sample temperature resulted in a calibration curve that lacked the accuracy and reliability needed to investigate changes in reaction temperature due to the presence of water.

The second approach taken to identify how the presence of water is causing a delay in the reaction rate was to use photo-differential scanning calorimetry. This work was performed using a differential scanning calorimeter equipped with a photocalorimetric accessory (Perkin Elmer, DSC-DPA 7) located at the University of Colorado, Boulder.

4.4. Isothermal Photo-Differential Scanning Calorimetry to Observe Water Effects.

Photo-differential scanning calorimetry (PDSC) offers a simple method to characterize the kinetics of photopolymerization reactions. Because the polymerizations are highly exothermic, the reaction rate may be measured by monitoring the rate at which

heat is released from the polymerizing sample. Therefore the profiles of reaction heat versus time provided by PDSC may be used to characterize the reaction kinetics and evaluate polymerization rate constants.[45] Several authors have used PDSC to characterize free radical photopolymerizations[1,45,46,47,48] however application of the technique to cationic photopolymerizations of divinyl ethers is more problematic. First, the polymerizations of divinyl ethers proceed very rapidly, and care must be taken to ensure that the reaction rate does not exceed the time resolution of the instrument. Since the DSC response time is on the order of 2-3 seconds,[21,22] relatively low light intensities must be used to increase the reaction time for the divinyl ether photopolymerizations.[23] Second, photopolymerizations of divinyl ethers are highly exothermic, and to maintain isothermal conditions during the reactions, very small sample sizes must be used (0.5 - 1.5 mg). If larger sample sizes are used, the heat evolved during the reaction generally cannot be removed on the time scale of the reaction.

In this study, PDSC was used to study the photosensitized cationic homopolymerization of a model divinyl ether monomer (DVE-3) containing different concentrations of water. A series of PDSC experiments were performed on cationic photopolymerizations of a divinyl ether initiated with a diaryliodonium salt of hexafluoroantimonate photosensitized by anthracene. The photosensitizer allowed the initiating wavelength to be shifted from the deep UV region of the spectrum to the near UV region around 350 nm.[41] Isothermal PDSC experiments were performed for a series of samples containing concentrations of water ranging from 0 to 1.5 wt %. The resulting profiles for the heat released per gram of sample as a function of reaction time provide

important insight into the nature of the effect of water on the cationic photopolymerization.

4.4a. Experimental

Materials. In these studies, 3,6,9,12-tetraoxatetradeca-1,13-diene (DVE-3) (ISP) was used as the monomer. The monomer was dried over molecular sieves to remove any traces of water. As in previous spectroscopic studies, [38,41,43] a commercially available initiator (UV9310C - GE Silicones) was used. The initiator formulation includes 5-10 wt % linear alkylate dodecylbenzene, ~50 wt % 2-ethyl-1,3-hexanediaol, and ~50 wt % bis(4-dodecyclophenyl) iodoniumhexafluoroantimonate. Initiator concentrations specified in the remainder of this section correspond to the total UV9310C concentration. The photosensitizer, anthracene, was purchased from Aldrich Chemical Company and was used as received. De-ionized water was added dropwise using a syringe to accurately control the amount added to each sample. A representative reaction sample contained 10^{-2} wt % anthracene, from 0 to 1.5 wt% water, and 1 wt % initiator in DVE-3.

PDSC Experiments. The PDSC experiments were conducted using the same differential scanning calorimeter equipped with a photocalorimetric accessory (Perkin Elmer, DSC-DPA 7) as described in chapter 3. As before, the strong mercury line at 365 nm was used to excite the anthracene photosensitizer. The polymerization reactions were run isothermally with small sample sizes of 0.5 - 1.5 mg. The samples were placed in uncovered aluminum DSC pans and cured with a constant UV light intensity and maintained isothermal at 30°C.

4.4b. Results and Discussion

Effect of Water on the Isothermal Reaction. PDSC provides a thermal reaction profile of the polymerization that was used to investigate the possibility that the addition of water to the divinyl ether system results in an extended reaction time due to heat effects. If the water is delaying the reaction through heat effects, then under isothermal conditions there should be no change in reaction time with the addition of water. As mentioned earlier the difficulty in making these DSC measurements with this particular system is that low light intensities and very small sample sizes are required to stay within the DSC's ability to keep the reaction isothermal. A sample size of approximately 1.0 mg and a light intensity of 1.6 mW/cm^{-2} was found to result in a polymerization reaction that could be maintained at an isothermal condition of 30°C over a range of water concentrations from 0 wt% to 1.5 wt%.

Figure 4-11 and *Figure 4-12* show the relationship between different water concentrations and reaction rate. In both of these figures, which differ by initiator concentration, there is no effect on reaction rate despite significant changes in water concentration. For samples containing 1 wt% initiator, *Figure 4-11* indicates that over a range of water concentrations from 0 wt% to near saturation for DVE-3 essentially no change in reaction rate, outside of experimental error, is observed. The curve for the sample containing no water has a peak at 4.5 ± 0.4 min. with a width of 3.0 ± 0.2 min., which compares closely to a peak of 4.0 ± 0.2 min., and a width of 2.6 ± 0.2 min. for the sample containing 1.5 wt% water. *Figure 4-12* indicates similar results for samples

containing 5 wt% initiator. The curves in *Figure 4-11* and *Figure 4-12* are averages of several profiles obtained at each water concentration, therefore these average curves are slightly shorter and wider than the original data, however the average curves represent the general shape and provide the correct average time at the peak maximum. These results suggest that during the initial part of the reaction even small concentrations of water are absorbing significant amounts of the heat generated by the polymerization probably through chain transfer reactions with the propagating cations. Chain transfer is further supported by the visibly different polymer properties between samples containing water and those without water. The cured polymers resulting from samples containing water remained tacky while "dry" samples resulted in a tack-free polymer indicating a much higher degree of conversion. PDSC measurements of heat capacity showed that water is not, however, simply acting as a heat sink by increasing the heat capacity of the solution. The heat capacity of samples were essentially constant despite the addition of small weight percents (0.0 % & 1.0 %) of water. Since the initiator in this system is capable of thermally initiating polymerization, it is believed that heat released by this exothermic polymerization increases the reaction rate leading to thermal runaway.[39] As long as the water is capable of absorbing heat from the reaction solution the sharp decrease in fluorescence attributed to thermal runaway is prevented resulting in a slower reaction rate.

4.5. Conclusions

In conclusion, Nelson *et al.* have previously shown that anthracene effectively photosensitizes the cationic polymerization of divinyl ethers initiated with iodonium salts

for wavelengths in the 350 nm range.[18,39,40,41,43] An anthracene fluorescence intensity decay, which was attributed to consumption of the photosensitizer, can be used to monitor the reaction progress.[40] The reaction of "dry" solutions of DVE-3 proceed to completion in under 2.0 seconds, while the presence of no more than a few weight percent of water in the monomer substantially slows the reaction. A sharp reduction in fluorescence intensity was attributed to large temperature increases arising from the heat of polymerization. It was found that increasing the anthracene concentration partially offset the effect of the water in the monomer.

In addition photo-differential scanning calorimetry (PDSC) was used determine the mechanism by which the presence of water slows down the reaction of the cationic photopolymerization of DVE-3. The PDSC method offers a direct way to evaluate the heat generated during a polymerization reaction. The heat of reaction profiles provided by the PDSC were used to monitor the isothermal reaction for samples containing different concentrations of water. However, the reaction system was extremely rapid and highly exothermic, which made DSC measurements particularly challenging. To maintain isothermal reaction conditions, low light intensities and very small sample sizes (0.5 - 1.5 mg) had to be used to increase the reaction time for the divinyl ether photopolymerizations. The DSC results indicated that under isothermal conditions the addition of water did not effect the rate of reaction. This suggests that during the initial part of the reaction even small concentrations of water are absorbing significant amounts of the heat generated by the polymerization probably through chain transfer reactions with the propagating cations. PDSC measurements of heat capacity showed that water is not simply increasing the heat capacity of the solution. As long as the water is capable of

absorbing heat from the reaction solution the sharp decrease in fluorescence attributed to thermal runaway is prevented resulting in a slower reaction rate.

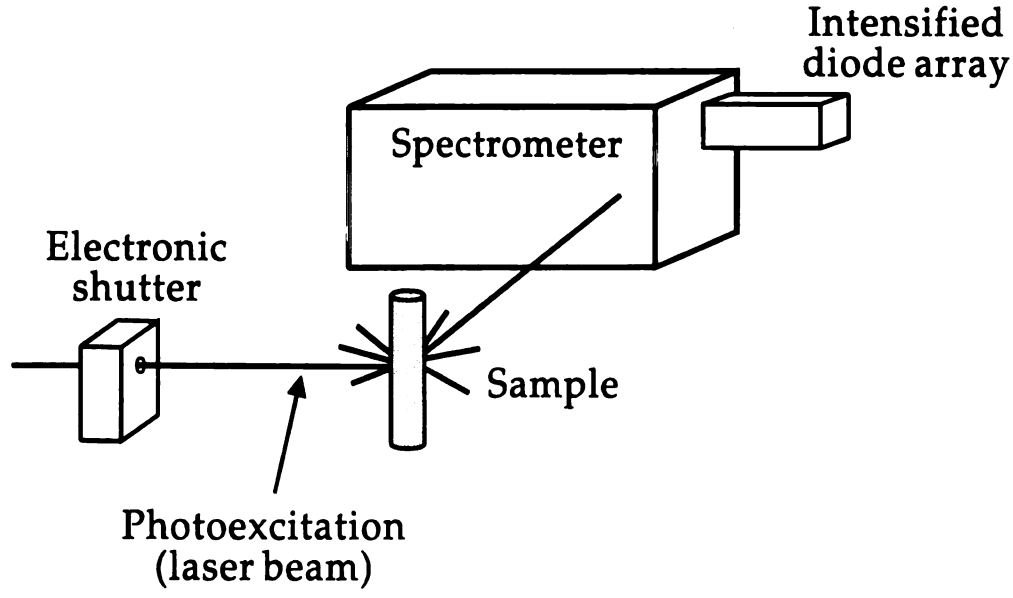

Figure 4-1. *Experimental setup for fluorescence cure monitoring.*

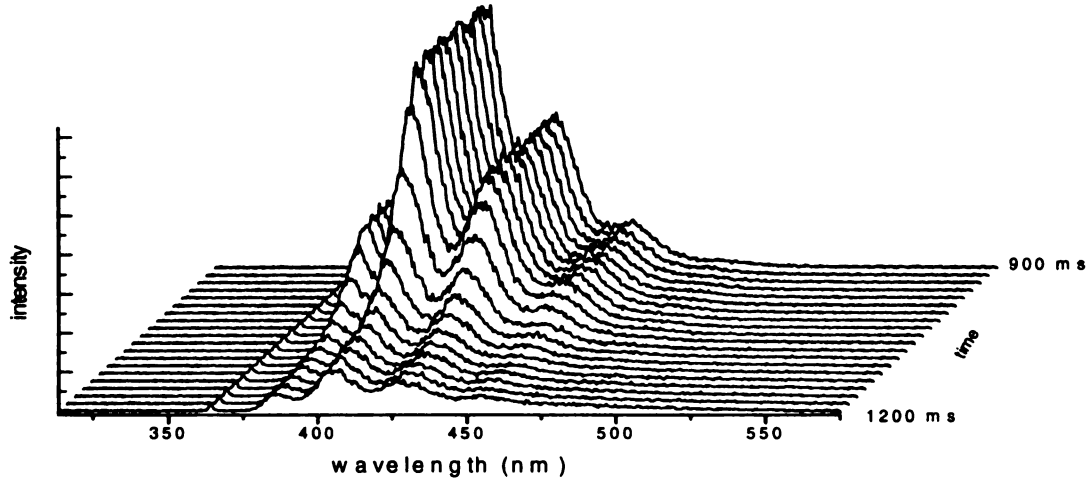

Figure 4-2. *Polymerization of DVE-3 monomer (0.5 wt% initiator) produced by exciting anthracene (2.8 x10^{-2} wt%), at 363.8 nm, and monitored by measuring the intensity of the anthracene fluorescence at time intervals of 17 ms.*[38]

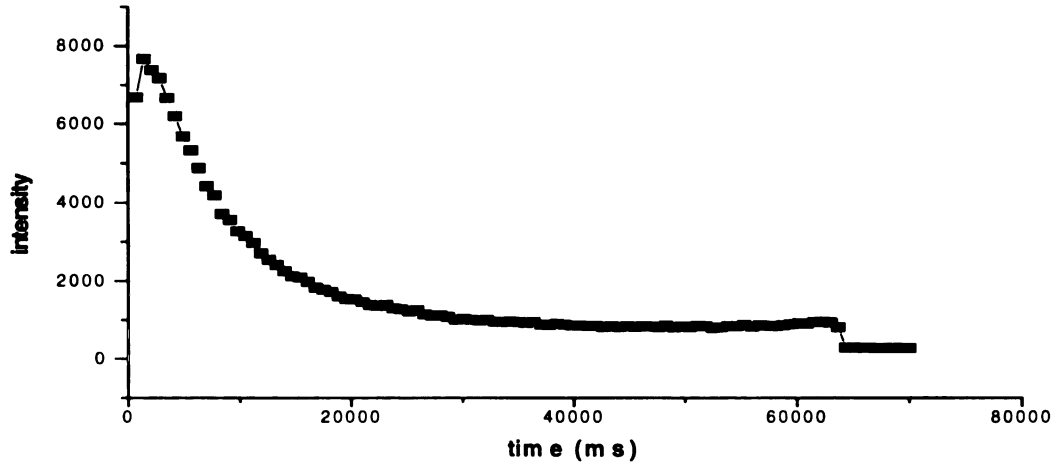

Figure 4-3. *Fluorescence intensity for polymerization of DVE-3 monomer with 1.0 wt% UV9310C, 10^{-2} wt% anthracene, and 2.25 wt% water.*

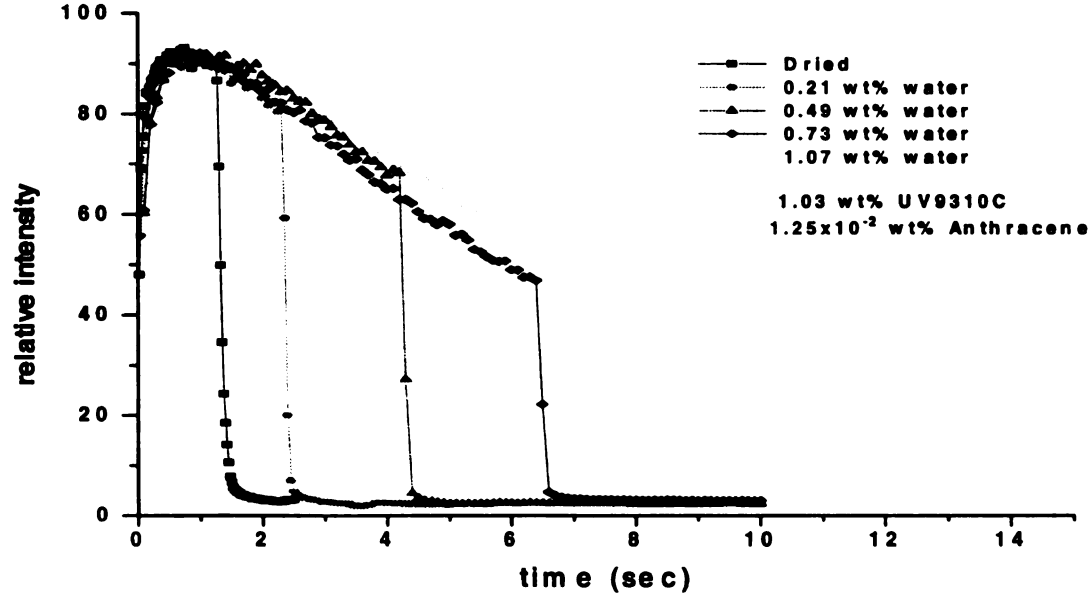

Figure 4-4. *Fluorescence intensity of anthracene as DVE-3 monomer in solution with varying concentrations of water polymerizes.*

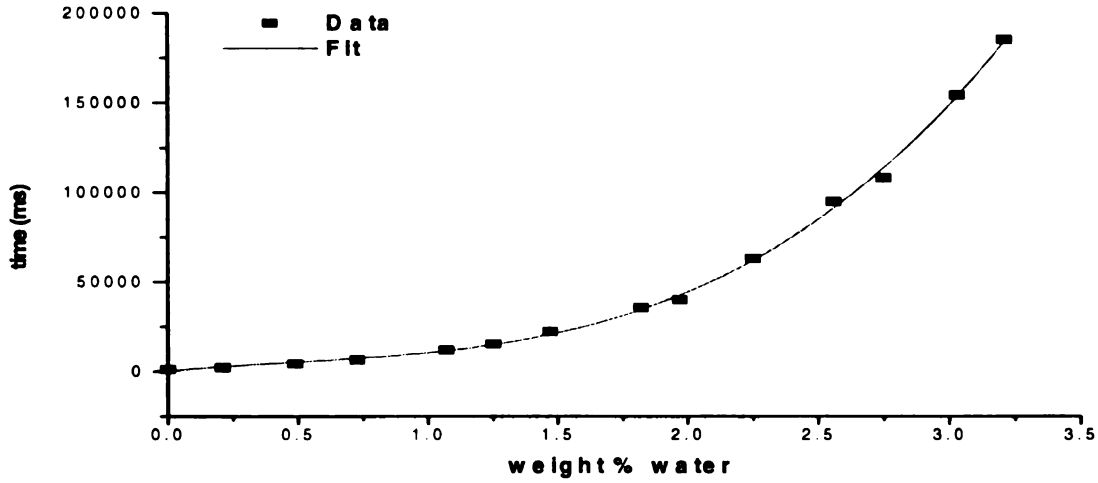

Figure 4-5. *Time for fluorescence decay of 10^{-2} wt% anthracene for the polymerization of DVE-3 with 1.0 wt% UV9310C and varying wt% water.*

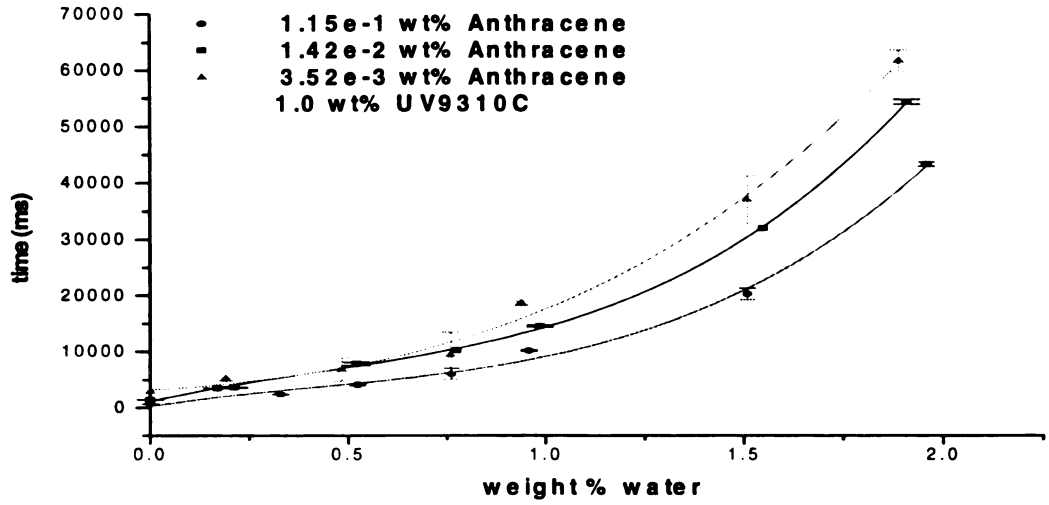

Figure 4-6. *Time for fluorescence decay of anthracene at 10^{-1}, 10^{-2}, and 10^{-3} wt% for the polymerization of DVE-3 with 1.0 wt% UV9310C and varying wt% water.*

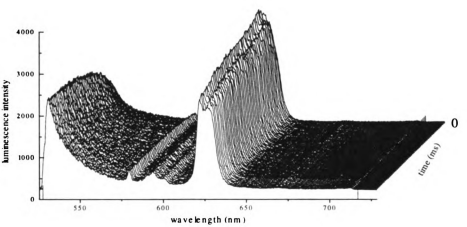

Figure 4-7. *Time-resolved, temperature-dependent luminescence of $Eu(hfa)_3$ (0.01 wt %) in DVE-3, photosensitized by 0.001 wt % anthracene. Polymerization was initiated with 15mW of 351 nm laser light.*

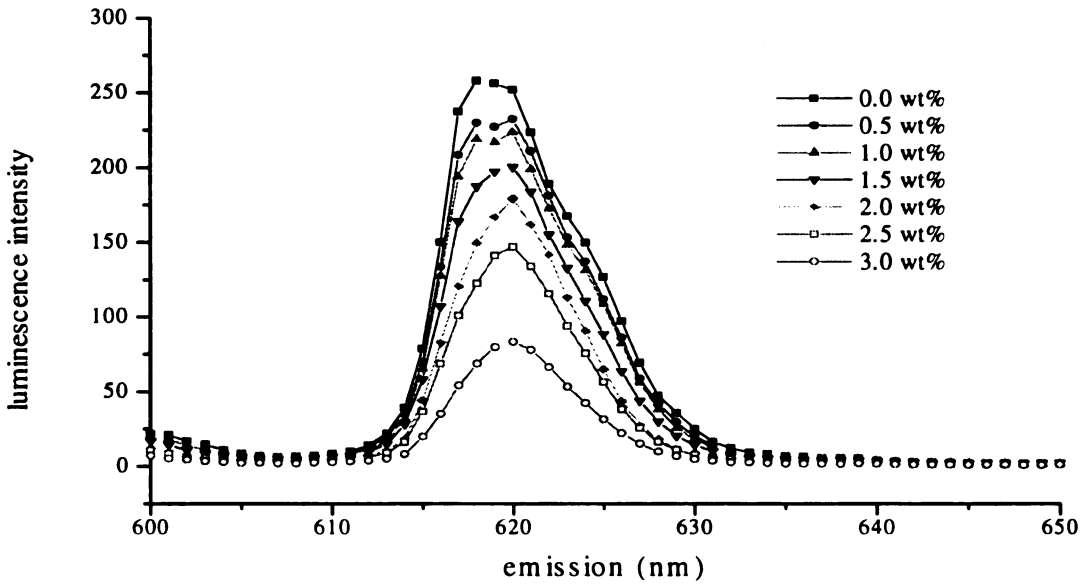

Figure 4-8. *Luminescence intensity of $Eu(hfa)_3$ (0.01 wt %) in DVE-3 monomer photosensitized with 0.001 wt % anthracene at 25 °C with various amounts of water.*

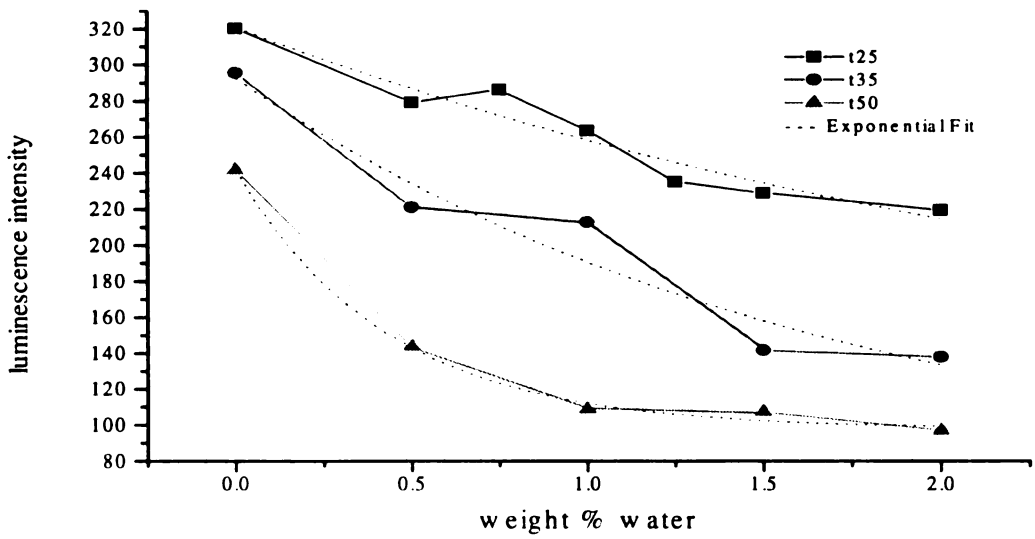

Figure 4-9. *Dependence of the luminescence intensity of Eu(btfa)3 (0.01 wt %) in DVE-3 photosensitized with 0.001 wt % anthracene on the weight percent of water at various temperature.*

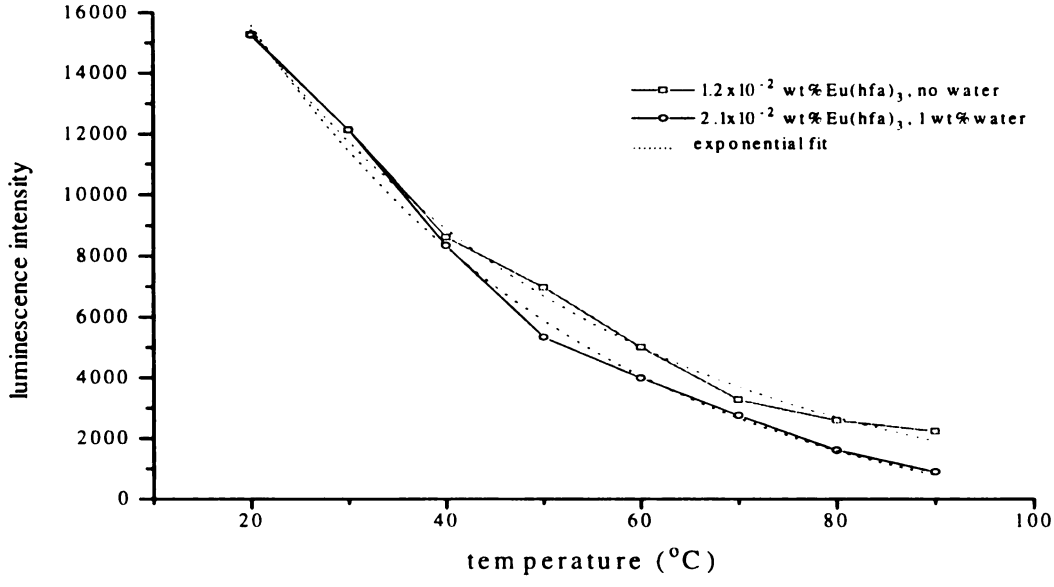

Figure 4-10. *Shift in the temperature calibration curve for $Eu(hfa)_3$ in DVE-3 photo-sensitized with 0.001 wt % anthracene due to the presence of water.*

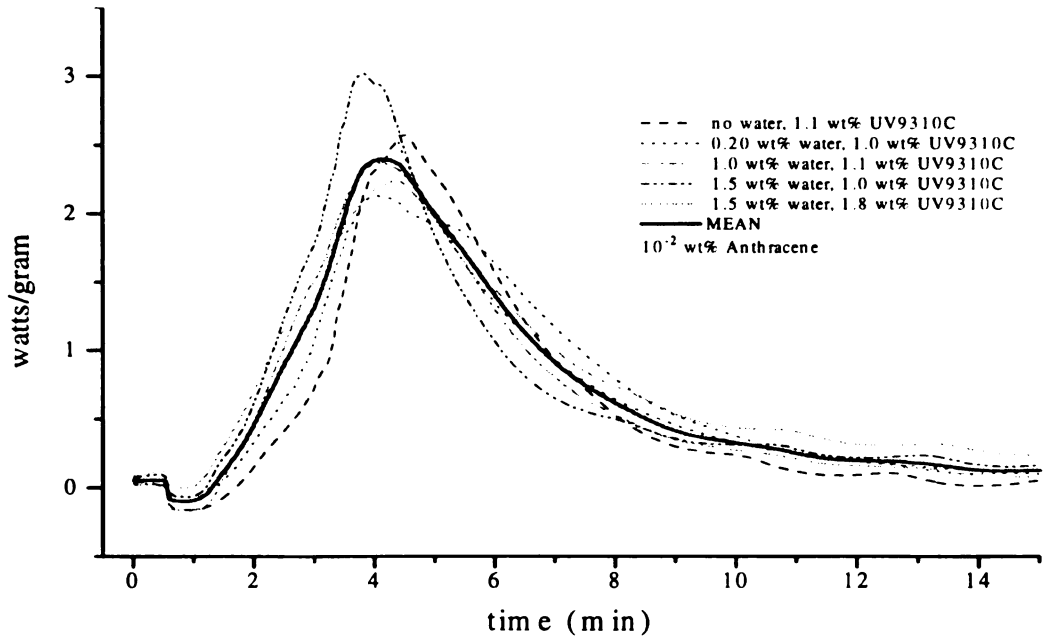

Figure 4-11. *Averaged PDSC results from isothermal (30°C) photopolymerizations of DVE-3 photosensitized with anthracene, containing 1 wt % initiator, and various concentrations of water.*

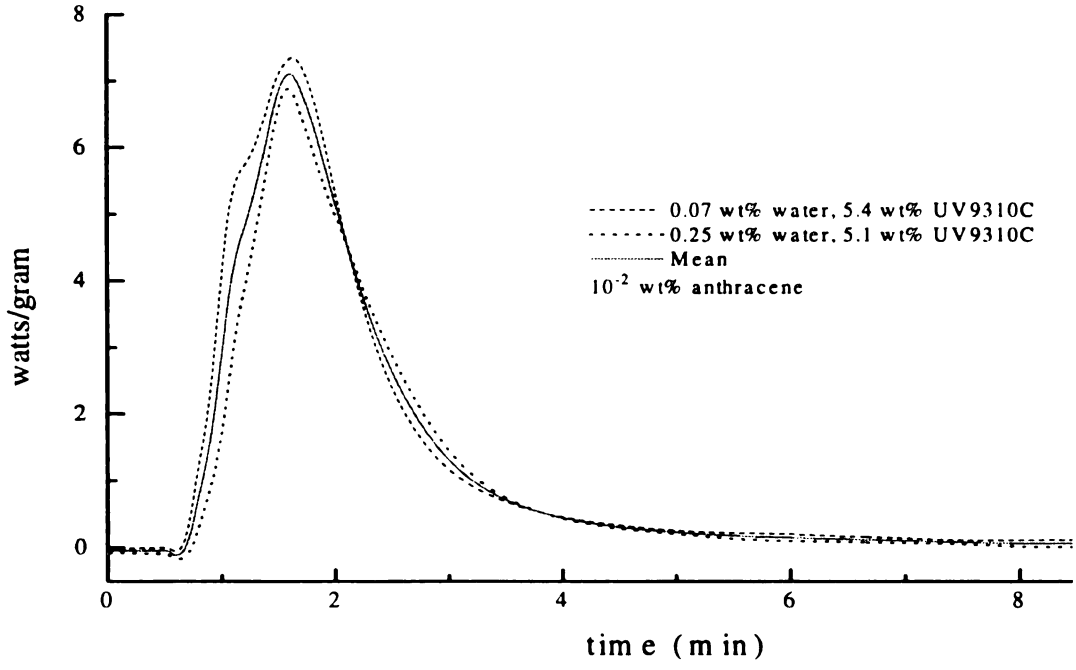

Figure 4-12. *Averaged PDSC results from isothermal (30oC) photopolymerizations of DVE-3 photosensitized with anthracene, containing 5 wt% initiator, and different concentrations of water.*

4.6. References

1. Kloosterboer, J.G., "Network Formation by Chain Crosslinking Photopolymerization and Its Applications in Electronics", *Adv. Polym. Sci.*, **84**, 1 (1988).

2. Roffey, C.G., *Photopolymerization of Surface Coatings,* Wiley, New York, 1981.

3. Pappas, S.P., "Photoinitiators," *UV Curing, Science and Technology,* Technology Marketing Corporation, Norwalk, CT, **2**, 1985.

4. Crivello, J.V., "Cationic Polymerization ---- Iodonium and Sulfonium Salt Photoinitiators," Adv. Polym. Sci., 62, 1 (1984).

5. Lapin, S.P., "Radiation-Induced Cationic Curing of Vinyl-Ether-Functionalized Urethane Oligomers", *Radiation Curing of Polymeric Materials;* Hoyle C.E.; Kinstle J.F., Ed.; ACS Symposium Series, American Chemical Society, Washington D.C., **417**, 363 (1989).

6. Reiser, A., *Photoreactive Polymers,* Wiley, New York, NY, 1989.

7. Pappas, S.P., "Photoinitiation of Cationic and Concurrent Radical-cationic Polymerization. Part V," *Prog. Org. Coat.*, **13**, 35 (1985).

8. Watt, W.R., "Photosensitized Epoxides as a Basis for Light-Curable Coatings," *Epoxy Resin Chemistry*; Bauer, R.S., Ed.; ACS Symposium Series, American Chemical Society, Washington D.C., **114**, 17 (1979).

9. Crivello, J.V.; Lam, J.H.W., "The Photoinitiated Cationic Polymerization of Epoxy Resins", *Epoxy Resin Chemistry*; Bauer,R.S., Ed.; ACS Symposium Series, American Chemical Society, Washington D.C., **114**, 1 (1979).

10. Crivello, J.V. *Organic Coatings, Science and Technology;* Parfitt, G.D.; Patsis, A.V., Ed., Marcel Dekker, Inc., New York, NY, **5**, 35 (1983).

11. Loshe, F.; Zweifel, H., *Adv. Polym. Sci.*, **78**, 61 (1986).

12. Crivello, J.V.; Conlon, D.A., "Aromatic Bisvinyl Ethers: A New Class of Highly Reactive Thermosetting Monomers," *J. Polym. Sci., Polym. Chem.*, **21,** 1785 (1983).

13. Crivello, J.V.; Lee, J.L., "Alkoxy-Substituted Diaryliodonium Salt Cationic Photoinitiators," *J. Polym. Sci., Polym. Chem.*, , **27**, 3951 (1989).

14. Crivello, J.V., "Recent Progress in the Design of New Photoinitiators for Cationic Polymerization," *Cationic Polymerization and Related Processes;* Goethals, E.J., Ed.; IUPAC, Oxford, UK, 289, 1984.

15. Sundell, P-E.; Jonsson, S.E.; Hult, A., "Photo-Redox Induced Cationic Polymerization of Divinyl Ethers," *J. Polym. Sci., Polym. Chem.*, **29**, 1525 (1991).

16. Anderson, V.S.; Norrish, R.G.W., "The Polymerization of Styrene Sensitized by Molecules in the Triplet State," *Proc. Roy. Soc. (London),* **51**, 1 (1959).

17. Manivannan, G.; Fouassier, J.P., "Primary Processes in the Phtotsensitized Polymerization of Cationic Monomers," *J. Polym. Sci., Polym. Chem.*, **29**, 1113 (1991).

18. Nelson, E.W.; Carter, T.P.; and Scranton, A.B., "Photosensitization of Cationic Photopolymerizations by Anthracene and its Derivatives," *Proc. ACS Polym. Mat. Sci. and Eng.*, **69**, 363 (1993).

19. Crivello, J.V., "The Synthesis and Cationic Polymerization of Novel Epoxide Monomers," *Polymer Eng. and Sci.*, **32**, 1462 (1992).

20. Crivello, J.V.; Lee, J.L., "The Synthesis, Characterization, and Photoinitiated Cationic Polymerization of Silicon-Containing Epoxy Resins," *J. Polym. Sci., Polym. Chem.*, **28**, 479 (1990).

21. Decker, C.; Moussa, K., "Real-Time Monitoring at Ultrafast Curing By UV-Radiation and Laser Beams," *J. Coatings Tech.*, **62**, 55 (1990).

22. Kloosterboer, J.G.; Lijten, G.F.C.M., *Cross-Linked Polymers;* Dickie, R.A.; Labana, S.S.; Bauer, R.S., Ed.; ACS Symposium Series 367; ACS: Washington DC, 1987.

23. Crivello, J.V.; Lee, J.L.; Conlon, D., "Photoinitiated Cationic Polymerization with Multifunctional Vinyl Ether," *J. Rad. Curing*, **6** (1983).

24. Decker, C.; Moussa, K., "Real-Time Kinetic Study of Laser-Induced Polymerization," *Macromolecules*, **22**, 4455 (1989).

25. Wang, F.W.; Pummer, W.J.; Fanconi, B.M.; Wu, En-Shinn, "Fluorescence Monitoring of Viscosity and Chemical Changes During Polymerization," *Photophysics of Polymers*; Hoyle, C.E.; Torkelson, J.M., Ed.; American Chemical Society, Washington D.C., 1987.

26. Wang, F.W.; Lowry, R.E.; Fanconi, B.M., "Novel Fluorescence Method for Cure Monitoring of Epoxy Resins," *Polymer*, **27**, 1529 (1986).

27. Stroeks, A; Shorhun, M.; Jamieson, A.M.; Shimha, R., "Cure Monitoring of Epoxy Resins by Excimer Fluorescence," *Polymer*, **29**, 467 (1988).

28. Wang, F.W.; Lowry, R.E.; Grant, W.H., "Novel Excimer Fluorescence method for Monitoring Polymerization: 1. Polymerization of Methyl Methacrylate," *Polymer*, **25**, 690 (1984).

29. Scarlata, S.F.; Ors, J.A., "Fluorescence Polarization: A Method to Monitor Polymer Cure," *Polymer Comm.*, **27**, 41 (1986).

30. Sung, C.S.P.; Chin, I-J.; Yu, W-C., "A Novel Fluorescence Technique for Monitoring Cure Reactions in Epoxy Networks," *Macromolecules*, **18**, 1512 (1985).

31. Sung, C.S.P.; Pyun, E.; Sun, H-L., "Characterization of EpoxyCure by UV-Visible and Fluorescence Spectroscopy: Azochromophoric Labeling Approach," *Macromolecules*, **19**, 2922 (1986).

32. Song, J.C.; Sung, C.S.P., "Intrinsic Phosphorescence of Curing Agent for Cure Characterization of Epoxy Composites," *ACS PMSE Proceedings*, **67**, 497 (1992).

33. Song, J.C.; Sung, C.S.P., *ACS Polymer Preprints*, **32:3**, 362 (1991).

34. Bondi, A., "Estimation of The Heat Capacity of Liquids," *I & E C Fundamentals*, **5**, 442 (1966).

35. Jonsson, S.; Sundell, P-E.; Hult, A., "Photoredox Induced Cationic Polymerization of Divinyl Ethers," *Radtech 90-North America, Radiation Curing Conference and Exposition Proceedings*, 417 (1990).

36. Allen P.E.M.; Patrick C.R., *Kinetics and Mechanisms of Polymerizatin Reactions*, John Wiley and Sons, New York, 79, 1974.

37. *Encyclopedia of Polymer Science and Engineering, Second Edition*, Kroschwitz, J.I., Ed., **17**, 453, 1989.

38. Nelson, E.W.; Carter, T.P.; Scranton, A.B., "Fluorescence Monitoring of Cationic Photopolymerizations: Divinyl Ether Polymerizations Photosensitized by Anthracene Derivatives," *Macromolecules*, **27**, 1013-1019 (1994).

39. Nelson, E.W.; Jacobs, J.L.; Scranton, A.B.; Anseth, K.S.; Bowman, C.N., "Photo-differential Scanning Calorimetery Studies of Cationic Polymerizations of Divinyl Ethers," *Polymer*, in press.

40. Nelson, E.W.; Carter, T.P.; Scranton, A.B., "Fluorescence Monitoring of Cationic Photopolymerization of Divinyl Ethers Photosensitized by Anthracene." *Polymer Preprints - ACS Division of Polymer Chemistry*, **34**, 779 (1993).

41. Nelson, E.W.; Carter, T.P.; Scranton, A.B., "The Role of the Triplet State in the Photosensitization of Cationic Polymerizations by Anthracene," *J. Polym. Sci., Polym. Chem.*, **33**, 247 - 256 (1995).

42. Alpha, B.; Ballardini, R.; Balzani, V.; Lehn, J.-M.; Perathoner, S.; Sabbatini, N., "Antenna Effect in Luminescent Lanthanide Cryptates: A Photophysical Study," *Photochemistry and Photobiology*, **52**, *2*, 299-306 (1990).

43. Jacobs, J.L.; Nelson, E.W.; Scranton, A.B., "Use of Fluorescence to Monitor Temperature and Observe the Water Effects of Cationic Photopolymerization of Divinyl Ethers Photosensitized by Anthreacene," *Proc. ACS Polym. Mat. Sci. and Eng.*, **70**, 74 (1994).

44. Kennedy, J. P.; Marechal, E., *Carbocationic Polymerization*, John Wiley & Son, New York, 1982.

45. Doornkamp, T.; Tan, Y. Y., *Polymer Commun.*, **31**, 362 (1990).

46. Kloosterboer, J. G.; Lijten, G.F.C.M., *Polymer*, **28**, 1149 (1987).

47. Anseth, K. S.; Wang, C. M.; Bowman, C. N., "Kinetic Evidence of Reaction Diffusion during the Polymerization of Multi(meth)acrylate Monomers," *Macromolecules*, **27**, 650 (1994).

48. Anseth, K. S.; Wang, C. M.; Bowman, C. N., "Reaction Behavior and Kinetic Constants for Photopolymerizations of Multi(meth)acrylate Monomers," *Polymer*, **35**, 3243 (1994).

CHAPTER 5. TEMPERATURE-SENSITIVE LUMINESCENCE OF EUROPIUM PROBES

5.1. Temperature-Sensitive Luminescence of Europium Probes

Introduction. Cationic photopolymerizations of divinyl ethers have received considerable attention in recent years (for example, see references 1-5). These solvent-free systems rapidly produce polymer films which exhibit exceptional clarity, adhesion, abrasion resistance, and chemical resistance.[6-8] Moreover, divinyl ether monomers have excellent rheological properties and low vapor pressure, making them attractive for applications as films and coatings. For example, the cationic photopolymerization of the divinyl ether, 3,6,9,12-tetraoxatetradeca-1,13-diene (DVE-3), proceeds very quickly to produce a highly crosslinked polymer with excellent chemical and abrasion resistance. This monomer also has a particularly low viscosity, which facilitates processing and handling. In addition, DVE-3 is attractive because of its low toxicity as compared to acrylate monomers, which are used in similar applications. Finally, the rapid reaction rate of these polymerizations allows for their use in compact continuous flow process lines.

Most of the early work on cationic photopolymerizations focused on the identification and synthesis of appropriate monomers and initiators (for reviews see references 9 and 10). Not until recently have the detailed studies of the reaction been reported.[4,11] For example, in a previous contribution[11] Nelson *et al.* reported a novel *in situ* laser-induced fluorescence technique for monitoring the initiation reaction in these high-speed polymerizations. Due to its extremely short intrinsic time scale, the fluorescence technique provided a means to characterize the kinetics of these

polymerizations which proceed too rapidly to be monitored by traditional methods such as differential scanning calorimetry (DSC). These studies indicate that although the reactions are extremely rapid (the systems typically react to completion in a few seconds), most of the conversion occurs in the last 100 milliseconds due to a dramatic increase in the reaction rate. Nelson *et al.* attributed this characteristic reaction profile to thermal runaway resulting from the large amount of heat released by the rapidly polymerizing system.

The objective of this contribution is to verify the importance of thermal runaway by monitoring the temperature *in situ* during cationic photopolymerizations of DVE-3. Because these studies are complicated by the rapid rate at which the reaction takes place as well as the thin-film geometry and the need for an optically-transparent, noninvasive probe, traditional methods of temperature monitoring are inadequate. For example, thermocouples are invasive, opaque, and even in their smallest form, have a size-scale comparable to the film thickness. Raman spectroscopy could theoretically be used to determine temperature by comparison of the magnitudes of the Stokes and the anti-Stokes lines. However Raman is characterized by an inherent signal weakness and is often obscured by sample fluorescence. Luminescence techniques for temperature monitoring have also been reported in the literature.[12] For example, temperature-sensitive excimer formation,[13] and a second technique based upon temperature-induced spectral shifts[12] have been used to characterize temperature in fuel sprays, and organic solvents. However these techniques are not applicable to polymerizing systems because they are sensitive to changes in viscosity.

In this chapter, a luminescence scheme is reported for *in situ* monitoring of temperature during cationic photopolymerizations of DVE-3 photosensitized by anthracene. Due to its short intrinsic time scale, luminescence techniques are attractive for monitoring the local temperature of these reactions which may proceed to completion in a few seconds. Furthermore, luminescence techniques provide a non-intrusive method for monitoring the temperature since trace amounts of the luminescence probe may be readily incorporated into the reaction mixture. Tris(β-diketone) chelates of europium fulfill the requirements of a temperature-dependent luminescence probe for our studies. As described in the remainder of this paper, these probes exhibit a linear response for a wide temperature range, and are insensitive to changes in viscosity. In addition, the excitation wavelength of these probes is ideally suited for our studies.

Probe Requirements. In addition to exhibiting a temperature-dependent response, the luminescence temperature probe for our studies must meet specific spectral requirements. Anthracene, which absorbs between 320 and 390 nm, was used as a photosensitizer to expand the initiating window to the near-visible region of the spectrum. The anthracene photosensitizer makes it possible to initiate polymerization in the near-UV or visible wavelengths as a result of a direct interaction between an excited state of a photosensitizer and the initiator.[11] In our experiment, 351 nm or 364 nm ultraviolet (UV) light was used to initiate the photopolymerization. Therefore, these wavelengths are the most convenient for excitation of the temperature probe, since they would eliminate the need for two laser beams. In addition, the emission wavelengths of the temperature probe must not overlap with the fluorescence of the anthracene photosensitizer in the 425 nm region.

A class of compounds which satisfies both spectral requirements is the lanthanide substituted tris(β-diketone) chelates, which absorb from 280 to 380 nm[14] and emit in the 620 nm range.[15] These compounds exhibit an interesting "antenna" effect which is responsible for the temperature dependence of the luminescence. The light absorption by the lanthanide itself is very weak, however the ligand plays the role of an antenna by absorbing light and efficiently transferring the excitation energy to the metal ion.[16] This non-radiative intramolecular transfer from the excited state of the ligand to the highly luminescent europium metal center results in a number of interesting luminescent properties. A number of authors[13,15-19] have characterized the chemical and photophysical properties of these chelates. These authors found that the luminescence efficiency varies greatly with the identity of the ligand, degree of coordination, temperature, and solvent.[14,16] Sager *et. al* reported that the underlying photophysical process proceeds by the following four-step mechanism: (1) ground singlet absorption to the excited singlet state; (2) radiationless intersystem crossing from the excited singlet to the lowest lying triplet state; (3) transfer of energy to the chelated ion; and (4) characteristic ionic fluorescent emission.[14]

5.1a. Experimental

Materials. The monomer, 3,6,9,12-tetraoxatetradeca-1,13-diene (DVE-3), photosensitizer, and the anthracene were purchased from Aldrich Chemical Co. The monomer was dried over molecular sieves to remove any traces of water and the photosensitizer was used as received. The cationic initiator (UV9310C-GE Silicones)

had a composition of 5-10 wt % linear alkylate dodecylbenzene, ~50 wt % 2-ethyl-1,3-hexanediol, and ~50 wt % bis(4-dodecylphenyl)iodonium hexafluoroantimonate. The initiator concentrations specified in the remainder of this paper correspond to the total UV9310C concentration.

A free radical polymerization system was used to identify any viscosity dependencies of the temperature probes. The monomer, 2-hydroxethyl acrylate (HEA), was purchased from Aldrich Chemical Co. This system was polymerized in solution with N,N-dimethyl-formamide (DMF) in order to maintain optical clarity. The initiator for this polymerization was 2,2-azobisisobutyronitrile (AIBN), purchased from Polyscience Inc.

Synthesis of Temperature Probes. The temperature probes under primary investigation were tris(benzoyl-1,1,1-trifluoroacetone) europium ($Eu(btfa)_3$), and tris(1,1,1,5,5,5-hexafluoroacetylacetone) europium ($Eu(hfa)_3$). Both of these probes were synthesized as described below. The ligands 1,1,1,5,5,5-hexafluoroacetylacetone (hfa) and benzoyl-1,1,1-trifluoroacetone (btfa) were purchased from Lancaster Synthesis Inc., and the europium (III) chloride hexahydrate was purchased from Aldrich Chemical. The europium compound was added to approximately 50 ml of distilled water. The pH was increased to 8.5 by the addition of ammonium hydroxide. As the europium solution was stirred, a stoichiometric amount of the ligand was added. After allowing the solution to react over night with stirring, the precipitate was filtered and dried for 24 hours at 70°C. This procedure was based on modifications of those reported in references 14,15,17-19.

Absorption and Luminescence Measurements. Absorption spectra of monomers, initiators, photosensitizers, and luminescent temperature probes were

obtained using a Hewlett Packard UV-vis 8452A diode-array spectrophotometer. For the temperature studies, the luminescence was monitored using an Aminco-Bowman Series 2 Luminescence Spectrometer. The excitation frequencies were varied from 340 to 364 nm. Based upon the absorption spectrum of each lanthanide chelate, the optimum concentration for measuring the luminescence was determined. A concentration that absorbed too strongly would result in an artificially low luminescence reading, due to a shorter path length resulting from the low penetration depth into the sample. The temperature was controlled with a Polyscience 9100 refrigerated constant-temperature circulator connected to a jacketed cuvette holder inside the luminescence spectrometer. A mixture of ethylene glycol and water was used as the heating fluid.

The luminescence monitoring of the temperature probes *in situ* during the cationic photopolymerization was performed in the MSU *LASER* laboratory. The luminescent temperature probe and cationic photopolymerization reaction were both excited with a Coherent Innova 200 Argon ion laser tuned at either 363.8 or 351.1 nm. A Newport 845HP-01 digital shutter system was opened with an electric pulse from the multichannel analyzer, ensuring that the illumination and the acquisition were started simultaneously. Fifteen milliwatts of unfocused laser radiation (measured with a Scientech 362 Power/Energy meter) in an ~3 mm dia. beam was directed on to the quartz capillary tube containing the sample. The sample geometry and instrument set-up have been described in further detail in an earlier publication.[11] The quartz capillary was approximately 2.5 cm in length with an inner diameter of 1 mm and an outer diameter of 2 mm. The fluorescent light was collected at an angle of 90° from the incident beam and 90° from the

longitudinal axis of the quartz tube. The temperature of the sample was controlled by a jacketed tube holder coupled to a thermostated water bath.

The luminescence signal was collected using a Spex 1877 Triplemate spectrometer with a subtractive dispersion filter stage and a spectrograph stage. An EG&G Princeton Applied Research Model 1530-C/CUV CCD detector, cooled to -120 °C to minimize dark charge levels, was used to detect the signal. The data was analyzed with an EG&G Princeton Applied Research Model OMA IV detector controller. Luminescence spectra spanning 50 to 100 nm centered at 620 nm were collected with 150 groove/mm gratings in both the filter and spectrograph stages. These spectra were typically collected in intervals of 50 ms.

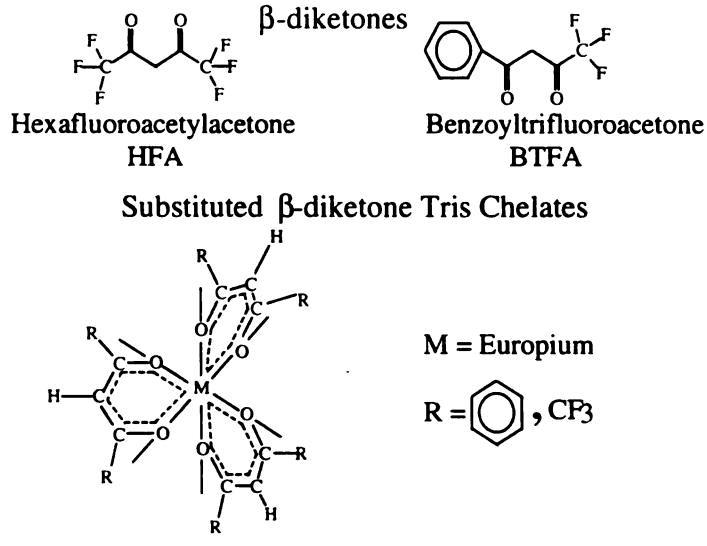

Figure 5-1. *The structure for the two lanthanide β-diketone chelates, $Eu(btfa)_3$ and $Eu(hfa)_3$.*

5.1b. Results & Discussion

Probe Selection. The two most promising temperature sensitive luminescence probes, $Eu(hfa)_3$ and $Eu(btfa)_3$, were selected based on their ability to meet the system requirements. The structures of these lanthanide β-diketone chelates are shown in *Figure 5-1.* In these chelates six of the nine coordination sites are occupied by organic ligands and the remaining three sites are occupied by water molecules. The choice of the organic ligand is important since it determines the absorption wavelength and helps to impart solubility in the monomer. These two chelates meet the solubility and spectral requirements for our studies.

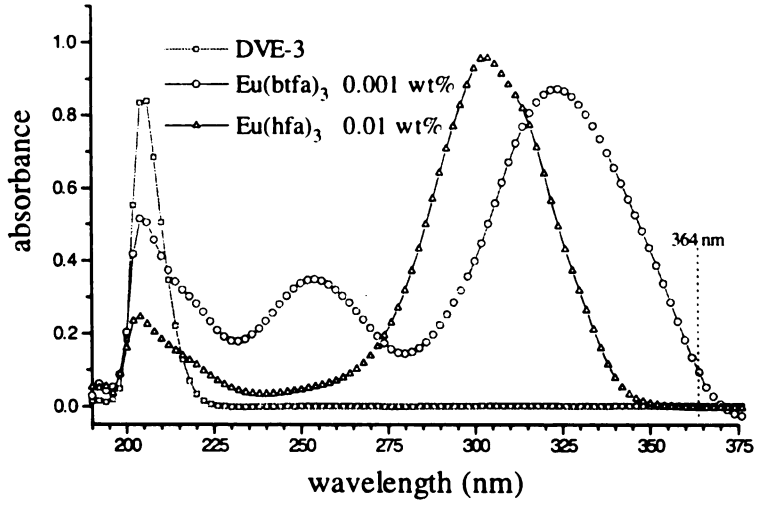

Figure 5-2. *Absorption spectra of $Eu(btfa)_3$ (0.001 wt %), $Eu(hfa)_3$ (0.01 wt %), and DVE-3 in methanol.*

The absorbance spectra of $Eu(btfa)_3$ and $Eu(hfa)_3$ are shown in *Figure 5-2*. The figure illustrates that the extinction coefficient of $Eu(btfa)_3$ is an order of magnitude larger than that of $Eu(hfa)_3$. In addition, the $Eu(btfa)_3$ spectrum is shifted toward the red compared to the $Eu(hfa)_3$ spectrum, and absorbs much more strongly then $Eu(hfa)_3$ at 364 nm. While it may appear that the 364 nm $Eu(hfa)_3$ absorbance is too low to produce

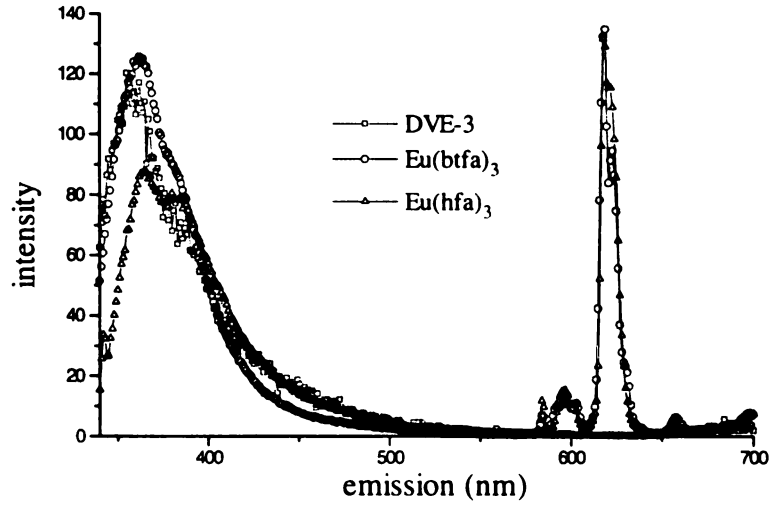

Figure 5-3 *Luminescence spectra of $Eu(btfa)_3$ (0.001 wt %) and $Eu(hfa)_3$ (0.01 wt %) in DVE-3 and of DVE-3.*

strong luminescence, $Eu(btfa)_3$ at 0.001 wt % and $Eu(hfa)_3$ at 0.01 wt % were found to have similar luminescence intensities (*Figure 6-3*). Due to its stronger absorption at 351 nm, the $Eu(hfa)_3$ emits a more intense signal when excited at this wavelength. Therefore the characterization of the cationic photopolymerizations was carried out using 351 nm as the excitation wavelength.

For the DVE-3 reaction system, it is important that the luminescence from the temperature probe does not overlap with the fluorescence signal from the anthracene photosensitizer (380-500 nm). For $Eu(btfa)_3$ and $Eu(hfa)_3$ the temperature sensitive emission peak occurs at around 620 nm (*Figure 5-3*), and therefore does not overlap with the anthracene peak. The fluorescence in the 375 nm range in *Figure 5-3* was attributed

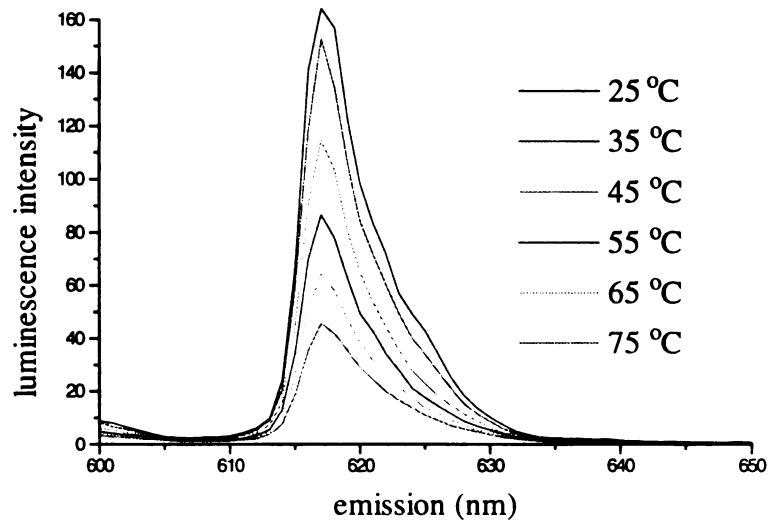

Figure 5-4. *Luminescence spectra at varying temperatures for $Eu(btfa)_3$ at 0.001 wt % in DVE-3, excited at 364 nm.*

to the organic ligands and does not change with temperature. As described earlier, the energy transfer from the organic ligands to the metal center becomes less effective, and the luminescence of the metal center decreases, as the temperature of the system increases.

Temperature Studies. The temperature-dependent luminescence of $Eu(btfa)_3$ in the monomer is shown in *Figure 5-4*. The figure illustrates that, as expected, an increase

in the temperature leads to a decrease in the luminescence intensity. A plot of the luminescence intensity at 618 nm (peak maximum) versus temperature, is shown in *Figure 5-5*. This intensity varies linearly with temperature (the correlation coefficient is 0.9976) and may therefore be used to estimate the temperature of a system if the measurement is performed using the same experimental conditions (concentrations and instrument settings).

The temperature-dependent luminescence of $Eu(hfa)_3$ is shown in *Figure 5-6*. Again, the luminescence intensity decreases with increasing temperature, however in contrast to the $Eu(btfa)_3$ profiles discussed above, the $Eu(hfa)_3$ luminescence exhibits two distinctive peaks centered at 618 and 622 nm. The intensities of these peaks undergo an inversion in relative intensity with the 622 nm peak exhibiting a larger intensity at low temperatures and the 618 nm peak exhibiting a higher relative intensity at high

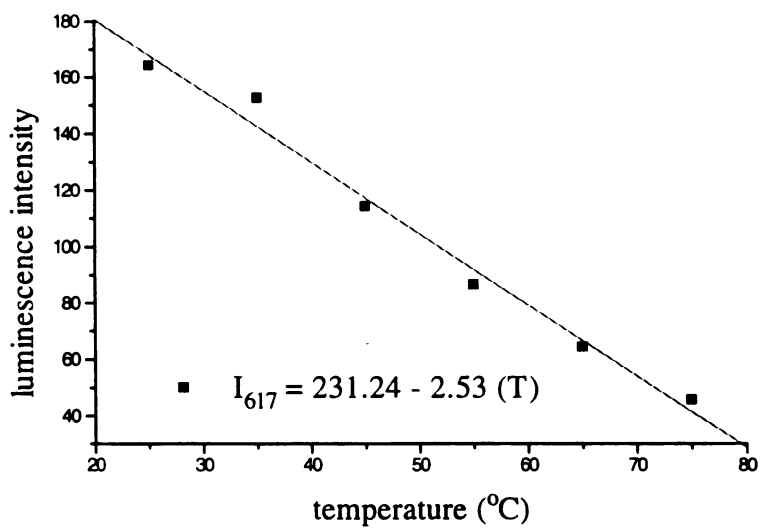

Figure 5-5. *The luminescence intensity of $Eu(btfa)_3$ at an emission of 617 nm plotted at different temperatures, resulting in a linear calibration curve.*

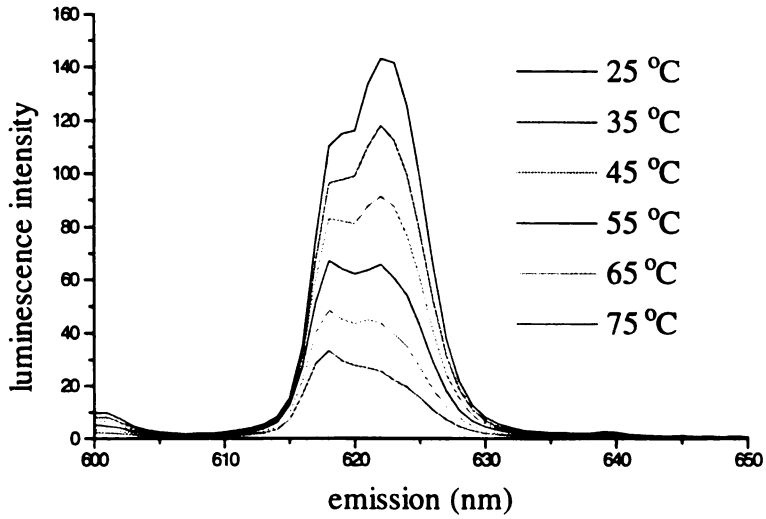

Figure 5-6. *Luminescence spectra at varying temperatures for $Eu(hfa)_3$ at 0.01 wt % in DVE-3 excited at 340 nm.*

temperatures. Equations 5-1 and 5-2 illustrate the linear dependence of each peak intensity on temperature (the correlation coefficients are 0.99849 and 0.99788 for the 618 and 622 nm peaks respectively).

$$I_{618} = 150 - 1.6(T) \qquad \text{Eq. 5-1}$$

$$I_{622} = 200 - 2.4(T) \qquad \text{Eq. 5-2}$$

To take advantage of the inversion in the relative intensities of the two peaks, a detector-insensitive calibration was developed based upon an intensity ratio defined as the intensity of the 618 nm peak divided by the modified intensity of the 622 nm peak (see *Figure 5-7*). As shown in the figure, a plot of the resulting intensity ratio versus reciprocal temperature is linear with a correlation coefficient of 0.99997). This calibration curve is independent of operating conditions such as instrument settings since the peaks act as internal standards.

To investigate the effect of elevated temperature on the luminescence of the lanthanide chelates, a series of studies were performed for temperatures ranging from 30 to 130 °C. The resulting luminescence/temperature calibrations for $Eu(hfa)_3$ and $Eu(btfa)_3$ are shown in *Figure 5-8*. As the figure illustrates, the $Eu(hfa)_3$ curve was best fit by a single straight line throughout the entire temperature range, while the $Eu(btfa)_3$ curve was best fit by an exponential decay. Therefore the $Eu(hfa)_3$ probe is better suited for the high temperature studies since it does not lose sensitivity as the temperature is increased. Theoretically this probe should be able to monitor much higher temperatures approaching its degradation temperature. However, since the luminescence intensity decreases as the temperature rises, the maximum measurable temperature is limited by the detector's low-level sensitivity. If the initial temperature is set to the maximum detector reading, the dynamic range of the detector limits the size of the temperature range.

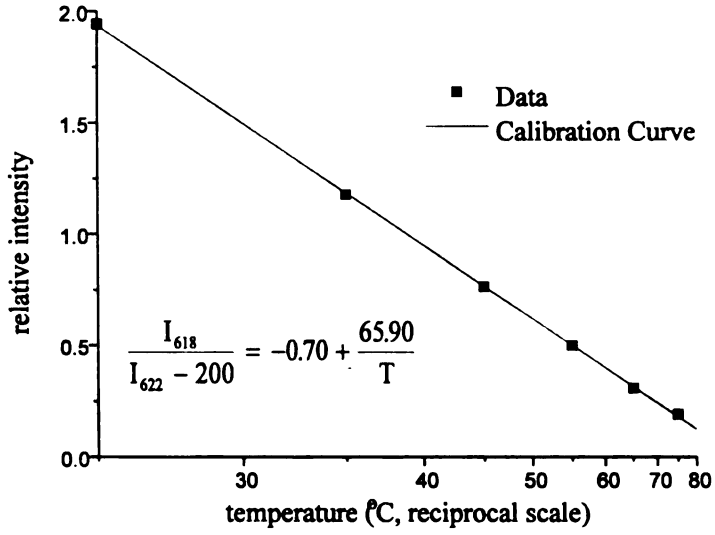

Figure 5-7. *The relative intensity, referring to the intensity of the 618 peak divided by the modified intensity of the 622 peak, of $Eu(hfa)_3$ in DVE-3 (0.01 wt %) plotted versus reciprocal temperature.*

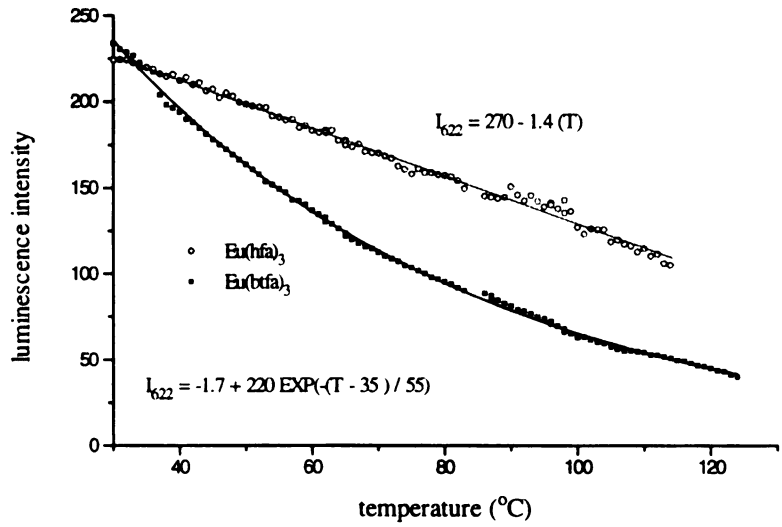

Figure 5-8. *High temperature calibration curves for Eu(btfa)$_3$ and Eu(hfa)$_3$ excited at 364 nm and monitored at an emission of 620 nm.*

Therefore, the maximum effective temperature range is effectively limited by the dynamic range of the instrument.

Viscosity Independence. Many probes which exhibit temperature-dependent luminescence are also sensitive to changes in viscosity.[12] However, a viscosity-dependent response is unacceptable for a luminescent probe used for monitoring temperature during polymerization. These systems undergo a large change in viscosity, and any viscosity-dependent response will likely dominate the desirable temperature-dependence. Therefore, a series of studies were performed to determine whether the luminescence of Eu(hfa)$_3$ and Eu(btfa)$_3$ were sensitive to viscosity. A calibration curve was produced for a liquid monomer system (~2 cps) and compared to a calibration for a solid polymerized system. Therefore, if the calibrations are the same for the two extremes of liquid and solid, the luminescence response is insensitive to viscosity.

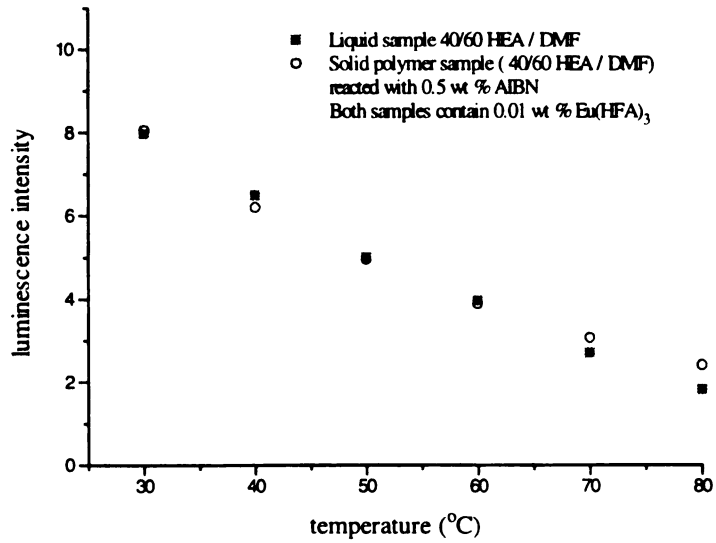

Figure 5-9. *Temperature calibration curves for 0.01 wt % Eu(hfa)$_3$ excited at 351 nm in liquid and solid systems.*

A solution polymerization was chosen for preparing the solid samples to ensure optical clarity and permit easy removal of the polymer from the quartz cuvettes. DMF was chosen as the solvent due to its relatively high boiling point (153 °C) and because the resulting polymer is optically clear. A suitable ratio of monomer to solvent was found to be 40/60. The polymerizations were carried out at a temperature of 65 °C with an initiator concentration of 0.5 wt % and a β-diketone tris chelate concentration of 10^{-2} wt %.

Profiles of luminescence intensity versus temperature for the HEA/DMF system are shown in *Figure 5-9*. When corrected for the presence of the AIBN initiator, the luminescence intensities show good agreement in both the liquid and solid state, indicating that the luminescence-temperature probe Eu(hfa)$_3$ is not sensitive to changes in viscosity. The viscosity independence of the europium probes is not surprising since the temperature dependent energy transfer is internal and should not be effected by the

translational or rotational motion of the molecule. Equivalent viscosity experiments were performed with $Eu(btfa)_3$ yielding similar results.

Inherent System Limitations. The above discussion illustrates the utility of the lanthanide chelates for *in situ* temperature monitoring. These molecular-level probes exhibit a linear temperature dependence over a wide temperature range and, in the case of $Eu(hfa)_3$, may provide a detector-insensitive calibration. However, these systems have several inherent limitations. Perhaps the largest limitation arises from the sensitivity of the luminescent response to solvent. Because water effectively competes with the β-diketones for the coordination sites on the lanthanides, the luminescence is diminished in the presence of water. Therefore these probes cannot be used with any aqueous systems. In DVE-3, the luminescence intensity decreases over a period of days possibly due to the

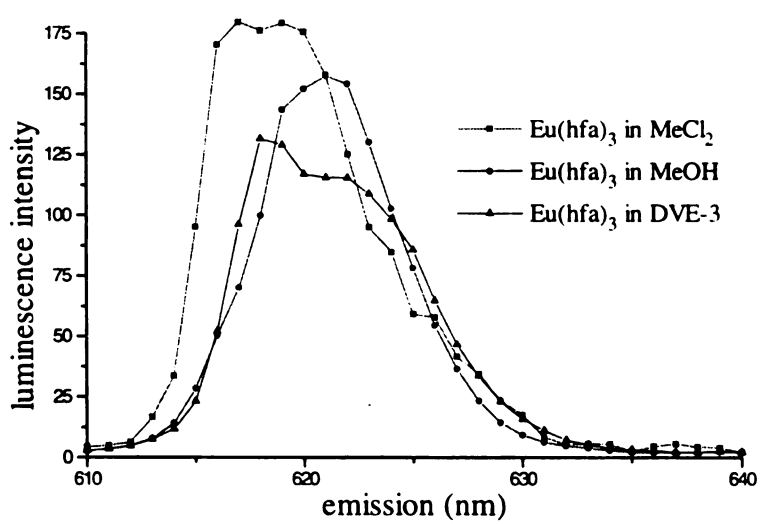

Figure 5-10. *The luminescence of $Eu(hfa)_3$ (0.01 wt %) in methanol, methylene chloride, and DVE-3.*

slow exchange of the ligand and the solvent. In addition, the shape of the luminescence spectra of the chelates is dependent on the solvent. For example, as shown in *Figure 5-10*, the two distinctive $Eu(hfa)_3$ peaks observed in DVE-3 are not present for experiments performed in methanol and methylene chloride. This dependence on solvent necessitates a calibration to be established for each system.

Temperature Profiles for the Cationic Photopolymerizations. Since the luminescence temperature probes were found to be sensitive to changes in temperature but insensitive to viscosity, they were investigated for use in monitoring the reaction temperature during the cationic photopolymerizations of DVE-3. A series of studies was performed to ensure that the lanthanide probes did not affect the polymerization kinetics and that the presence of the initiator and photosensitizer did not disrupt the luminescence response of the temperature probes. The β-diketone tris chelates are electronically neutral, therefore they will not undergo electrostatic interactions with the propagating active centers. However it was anticipated that the lanthanide probes could possibly affect the reaction by interacting with the initiator or the anthracene photosensitizer.

A non-reacting system (a sample containing DVE-3, anthracene, and an europium probe) was tested to determine the time stability of the temperature-sensitive probe. No initiator was added to ensure that the system was non-reactive and remained isothermal when exposed to the beam from the argon ion laser. Essentially no change in luminescence was observed over the time scale of the experiment (30 sec) for both $Eu(hfa)_3$ and $Eu(btfa)_3$. Next, to investigate the effect of the initiator, the temperature-sensitive luminescence of a sample containing hexanol, anthracene, initiator, and an europium probe was monitored. Hexanol was chosen to approximate DVE-3 in this non-

reactive system. The hexanol system was then exposed to the initiating wavelength causing the photosensitization to begin. For both probes ($Eu(hfa)_3$ and $Eu(btfa)_3$), there was no change in the temperature sensitive probe luminescence over a substantial period of time. This indicates that the temperature probes were not being consumed during the photosensitization reaction. By monitoring the anthracene fluorescence intensity as a function of time, the photosensitization reaction rate was found to be unaffected by the addition of the europium probes, indicating that the temperature probes are not adversely affecting the photosensitization reaction.

The cationic photopolymerizations were carried out in the MSU *LASER* laboratory, therefore calibration curves were generated using the Triplemate spectrometer and CCD detector. To produce the calibration curve, a non-reacting sample containing

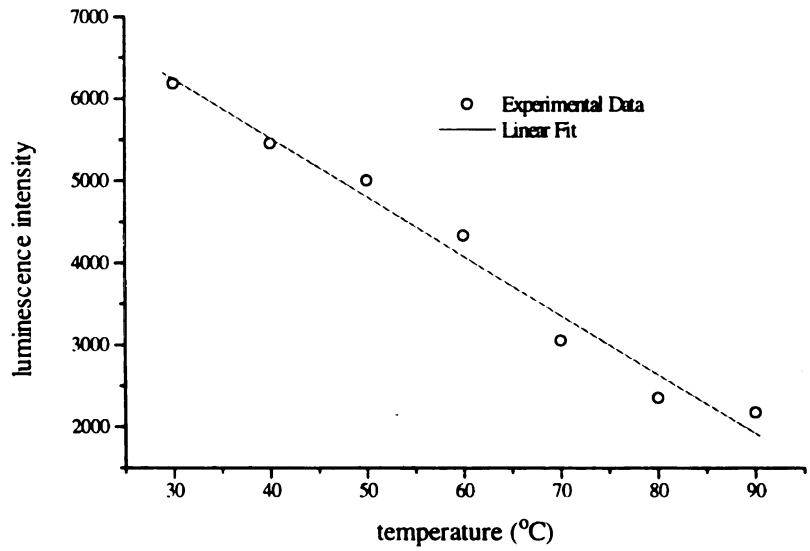

Figure 5-11. *Temperature calibration for 1.6 x 10^{-2} wt % $Eu(hfa)_3$ in DVE-3 with 1.4 x 10^{-2} wt % anthracene excited with 15 mW at 351 nm using an argon ion laser.*

anthracene and an europium probe in DVE-3 was used. The sample tube was placed in a jacketed cell holder (as described in the experimental section), then the temperature was increased while the luminescence at 620 nm was measured (*Figure 5-11*).

In preliminary reaction-monitoring experiments, the europium luminescence at 620 nm was measured at 50 ms intervals, and the calibration curve was used to generate the temperature profile. The temperature reading at the start of the reaction was adjusted to match room temperature (25 °C). The luminescence from the europium probe indicated that the temperature increased gradually from ~25 to ~55 °C at which point the reaction temperature increased rapidly (*Figure 5-12*). Therefore these studies illustrate that, as expected, a marked increase in temperature is associated with the sudden increase in the reaction rate. The reaction temperature continues to increase, however, due to the

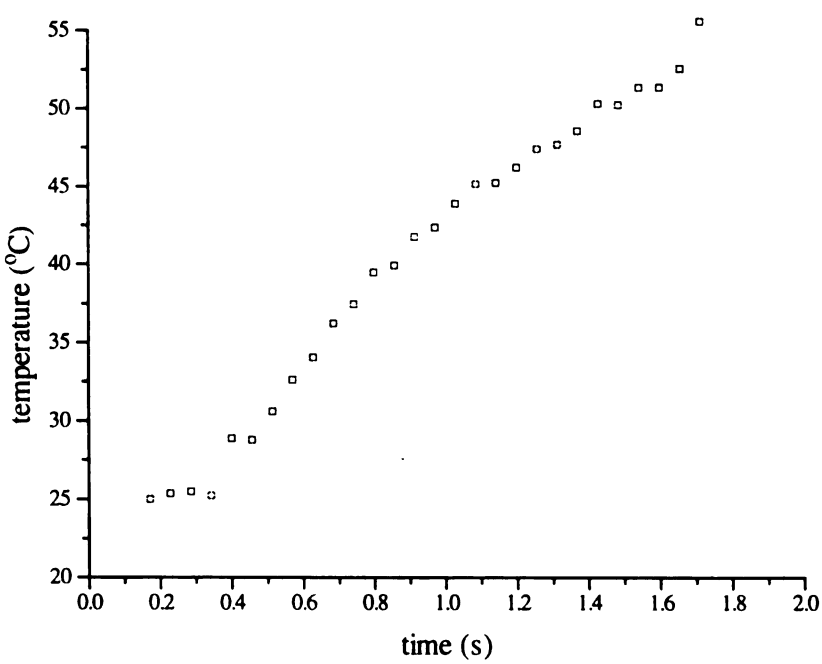

Figure 5-12. *Temperature profile of the cationic polymerization of DVE-3 1.6 x 10^{-2} wt % anthracene and 1.0 wt % initiator monitored with 1.0 x 10^{-2} wt % $Eu(hfa)_3$.*

instrumental dynamic range limitations mentioned above, we are not able to monitor higher temperatures in this system. In addition, at elevated temperatures the sample loses optical clarity. However, the important temperature at which the thermal runaway occurs (~55 °C for these specific reaction conditions) can be readily obtained from the temperature profile.

Further Applications. Due to their temperature dependence and viscosity insensitivity, the β-diketone tris chelates of europium may be attractive for temperature monitoring in a variety of systems. The technique could find application in any system in which an *in situ*, non-intrusive measurement of temperature is desired. Moreover, due to their viscosity insensitivity, the probes are appropriate for systems in which a change in phase occurs.

To illustrate the broader applicability of this technique in other reaction systems, the *in situ* luminescence during a free radical polymerization of 2-hydroxyethyl acrylate (HEA) was investigated for both probes. The reaction was a solution polymerization of 40/60 HEA/DMF in order to insure optical clarity during the reaction. The polymerizations were performed in 3.5 ml cuvettes heated to 65°C by a jacketed cell holder. AIBN was used as the initiator, and the lanthanide probes were present in concentrations of 10^{-2} wt %. Temperature excursions may occur due to the heat of polymerization, and the luminescence technique provides a temperature measurement which is averaged over the width of the cuvette. Luminescence measurements were easily performed in a standard luminescence spectrometer since the reaction takes minutes to complete as opposed to seconds in the case of cationic polymerizations.

Figure 5-13 shows the temperature profile produced from the luminescence intensity at 620 nm (the peak maximum) during a free radical polymerization of HEA. A calibration curve was prepared using the procedures described previously for the cationic system. As the reaction proceeds the exothermic heat of polymerization will cause the system temperature to increase above the jacket temperature, if heat evolution rate is higher than the heat transfer rate. Therefore, a dramatic increase in the temperature was observed at ~15 minutes, corresponding to an increase in the reaction rate due to autoacceleration. After reaching a peak value of around 100 °C, the reaction is essentially complete and the temperature of the solution returns to that of the jacket (65°C). Therefore, the luminescence ultimately returns to approximately the same intensity as when the sample was a liquid (confirming that the luminescence is independent of viscosity). The profile shown in *Figure 5-13* has the well-characterized shape indicative of free radical polymerizations undergoing the gel effect[20], thereby illustrating the broader

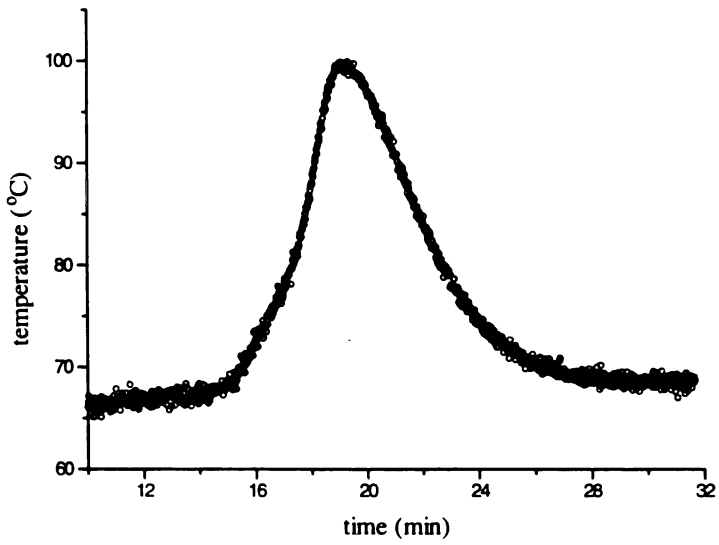

Figure 5-13. *The temperature profile generated from the luminescence intensity of $Eu(hfa)_3$ in a free radical polymerization of HEA/DMF (40/60) with an initiator concentration of 0.2 wt %.*

applicability of these temperature probes.

5.2. Conclusions

In conclusion, luminescence can provide a novel *in situ*, non-destructive method for monitoring the temperature in high speed reactions. Molecular-level luminescent probes provide extremely rapid response without requiring a macroscopic probe to be imbedded in the sample. For temperature monitoring during photopolymerizations of vinyl ethers, two β-diketone tris chelates of europium [$Eu(hfa)_3$ and $Eu(btfa)_3$] were found to meet several stringent requirements. These probes exhibit a reproducible temperature dependence over a wide temperature range and, in the case of $Eu(hfa)_3$, may provide a detector-insensitive calibration. Calibration curves of luminescence intensity versus temperature were generated for the temperature range of interest (between 20 and 90 °C). In addition, these probes meet specific spectral requirements, such as excitation in the 350 nm range and emission above 500 nm. Finally, the luminescence response of these probes was found to be independent of viscosity.

Our temperature profiles for cationic photopolymerizations verified the importance of thermal effects in these high-speed polymerizations. The luminescence from the europium probe indicated that the temperature increased gradually from ~25 to ~55 °C, then increased dramatically in a period of a few hundred milliseconds. These results confirm that a thermal runaway effect is responsible for the large increase in polymerization rate, as previously postulated by Nelson *et al.*[11]. While the temperature-sensitive probes appear to accurately monitor the temperature prior to thermal runaway,

they are unable to determine the maximum reaction temperature due to detector dynamic range limitations and problems associated with the sample losing optical clarity. Furthermore, the luminescence of the probes was found to be sensitive to sample components (solvent, initiators, and water) and seemed to degrade at long times. However, this can be overcome with the use of system specific calibration curves and the use of fresh samples.

Our studies have demonstrated the utility of the temperature-dependent luminescence of tris(β-diketone) europium chelates for characterizing the temperature during high-speed photopolymerizations that cannot be monitored using conventional techniques. However the applicability of these probes is not limited to this reaction system. These probes could find application in any system in which an *in situ*, non-intrusive measurement of temperature is desired. For example, due to their temperature dependence and viscosity insensitivity, the probes are appropriate for systems in which a change in phase occurs. The broader applicability of these probes was illustrated by our studies of the HEA free radical polymerizations. Finally, a host of other lanthanide compounds could possibly be used as temperature sensitive fluorescent probes. For example, commercially available probes worthy of further study include tris(6,6,7,7,8,8,8-heptafluoro-2,2-dimethyl-3,5-octanedionato) europium and tris(2,2,6,6-tetramethyl-3,5-heptanedionato) europium.

Acknowledgments. This work was supported by the National Science Foundation Grant number CTS 9216939, including an REU Supplement for C.L. Crofcheck. The laser luminescence studies were performed in the MSU *LASER* Lab.

5.3. References

1. Herzig, C.; Deubzer, B., *RadTech 94 North American Proceedings*, RadTech International North America, 635 (1994).

2. Dougherty, J. A.; Crivello, J. V., *RadTech 94 North American Proceedings*, RadTech International North America, 627 (1994).

3. Chawla, C. P.; Julian, J. M., *RadTech 94 North American Proceedings*, RadTech International North America, 617 (1994).

4. Decker, C.; Decker, D., *RadTech 94 North American Proceedings*, RadTech International North America, 602 (1994).

5. Bok, H.; Quade, R. M., *RadTech 94 North American Proceedings*, RadTech International North America, 48 (1994).

6. Kloosterboer, J. G., "Network Formation by Chain Crosslinking Photopolymerization and its Applications in Electronics," *Adv. Polym. Sci.*, **84**, 1 (1988).

7. Roffey, C. G., *Photopolymerization of Surface Coatings*, Wiley, New York, 1981.

8. Pappas, S. P., "Photoinitiators", *UV Curing, Science and Technology*, Technology Marketing Corp., Norwalk, CT, **2**, 1985.

9. Crivello, J. V., "Cationic Polymerization ---- Iodonium and Sulfonium Salt Photoinitiators," *Adv. Polym. Sci.*, **62**, 1 (1984).

10. Crivello, J. V.; Lee, J. L., "Alkoxy-Substituted Diaryliodonium Salt Cationic Photoinitiators," *J. Polym. Sci., Part A Polym. Chem.*, **27**, 3951 (1989).

11. Nelson, E.W.; Carter, T.P.; Scranton, A.B., "Fluorescence Monitoring of Cationic Photopolymerizations: Divinyl Ethers Photosensitized by Anthracene Derivatives," *Macromolecules*, **27**, 1013-1019 (1994).

12. Schrum, K. F., Williams, A. M., Haerther, S. A., Ben-Amotz, D., *Anal. Chem.*, **66**, 2788-2790 (1994).

13. Murray, A. M.; Melton, L. A., *Appl. Opt.*, **24**, 2783-2787 (1985).

14. Sager, W. F.; Filipescu, N.; Serafin, F. A., *J. of Phys. Chem.*, **69**, *4*, 1092-1100 (1965).

15. Halverson, F.; Brinen, J. S.; Leto, J. R., *J. of Chem. Phys.*, **40**, *10*, 2790-2792 (1964).

16. Alpha, Beatrice; Ballardini, Roberto; Balzani, Vincenzo; Lehn, Jean-Marie; Perathoner, Siglinda; Sabbatini, Nanda, "Antenna Effect in Luminescent Lanthanide Cryptates: A Photophysical Study," *Photochemistry and Photobiology*, **52**, 2, 299-306 (1990).

17. Richardson, M. F.; Wagner, W. F.; Sands, D. E., *J. Inorg. Nucl. Chem.*, **30**, 1275-1289 (1968).

18. Sato, S.; Wada, M., *Bulletin of the Chemical Society of Japan*, **43**, 1955-62 (1970).

19. Schimitschek, E. J.; Trias, J. A., *J. Inorgan. Nucl. Chem.*, **32**, 811-831 (1970).

20. Odian, G., *Principles of Polymerization*, John Wiley & Sons, Inc.: New York, NY, 286, 1991.

CHAPTER 6. THE MORPHOLOGY OF CATIONICALLY PHOTOPOLYMERIZED DIVINYL ETHERS

6.1. Transmission Electron Microscopy

Transmission electron microscopy (TEM) has become established as a valuable tool for identifying and characterizing the morphology of polymer systems. Traditionally, TEM has been used to examine composite materials, blends, and copolymers in order to identify quantities such as the size and shape of fillers and additives, and the size and distribution of microstructures within a copolymer.[1] More recently, electron microscopy has been used to identify the presence of heterogeneities, such as microgels, in epoxy resins.[2,3] However, while the literature contains numerous examples of electron microscopy for investigation of copolymers and polymer composites, relatively little work has been reported on the use of TEM to identify microstructures in crosslinking homopolymers.

This contribution reports the use of transmission electron microscopy to characterize the morphology in the homopolymer of a cationically polymerized divinyl ether. These systems are crosslinked due to the presence of two polymerizable vinyl bonds within each monomer unit. However, the extent to which the polymer crosslinks under various reaction conditions can be difficult to determine due to the extremely rapid rate of polymerization. There has been significant interest in the characterization of cationic photopolymerizations of bisvinyl ethers due to their tremendous potential for development as high-performance films and coatings which emit no volatile organic components (VOCs). These polymerizations proceed rapidly at room temperature to

form highly crosslinked polymers exhibiting excellent adhesion, abrasion resistance, and chemical resistance. Moreover, because the unreacted monomers exhibit excellent rheological properties and low vapor pressures, no solvents are required, eliminating VOCs. Cationic photopolymerizations exhibit several advantages over the more extensively employed free-radical photopolymerizations. For example, the cationic photopolymerizations are not inhibited by oxygen,[4] which eliminates the need to blanket the system with nitrogen.

Despite the advantages of cationic photopolymerizations discussed above, these reactions have received only limited attention and are not well understood. This fact may be largely attributed to three factors: the lack of suitable cationic photoinitiators until recently,[5,6] the difficulty in obtaining reproducible kinetic data on these extremely rapid polymerizations, and the difficulty in preparing samples from the resulting polymer for electron microscopy. Therefore, these polymerizations, as well as the resulting polymers, are not well characterized. Currently analytical techniques such as real-time infrared spectroscopy[7] and fluorescence spectroscopy, [8,9] which have response times on the order of several milliseconds, are being used to investigate the polymerization kinetics. However, there is still the need to characterize the structural properties of the resulting photopolymer. Transmission electron microscopy has the advantage of offering a unique visual insight into how the polymer chains are arranged and to what extent crosslinking has occurred.

6.1a. Experimental

In these studies, 3,6,9,12-tetraoxatetradeca-1,13-diene (triethylene glycol divinyl ether-DVE-3) (Aldrich Chemical Company) was the divinyl ether monomer used. Molecular sieves were added to remove any traces of water. The initiator (UV9310C - GE Silicones) had a composition of 5-10 wt. % linear alkylate dodecylbenzene, ~50 wt. % 2-ethyl-1,3-hexanediol, and ~50 wt. % bis(4-dodecylphenyl)iodoniumhexafluoro-antimonate as the active initiating species. Initiator concentrations specified in the remainder of this paper correspond to the total UV9310C concentration even though the iodonium ion is the actual initiating species. The anthracene photosensitizer (Aldrich Chemical Company) was used as purchased. Since the UV9310C initiator absorbs light in the deep UV region of the spectrum it is desirable to use a photosensitizer to increase the range over which the reaction can be initiated to include the near UV and visible wavelengths. This allows the use of common mercury arc lamps as the excitation light source.

The reaction solutions consisted of DVE-3 monomer with approximately 1.0 wt. % initiator, and 10^{-2} wt. % anthracene. Polymer samples were cured in two different ways in order to determine the effect of cure on the morphology. In the first method, the monomer solutions were placed in a mold and cured slowly in a desiccator by exposing the monomer solution to only the laboratory lighting. It was necessary to carry out these reactions in a desiccator to prevent the absorption of water from affecting the cationic polymerization by chain transfer. These samples required several days to reach the tack-

free point. In the second method the polymer was cured rapidly as a film on a glass slide under a Spectoline model XX-15G ultraviolet lamp with 84 W at 254 nm.

Once the polymer was formed it was prepared for use in the TEM by either grinding to form a fine powder or cryo-ultramicrotoming to form an ultrathin section. In the former case, the polymer sample was cooled with liquid N_2 to make it brittle and then ground to a fine powder with a mortar and pestle. The finest particles were then separated from the larger ones by sedimentation from an acetone suspension. The smallest particles remain in suspension much longer than the large ones allowing an aliquot of acetone with fine particles of DVE-3 to be removed with a micropipet. A drop of this suspension was then placed on a the Formvar coated sample grid. The acetone was allowed to evaporate off leaving the fine DVE-3 particles on the grid. Acetone was chosen because it evaporates from of the specimen support grid rapidly, and the DVE-3 is insoluble in it. The grids used were 3 mm x 300 mesh copper Gilder grids coated with a Formvar plastic specimen support film. In order to prepare more uniform samples, cryo-ultramicrotomy was used. Ambient temperature microtomy was unsuitable for the DVE-3 samples because they were soft and tended to swell in the water. Sections of thicknesses ranging from 150 to 95 nm were prepared with a glass knife at - 30 °C and a cutting speed of 1.0 mm/sec using a Reichert - Jung Ultracut E microtome with a FC 4D temperature controlled cutting stage. These sections were placed on uncoated 3 mm x 100 mesh copper folding grids.

Since contrast in TEM photographs is largely dependent on differences in electron density within the sample,[1,10] a stain may be used to increase the electron density of morphological features in the sample. In our studies osmium tetroxide was used to

selectively stain any remaining carbon-carbon double bonds in the polymer, thereby increasing their electron density.[1] The polymer samples were stained by contact with osmium tetroxide (obtained from Stevens Metallurgical) vapor for at least 2 hours, as suggested by Sawyer and Grubb.[1] The osmium tetroxide was prepared for use by dissolving OsO_4 crystals in water and diluting to a 2 % aqueous solution. Once the samples were stained they were generally coated with a conductive carbon layer in order to increase the stability of the polymer while in the electron beam. A Ladd vacuum evaporator was used to place a thin layer of carbon on the stained samples.

Micrographs were obtained using a JEOL 100CX II electron microscope operated in the TEM mode. Typical operating parameters included an accelerating voltage of 100 keV, a cryogenically cooled Gatan sample stage, and magnifications from 19,000x to 100,000x. Further magnification was obtained by photographic enlargement of the negatives. We found it necessary to use a Gatan cryostage cooled to -150 °C with liquid nitrogen to prevent sample degradation and distortion from the electron beam. The Gatan is equipped with a temperature controller that allows the temperature of the sample to be maintained at a set point above -195.8 °C (the boiling point of nitrogen) to within a couple degrees. A through-focus series of photographs was taken in order to help identify artifacts. Photographs were taken using Kodak electron image film #4489, $3^1/_4$ x 4 inches. Prints were made using Kodak polycontrast III RC paper, glossy F surface.

6.1b. Results and Discussion

Investigation of divinyl ethers by transmission electron microscopy presented a number challenges that had to be overcome before reliable micrographs could be obtained. Transmission electron microscopy requires specimen thicknesses on the order of nanometers in order for the electron beam to penetrate through the sample. Due to the lack of literature reports on investigations of vinyl ethers using TEM, preparation procedures to obtain DVE-3 samples with thicknesses of 100 nm or less were established. We developed two different techniques that are described in the experimental section. Unlike the epoxies studied,[2] the soft nature of the DVE-3 polymer, as well as its tendency to swell significantly in water prevented sample preparation by traditional microtoming. The grinding technique used to prepare powder samples resulted in samples that were of suitable thicknesses for electron beam penetration for regions on the order of several tenths of a micron near the edges of the particles. The disadvantage of these powders is that only this limited area is visible, and stained regions indicative of heterogeneities in polymer structure are difficult to distinguish from dark areas arising from increasing sample thickness.

In order to overcome this limitation, an adaptation of the ultramicrotomy technique called cryo-ultramicrotomy was employed. This technique uses liquid N_2 to harden the DVE-3 polymer so that the polymer is rigid, but still flexible enough to prevent a brittle fracture.[11] Furthermore, the cryosectioning technique has the advantage of not involving water which tends to swell the DVE-3 polymer. Finally, since the sectioned samples can be held in place by being pinched between the two halves of a

folding grid, no support film is needed. This has the advantage of allowing examination of thicker samples because the electron beam doesn't have to penetrate the support film as well as the sample. The cryosections, although much more tedious to obtain, provide larger regions of a uniform thickness than the grinding technique.

Osmium tetroxide has been used successfully for studying heterogeneities in epoxies containing a stainable diamine hardener,[2] and is ideally suited to polymer systems involving vinyl bonds. The osmium tetroxide reacts across the double bond (Equation 6-1), thereby increasing its electron density and "fixing" the bond to prevent it from crosslinking while in the electron beam.[1]

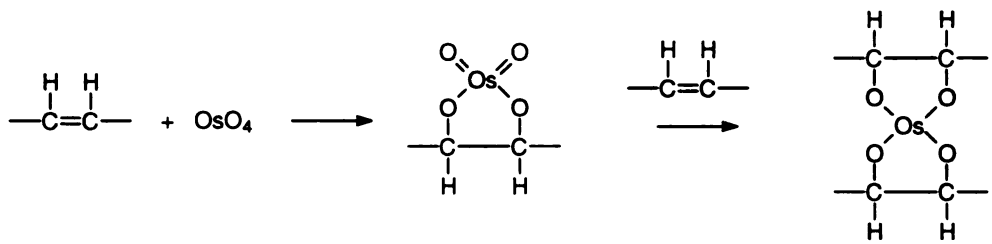

Eqn. 6-1

Damage of a polymeric material due to radiation from the electron beam may present a significant problem.[11] In order to minimize this degradation of the polymer, we used a cryogenically cooled Gatan sample stage to keep the sample at a temperature of -150 °C. We found that the DVE-3 polymer samples, when maintained at this temperature, suffered no visible degradation over the period of an hour, with or without carbon coating. However, the smaller particles in the powder samples had a tendency to move around on the grid and even be sucked off by the vacuum in the column if they were not carbon coated. The cryotomed samples, however, did not require a carbon coating.

Figure 6-1 is a transmission electron micrograph of an unstained section of DVE-3 polymer, while *Figure 6-2* is an identically cured and prepared section that was stained with OsO_4. *Figure 6-1* is representative of the 7 micrographs taken of 3 separate but identically prepared samples. The micrograph in *Figure 6-2* is representative of nearly 70 micrographs taken of various areas on a total of 6 different OsO_4 stained samples prepared by either of the two methods described earlier. Similar results were seen regardless of the sample preparation method used. A comparison of these micrographs demonstrates the function of osmium tetroxide. The polymer in *Figure 6-2* has areas of increased contrast not visible in *Figure 6-1*. The dark regions are attributed to areas with high concentrations of vinyl bonds that reacted with the osmium tetroxide. These regions are probably a result of trapped oligomer or monomer. In addition, careful examination of *Figure 6-2* shows a number of light regions surrounded by a darker border. These light regions appear to arise from microgel regions of very highly crosslinked polymer containing almost no vinyl bonds. Gupta *et al.*[2] offered a similar explanation for their observations in micrographs of epoxy materials. In both cases these regions were found to be present in sizes ranging from 5 nm to 100 nm in diameter. Care must be taken in identify these regions so as to minimize the risk of mistaking differences in contrast due to variations in sample thickness as differences in stain concentration. The presence of these inhomogeneities suggests that the reaction takes place in localized "hotspots" that become highly crosslinked by local propagation of active centers. Expansion of these microgels may entrap small pockets of unreacted double bonds resulting in the dark, highly-stained regions of the sample.

Figure 6-3 contains an x-ray spectra of an unstained slow cured DVE-3 polymer similar to the sample in *Figure 6-1* and an x-ray spectra of an OsO_4 stained sample corresponding to *Figure 6-2*. These x-ray spectra were obtained using the LINK systems x-ray detector attached to the JEOL electron microscope. They were obtained with an accelerating voltage of 60 keV and an ambient temperature carbon sample rod. The strong peaks at 8.041 and 8.910 keV are largely due to the copper grids on which the samples were mounted. In addition the gold peaks are due to the gold traces present in the instrument column. There is an osmium $L_{\alpha 1}$ peak overlaying the second copper peak. However, there are two beta peaks, $L_{\beta 1}$ and $L_{\beta 2}$, for osmium in an otherwise clean region at 10.354 and 10.597 keV, respectively. An additional osmium peak, $L_{\gamma 1}$, at 12.094 keV for the stained sample. This figure indicates that osmium is definitely present in the stained samples.

Finally, *Figure 6-4* is a micrograph of a DVE-3 sample identical to that in *Figure 6-1* and *Figure 6-2* except that it was cured rapidly (several minutes) using an 84 W UV lamp (254 nm). This sample was prepared for observation in the TEM by cryo-ultramicrotoming to a thickness of approximately 100 nm and stained by OsO_4 vapor deposition for 8 hours. *Figure 6-4* is representative of 10 micrographs taken of two samples. In contrast to the distinct stained regions that can be observed in *Figure 6-2*, *Figure 6-4* shows no indication of having stained regions at all. Several identically prepared samples that were cured rapidly under a UV lamp were examined at various levels of magnification and with different objective apertures. Stained regions were not

observed in any of these samples, indicating that little, if any, unreacted double bonds remained.

6.2. Conclusions

In this chapter, a procedure was developed for preparing sections of soft, brittle divinyl ether polymers for transmission electron microscopy. Cryo-ultramicrotomy was used to section DVE-3 with thicknesses on the order of 100 nm. In addition, osmium tetroxide was found to be a suitable stain for selectively increasing the contrast (electron density) of vinyl bonds in the polymer structure. Finally, a Gatan cold stage maintained at -150 °C was found to successfully prevent radiation damage of the DVE-3 sections while exposed to an electron beam accelerated by 100 keV. This technique offers the ability to characterize the morphology of polymers of divinyl ethers with resolutions down to several nanometers.

Our electron microscopy results indicate that heterogeneities are present in the polymer morphology due to unpolymerized vinyl bonds in the cationically photopolymerized divinyl ether. Two different types of inhomogeneous regions were identified. The first type of inhomogeneity (dark regions on the micrograph) is suspected to be a result of trapped pockets of unreacted double bonds. The second type (light regions on the micrograph) suggests the presence of microgels of highly crosslinked polymer. In DVE-3 we identified heterogeneities ranging in size from 5 nm to 100 nm.

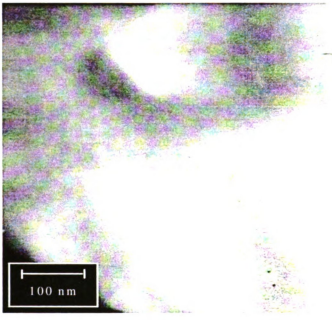

Figure 6-1. *Unstained DVE-3 polymer containing 1 wt. % UV9310C, and 10^{-2} wt % anthracene cured in a desiccator.*

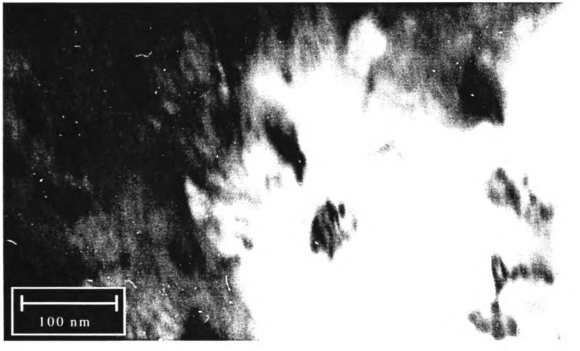

Figure 6-2. *The DVE-3 polymer stained with OsO_4 by vapor deposition indicates areas of varying contrast due to stained vinyl bonds.*

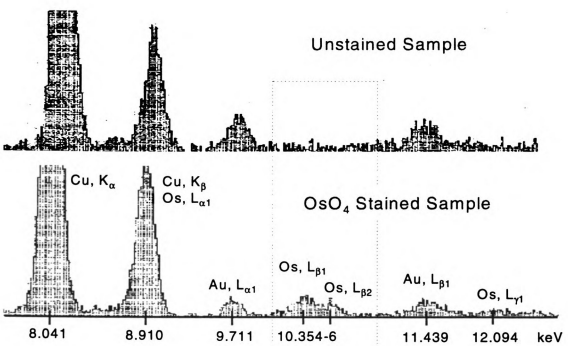

Figure 6-3. *X-ray spectra of OsO_4 stained and unstained DVE-3 polymer on copper grids. The vertical intensity axises are approximately equivalent.*

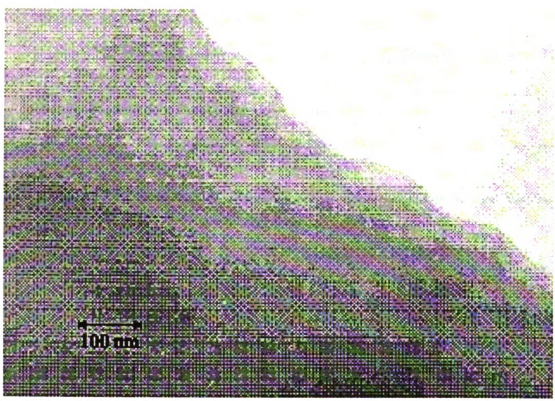

Figure 6-4. *Lamp cured DVE-3 sample stained with OsO_4 by vapor deposition. Notice the absence of stained regions indicating a low concentration of unreacted double bonds.*

6.3. References

1. Sawyer, L.C., Grubb, D.T., *Polymer Microscopy*, Chapman and Hall, London, 1987.

2. Gupta, V.B.; Drzal, L.T.; Adams, W.W.; Omlor, R., "An Electron Microscopic Study of the Morphology of Cured Epoxy Resins," *Journal of Materials Science*, **20**, 3439 (1985).

3. Dusek, K.; Plestil, J.; Lednicky, F.; Lunak, S., "Are Cured Epoxy Resins Inhomogeneous?," *Polymer*, **19**, 393 (1978).

4. Roffey, C.G., *Photopolymerization of Surface Coatings*, Wiley, New York, 1981.

5. Crivello, J.V., "Cationic Polymerization ---- Iodonium and Sulfonium Salt Photoinitiators," *Adv. Polym. Sci.*, **62,** 1 (1984).

6. Pappas, S.P., "Photoinitiation of Cationic and Concurrent Radical-cationic Polymerization. Part V," *Prog. Org. Coat.*, **13**, 35 (1985).

7. Decker, C.; Decker, D., *RadTech 94 North American Proceedings*, RadTech International North America, 617 (1994).

8. Nelson, E.W.; Carter, T.P.; Scranton, A.B., "The Role of the Triplet State in the Photosensitization of Cationic Polymerizations by Anthracene," *J. Polym. Sci., Polym. Chem.*, **33**, 247 - 256 (1995).

9. Jacobs, J.L.; Nelson, E.W.; Scranton, A.B., "Use of Fluorescence to Monitor Temperature and Observe the Water Effects of Cationic Photopolymerization of Divinyl Ethers Photosensitized by Anthreacene," *Proc. ACS Polym. Mat. Sci. and Eng.*, **70**, 74 - 75 (1994).

10. Heckman, J.W., Jr.; Flegler, S.L.; Klomparens, K.L., *Scanning and Transmission Electron Microscopy, An Introduction*, W.H. Freeman and Company, New York, 1993.

11. Voigt-Martin, I.G., "New Developments in the Characterization of Polymers by Transmission Electron Microscopy," *Applied Polymer Anal. Charact.*, 277, 1987.

CHAPTER 7. FEASIBILITY OF IR SPECTROSCOPY FOR CURE MONITORING

7.1. Background on Fourier Transform Infrared Spectroscopy

Due to technological advances, infrared (IR) has become an increasingly important tool for the investigation of polymers. With the development of Fourier transform infrared (FTIR) spectroscopy, spurred by the discovery of the fast Fourier transform (FFT) algorithm by Cooley and Tukey[1] in 1965, the usefulness of IR spectroscopy was greatly expanded. Even today as sampling techniques, lasers, detection systems, computers and software become more sophisticated previous limitations continue to be overcome. For example, it is now possible, and desirable in many cases, to examine polymer systems *in situ*.[2] High speed FTIR instruments are now capable of collecting an entire spectrum in times as short as 5 ns.[3]

IR is a useful technique for polymers, since the infrared absorption spectra for polymers are often surprisingly simple considering the large number of atoms involved.[6] The simplicity results first from the fact that many of the normal vibrations have almost the same frequency and appear as one band. Furthermore, the strict IR selection rules prevent many of the vibrations from producing absorptions[6], therefore simplifying the spectrum.

The usefulness of IR and also Raman spectroscopy ultimately lies in the variety of qualitative and quantitative information they can provide about the nature of the polymer under investigation. Information that can be obtained using these techniques includes: the chemical nature (structural units, branching, end groups, additives, and impurities),

steric order (isomerism and stereoregularity), conformational order (physical arrangement of the chain), state of aggregation (crystalline, mesomorphous, amorphous phases, number of chains per unit cell, etc.), and orientation of the polymer chain and side groups.[4]

The nice thing about IR and Raman spectra is that they provide complementary rather than duplicate information. For example, IR spectroscopy is generally better suited for the identification of polar groups, while Raman is especially good for the investigation of the homonuclear polymer backbone.[4] Raman spectroscopy is potentially well suited for the study of low concentration aqueous systems such as hydrogels, since water is an ideal solvent due to its poor Raman scattering. This is a distinct advantage over IR techniques since water absorbs strongly in the IR region and overwhelms the spectrum.[7] Other advantages of Raman spectroscopy arise from the fact that Raman scattering from molecular vibrations can be measured in the visible region of the spectrum. Intrinsic limitations of Raman spectroscopy arise from the requirement of an intense monochromatic (preferably columnated) light source, and the possible interference from highly colored or fluorescence materials.[8]

IR and Raman spectroscopy are based upon distinctly different physical processes. Fundamentally, Raman is a scattering technique while IR spectroscopy is based upon light absorption, therefore the sampling techniques of the two methods are significantly different. In transmission IR spectroscopy the light is required to pass through the sample to reach the detector, therefore severe constraints are imposed on the sample thickness (typically the thickness must be less than about 40 μm). Methods such as attenuated total reflectance (ATR) may be used with thick samples, but present their own problems and

limitations associated with the contact to the ATR crystal, and the limited depth of penetration. In contrast, since Raman spectroscopy is based upon light scattered by the sample, thick samples are not a problem since back-scattered light may be collected and analyzed. Therefore Raman spectroscopy generally requires very little if any sample preparation.

The most significant limitations of Raman spectroscopy arise from interference from samples that are highly fluorescent or colored. This limitation ultimately arises from the relatively low intensity of the scattered Raman light, which necessitates intense light sources. In colored samples, the incident light may lead to significant heating of the sample. If the incident light induces fluorescence, the Raman signal must be resolved from the fluoresced light (fluorescence is typically several orders of magnitude more intense than Raman scattering). Both techniques are good for analysis of microscale sample sizes. Although, IR spectroscopy has the advantage of better resolutions with resolutions down to approximately 0.05 cm^{-1}, while Raman instruments are limited to about 0.25 cm^{-1}.[8] In addition, both techniques are fairly easily adapted to high and low temperature work.[8]

There are two general types of infrared spectrometers. The older of the two types is referred to as a dispersive spectrometer. This type of spectrometer uses a monochromator and slits to separate the infrared radiation into individual frequencies.[9] The more recently developed type of instruments is known as a Fourier transform infrared spectrometer (FTIR). These instruments are based on the Michelson interferometer and require no monochromators or slits.[9] The areas of continuing improvement in FTIR instrumentation include increased scan speed and resolution, improved signal-to-noise

ratios, expansion of the range of wavelengths over which the instrument operates, data handling software, and automation. Examples of these improvements include FTIR instruments which are capable of resolutions down to 1 cm^{-1} and signal-to-noise ratios of 2,000:1 with high speeds capable of obtaining spectra in intervals as short as 5 nanoseconds.[3]

The most significant area of improvement in Raman spectroscopy has been the development of relatively low cost, high power lasers. Some of the more recent improvements include enhanced detection systems, such as charge coupled devices (CCD), and the use of fiber-optics for remote process analysis.[3] Other improvements in IR and Raman instrumentation make use of the increased power of personal computers and computer software. It is now possible to collect, analyze, annotate, and even "cut and paste" selected spectrographs into reports and presentations all within the same computer. In addition, computerized libraries of known IR and Raman spectra continue to grow, allowing for more extensive computer matches of characteristic group frequencies.[3]

There are many applications of IR and Raman spectroscopy to the investigation of polymers. Specific applications include investigations of controlled drug release delivery systems, and contact lens materials; identification of biocompatible polymers; and characterization of synthesis products.

7.1a. Physical Basis and Instrumentation for IR Spectroscopy

A brief introduction to the basic principles of infrared spectroscopy is presented in this section. The infrared (IR) region of the spectrum consists of light with wavenumbers

between 10,000 cm^{-1} and 10 cm^{-1} (wavelengths between 1.0 μm and 1,000 μm), with the range from 10,000 to 4,000 cm^{-1} (1,000 - 2.5 μm) referred to as the near infrared; 4,000 to 400 cm^{-1} (2.5 - 25 μm) the mid-infrared; and 400 to 10 cm^{-1} (25 - 1,000 μm) the far infrared regions.[8] The basic premise behind IR spectroscopy is that when infrared light is passed through a sample, certain frequencies are absorbed while others are transmitted, resulting in an absorption spectrum that is dependent on the molecular vibrational frequencies.

In polymers, molecular bonds have different vibrational frequencies which correspond to characteristic IR absorption bands. Therefore an IR spectrum may be used for identification of the types of bonds and functional groups present in a specific polymer sample.[10] IR absorption bands due to rotational transitions may be observed for gases[4], however the rotation of the molecule is highly restricted in solids, and rotational transitions are not observed. Therefore, for the study of polymer systems concern is focused on molecular vibrations, with characteristic absorption bands throughout the IR spectrum.

In an infrared spectrometer, the sample under investigation is exposed to the light which spans the entire IR region (either simultaneously as in an FTIR or one wavelength at a time as in a dispersive IR). Both the classical and quantum mechanical viewpoints are useful in describing fundamentally what occurs on the molecular level. The sample absorbs the light only at the specific frequencies that match the natural vibrational frequencies of its constituent molecules.[11] In order for a molecular vibration to absorb in the IR region it must cause a change in the magnitude of the dipole moment.[4, 12, 14] The intensity of this absorption is dependent on how effectively the molecule transfers the

infrared photon energy to molecular vibrational energy. This is dependent on the change induced in the dipole moment.[11] It has been shown that the intensity of an IR absorption band is proportional to the square of the change in its dipole moment.[11, 12, 14] If a molecule has a center of symmetry in its equilibrium configuration, then any vibrations for which this symmetry is retained will be infrared inactive.[11]

The frequency of a photon, ν_p, is determined by its energy, E_p, according to Equation 7-1.[11]

$$E_p = h\nu_p \qquad \text{Eq. 7-1}$$

Quantum mechanical considerations dictate that molecular energy assumes only specific discrete values. The values of the vibrational energy levels, E_{vib}, are given by[11],

$$E_{vib} = (n + {}^1/_2)h\nu \qquad \text{Eq. 7-2}$$

Where h is Planck's constant, ν is the classical vibrational frequency of the oscillator, and n is a quantum number. If this equation is applied to the infrared absorption of a photon where the vibrational energy of the molecule is E_m, and the frequency of the induced vibration is ν_m, then by substitution,

$$E_m = (n + {}^1/_2)h\nu_m \qquad \text{Eq. 7-3}$$

The only variable in this equation is the quantum number, which can only have integer values. If the quantum number changes by +1 or -1, then the molecule gains or loses energy, respectively. For an unsymmetrical diatomic molecule this amount of energy is ΔE_m, which is equal to the difference between the energy of the n quantum level the energy of the n+1 level. This gives the result[11],

$$\Delta E_m = h\nu_m \qquad \text{Eq. 7-4}$$

Since the change in energy, ΔE_m , is due to the transfer of energy from the photon to the molecule, $\Delta E_m = E_p$. Therefore $\nu_p = \nu_m$. This states that the frequency, ν_p, of a photon which has the proper energy to cause the vibrational quantum number to jump up one level is equal to the classical vibrational frequency of the molecule, ν_m.[11] For harmonic vibration the vibrational quantum number may only change by ±1, all other transitions are forbidden. This selection rule corresponds to conditions where the electric field of the photon causes the molecule to vibrate at the field's frequency, and induces a molecular dipole moment. For an anharmonic quantum mechanical oscillator the selection rule allows for integer changes in the quantum number of ±1, ±2, ±3, etc. In this case, the excited molecule vibrates at the corresponding integer multiple of the molecular frequency.[11] At room temperatures most molecules are in the ground vibrational state, therefore, the allowed transition that dominates infrared spectroscopy and is of most interest is from $n = 0$ to $n = 1$. This is referred to as the fundamental transition. The relative intensities of other allowed transitions are low since the populations of the higher energy levels are low compared to the ground state at room temperatures.[11] Although additional bands, known as overtones and combination bands, may result from anharmonic terms in the potential energy of the molecule.[13] Since anharmonic oscillator energy levels are not equally spaced, the frequency is no longer completely independent of amplitude.[11] The additive effect of the harmonic and anharmonic terms results in the appearance of absorption bands that are shifted from their characteristic absorption wavelength.

Instrumentation for Infrared Spectroscopy. The original type of infrared technique is known as a dispersive IR. A dispersive IR instrument consists of prisms or

gratings that separate or disperse the IR radiation into its component wavelengths.[13] Generally modern dispersive infrared spectrometers are made using gratings rather than prisms with a series of diffraction gratings used to separate the entire IR region.[11] The diffracted light is then reflected with an off-axis paraboloid through an exit slit into a detector. A movable mirror allows a progressive scanning of the individual wavelengths. As a whole, this setup acts as a monochromator thus focusing one wavelength at a time onto the detector. Before reaching the monochromator, the IR radiation is first passed through the sample. In a double beam instrument the IR radiation is split into two beams, one of which is passed through the sample; the other is passed through a reference cell. A rotating sector mirror, called a chopper, alternately reflects or transmits each beam to the monochromator.[10] By comparing the two intensities, the absorption of the sample can be determined.

In contrast to the traditional dispersive instruments, the modern Fourier transform infrared (FTIR) spectrometers do not require a system of slits or a monochromator. Instead, light containing all IR frequencies is passed through the sample simultaneously and those not absorbed reach the detector. The advantage is an improved signal-to-noise ratio and a higher throughput compared to the dispersive IR method.[4, 11, 15] The key component of the FTIR instrument is the Michelson interferometer, which was first developed around the turn of the century, but was not applied to infrared spectroscopy until the development of digital computers that could quickly and accurately derive the IR spectra from the interferograms by taking the inverse Laplace transform.[4]

In the Michelson interferometer, a beamsplitter is used to transmit half of the source radiation to a movable mirror and to reflect the other half to a fixed mirror. The

two beams are then reflected back to the beamsplitter and recombined either constructively or destructively depending on the position of the movable mirror.[11] In an FTIR spectrometer, this recombined beam is then generally passed through the sample to a detector[4], where the interferogram is obtained. In the simplest case of a monochromatic radiation source the intensity (amplitude) of the detector signal is merely the cosine function of the mirror position.[4,11] For polychromatic radiation, however, the interferogram is a summation of all of the constructive and destructive interferences resulting from the interactions between all of the wavelengths.[11] The cosine Fourier transform provides the mathematical relationship between the detected interferogram intensity, *I(x)*, which is a function the mirror position, and the infrared absorption intensity, *I(v)*, as a function of frequency [11, 15],

$$I(x) = \int_{-\infty}^{\infty} I(v)\cos(2\pi xv)dv \qquad \text{Eq. 7-5}$$

In order to obtain the infrared spectrum from this interferogram quickly, a computer is required to calculate the following inverse transform[11, 15],

$$I(v) = \int_{-\infty}^{\infty} I(x)\cos(2\pi xv)dx \qquad \text{Eq. 7-6}$$

The optical path difference, x, is a function of the position of the moveable mirror and is very accurately determined through the use of an internal standard (typically a helium-neon laser).[15]

Ideally, the light source for infrared spectroscopy should be continuously tunable over the entire infrared region at power levels above the microwatt range.[11, 16] One source that provides an ideal continuous high energy output is a blackbody slit cavity;

however this source is impractical since it requires high temperatures.[11] There are several common types of infrared light sources that come close to matching the ideal characteristics of the blackbody radiator in the infrared region. These include the Nersnst Glower and the Globar.[11] The Nernst Glower consists mainly of rare earth oxides such as zirconium, yttrium, and thorium oxide which are fashioned into rods about 20 mm long and 1 mm in diameter. They are normally operated at 1900 °C since they are nonconducting at room temperature and must be heated to reach a conducting state.[11] The Globar is a silicon carbide rod, 50.8 mm long and 4.8 mm in diameter that operates at about 1200 °C.[11] The disadvantage of the Globar is that it requires a water-cooled jacket to protect the silvered electrical contacts. In comparison, the Globar has similar radiator properties as the Nernst Glower, although the Nernst Glower gives better performance in the region below 15 μm.[11] However, unless high performance in this region is specifically needed, the Globar is recommended due to its advantage of being more rugged.

A recently developed source of infrared light is a laser pumped nonlinear optical parametric device, such as an optical parametric oscillator (OPO).[16] Optical parametric devices were identified some time ago as promising sources of tunable infrared radiation. However, until recently they proved to be less than ideal due to difficulties such as low optical damage thresholds, spectral bandwidth limitations, and complicated wavelength control methods.[16] Lately, significant improvements in the production of nonlinear optical materials and the availability of stable injection-seeded single-mode or ultrashort-pulse high-peak-power solid-state laser pump sources has resulted in new developments in optical parametric devices.[16] These devices require a coherent diffraction-limited

pump source, such as an injection-seeded Nd:YAG laser, to deliver the necessary beam quality, peak power, and pulse energy, as well as the high pulse-repetition rate, and narrow bandwidths. The Nd:YAG lasers operate in the nanosecond and picosecond regimes. For ultrafast spectroscopic applications, femtosecond-pulse lasers such as Ti:Al_2O_3 /dye lasers have proven useful.[16] Parametric devices using these pump sources and newly developed nonlinear optical materials such as $AgGaS_2$ and $AgGaSe_2$ can now generate infrared radiation throughout the mid-IR (fingerprint) region.[16] Previously identified materials such as $LiNbO_3$ and $LiIO_3$ had transmission characteristics that limited them to wavelengths shorter than 4 μm and 5 μm, respectively. Now essentially any wavelength from the UV to the mid-IR can be produced by selecting different crystals (nonlinear optical materials) and pump sources.[16] Use of this type of light source is currently limited to high end systems because of its relatively high cost compared to the Glower or Globar sources.

Infrared detectors consist of two general types, thermal and photon detectors. Thermal detectors measure a change in a physical property of a material as it is heated, whereas, photon detectors use changes in the electrical properties of a semiconductor caused by incoming photons to detect IR radiation.[17] Thermal detectors tend to be nonselective detectors, in that, they have a response that is directly proportional to the incident energy and largely independent of the wavelength.[11] Photon detectors, on the other hand, are much more selective detectors since they have a response curve that is strongly dependent on the wavelength of the incident radiation. Because of their relative wavelength independence[11] and versatility[17], nonselective thermal detectors have traditionally been the better choice for spectroscopy. However, these types of detectors

tend to have slow response times and low relative sensitivity.[17] With improvements in semiconductor technology and the increasing need for fast response times and better sensitivity, photon detectors are gaining favor. Thermal detectors include thermocouples, thermopiles, thermistors, bolometers, and pyroelectric detectors. Some examples of photon detectors include photoconductive, and photovoltaic cells.[17]

Thermocouples and bolometers are two commonly used detectors. Bolometers have the advantages over thermocouples of faster response times and greater sensitivities. A bolometer uses the temperature dependence of a material's electrical resistance to measure the intensity of incident radiation. Bolometer's are often constructed of semiconductors. However, superconducting materials have been used for improved sensitivities and faster response times.[11]

The fast response requirements of the rapid-scanning interferometers in FTIR instruments, and the convince of room temperature operation is often meet by the use of a pyroelectric detector.[4] This detector's response is based on the temperature sensitivity of the residual electrical polarization that can be induced in pyroelectric crystals, such as triglycine sulfate.[11] When this type of material is polarized by an electrical field a residual polarization is retained by the material after the field is removed. The voltage across this crystal is then temperature dependent and is measured by electrodes placed on the crystal faces. This device is essentially independent of wavelength from the near infrared through the far infrared.[11]

Photoconductive and photovoltaic detectors have the advantages of rapid response times and high sensitivity compared to thermal detectors. However, they have the disadvantage of being limited in their detection range, providing poor performance in the

far-IR region.[17] In addition, they often require liquid nitrogen or helium cooling. Both of these detectors depend on the quantum interaction between photons from the incident light and the semiconductor material in the detector.[17]

Overall for the slower dispersive IR instruments, the cheaper thermal detectors are generally the best choice. For high speed applications and especially rapid FTIR work, a photon detector is essential.[17] More detailed information on the various types of detectors available for IR spectroscopy is presented by Colthup *et. al* in reference[11] and Cuirczak in reference.[17]

7.1b. Sampling Techniques for Infrared Spectroscopy.

The physical state (*i.e.* solid, optically dense) of most polymers makes careful sample preparation imperative since it is generally necessary for the IR beam to be transmitted through the sample. Therefore, at least some sample preparation is necessary before a spectrum can be obtained. In addition, the quality of the spectrum is often dependent on the care taken in preparing the sample. Poorly prepared samples that are too thick, nonuniform; or contain impurities, can result in poor or misinterpreted data. There are a number of methods for polymer sample preparation available depending on the physical state of the sample. For solid polymers, IR samples may be prepared by dissolution, dispersion into KBr pellets or mulls, thin film casting, microtoming, microsampling, and attenuated total reflectance (ATR).[4, 10, 18] For liquid polymer samples, liquid films can be examined by placing several drops between two salt plates.[10]

The method of dissolution requires the identification of a solvent that dissolves the polymer under investigation but does not absorb in the IR region of interest. For this reason this method is seldom used despite the advantage of excellent reproducibility.[4] A number of authors, such as D. O. Hummel and J. E. Stanfield have summarized the IR absorption spectra of commonly used solvents.

For dispersive IR systems, the spectrum of the solvent is removed from the polymer spectrum by placing the solvent in the reference beam. It is generally advantageous to prepare solutions with as high a concentration as possible. For polymer systems, this method is often most valuable for cases where only a narrow spectral region is of interest for which a suitable solvent exists.[4] With FTIR systems there is no problem removing the solvent absorption bands, unless water is the solvent. The strength and breadth of the IR absorption spectrum of water in aqueous systems, such as hydrogels, can easily surpass the dynamic range limitation of the instrument. In order to subtract the water spectrum, the FTIR spectrum must be examined so that the dynamic range of the detector is not exceeded by the presence of excessive amounts of water.[4]

One of the more commonly used sample preparation techniques for the investigation of polymer systems is to make film samples. This method has the advantage of providing a means for studying polymers in their solid state. The dimensional requirements of the film are such that it is large enough to cover the entire cross section of the light beam and that it is thick enough to provide sufficiently intense bands for groups that are present in low concentrations, but thin enough to allow beam penetration. The film thickness may also need to be reduced to prevent saturation of the detector in IR regions that absorb more strongly than others. Typical dimensions are on

the order of 15 mm x 5 mm with thicknesses in the range of 0.001 to 1 mm.[4] Some of the techniques for forming polymer films include solvent casting, melt casting, and hot pressing. Solvent casting is useful for polymers that can be readily dissolved in a volatile solvent. While melt casting can be used for thermoplastics, some samples require hot pressing in which a hydraulic press is used to provide thinner sample films.[4]

Another IR sample preparation method often used for polymers is the pressed disk technique. This technique involves grinding the polymer sample into a fine powder, and then mixing a small amount with an IR transparent matrix, such as powdered potassium bromide. This mixture is then molded at high pressures in a special die. Often the die is evacuated[11] and pressures range up to 1,000 N/mm^2.[4] A disadvantage of this technique is that many of the matrix materials (salts) absorb water and exhibit water absorbance peaks near 3450 cm^{-1} and 1635 cm^{-1}.[4] A similar technique which is more useful for water-sensitive samples, is the mull method. In this method the polymer is ground into a powder and dispersed into a liquid phase, commonly mineral oil (Nujol)[11], hexachlorobutadiene, or perfluorocarbon.[4] This paste is squeezed between two IR transparent plates. The major disadvantage of this method is the limitation of spectral regions that can be observed due to absorbance bands of the dispersion material.[4] A table of transmission ranges and refractive indices for a number of common matrix materials is presented by Siesler in reference.[4]

Two final sample preparation methods are microtoming and microsampling. Microtoming involves the use of a sharp glass or diamond knife to cut extremely thin samples with thicknesses down to the nanometer scale. The technique is rather tedious and requires considerable practice to master, but may be useful for highly crosslinked

polymers for which a solvent can't be found. In order be microtomed, a sample it must be suitably hard so as not to deform greatly under the knife pressure. Softer samples often must be microtomed under cyrogenic conditions. Microsampling is a technique that is used to obtain IR spectra from very small specimens, such as a microtomed sample.[4] This technique requires the attachment of an optical device that reduces the image of the monochromator slit at the sample position.[4] This type of system can introduce several sources of error that need to be considered. As an example, diffraction phenomena or imperfections in the optical system can cause false radiation that will result in smaller intensities of the absorption bands.[4]

Finally, for polymer samples for which satisfactory transmission spectra can not be obtained by any of the above techniques it may be possible to use attenuated total refection (ATR) to acquire an IR spectra.[19,20] ATR is based on the phenomenon of total internal reflectance between two materials of different refractive indices. Experimentally, the sample under investigation with a refractive index of n_2 is placed in direct contact with the reflecting surface of a prism. The prism has a refractive index of n_1 that is larger than n_2. Total internal reflectance occurs at an angle above the critical angle of incidence, α_c, of the light beam. This angle is defined by the relation[4,11],

$$\sin \alpha_c = n_2/n_1 \qquad (n_1 > n_2) \qquad \text{Eq. 7-7}$$

The penetration depth of the light beam into the sample is generally on the order of several micrometers. This provides the absorption path without requiring transmission of the radiation through the entire thickness of the sample. The spectrum obtained is very similar to the transmission spectrum. The only difference is that the absorption bands

observed with ATR at longer wavelengths have higher intensities compared to transmission spectra.[4]

A second type of reflection spectroscopy is reflection-absorption (RA) spectroscopy. This technique makes use of external reflections. A thin film of the sample is placed on a reflecting metal surface and irradiated with a light beam having an angle of incidence usually between 70° and 89°. This technique has been used for the detection of thin polymer films on metal surfaces, and investigations of the adhesion between polymers and metals.[21]

7.1c. Application to Polymers.

Infrared spectroscopy, especially FTIR, is very useful in both the qualitative and quantitative characterization of the functional groups present in polymers. Additionally, infrared spectroscopy can be used for the detection and identification of additives, the study of oxidation and degradation reactions, and the investigation of molecular interactions, configurations, and hydrogen bonding.[4] IR spectra have also found use in the study of polymer deformation, stress relaxation, fracture, and fatigue.[15] Finally, IR techniques can be used to investigate kinetics[22], network formation and identification[23], and diffusion.[4,2]

Infrared spectroscopy has been successfully used in the analysis of the polymerization process. With the use of high speed FTIR spectrometers, kinetic studies can often be performed *in situ* to determine reaction order and activation energy. IR spectra can also be used to identify the structural changes and the extent of cross-linking

that occur in a polymerization reaction.[13] The extent of cross-linking can often be followed from the decrease in the double bond stretching mode at 1640 cm^{-1} if a suitable internal intensity standard can be found.[15] Hasirci used IR spectra to identify the major source of cross-links in hydrogels synthesized from 2-vinylpyridine and divinyl-benzene/ethylbenzene monomers initiated with gamma radiation. He found that the major source of cross-links was the bifunctional divinylbenzene monomer.[23] Earhart *et. al* used FTIR spectroscopy in their investigation of the effect of poly(vinyl alcohol) on the mechanism and kinetics of the copolymerization of vinyl acetate and butyl acrylate. These investigators used the FTIR spectra to monitor the increase in the concentration of acetate moieties on the polymer chains resulting from the grafting of vinyl acetate onto poly(vinyl alcohol).[26] Finally, Gulari *et. al* used FTIR spectroscopy to follow, in real time, the conversion of the bulk polymerization of both styrene and methyl methacrylate. By monitoring the integrated peak area for the IR absorbance of the carbon-carbon double bond (1643 cm^{-1}), they were able measure conversion with less error than methods involving the ring breathing mode of the aromatic ring at 1000 cm^{-1} as an internal reference.[27]

Changes in the structure of the crystalline regions of poly (tetramethylene terephthalate) due to an applied stress were studied by Ward and Wilding using FTIR.[35] They found that differences in the spectra between the stressed and unstressed state could be attributed to changes in the *trans/gauche* isomerism of the polymer chains. Under stress the conformation changed from a *gauche-trans-gauche* form (identified by C-H rocking bands at 917 cm^{-1} and 752 cm^{-1}) to an all *trans* conformation (identified by C-H rocking bands at 962 cm^{-1} and 840 cm^{-1}).[35] In additional use has been made of infrared

spectroscopy in the study of the stereoregularity of poly(methyl methacrylate) (PMMA).[36,37,38] Dybal *et al* used the infrared spectra of PMMA to find that in a stereocomplex of isotactic and syndiotactic PMMA the extended chain form of the syndiotactic PMMA is preferred.[37]

7.2. Conclusions for Cure Monitoring of Polymerizations Using FTIR Spectroscopy

The objective of using an FTIR to look at the DVE-3 system was to try and characterize the polymerization by monitoring the changes in the IR absorption bands due to the vinyl group. In this reaction the carbon-carbon double bonds react with an active center or crosslink to form a carbon-carbon single bonds. The double bond has a strong absorption peak due to stretching at 1635 cm^{-1} and an out-of-plane bending peak at 810 cm^{-1}, while the single bond doesn't absorb in these regions at all. Theoretically by monitoring these peaks compared to an internal standard the degree of cure can be observed. The major problem in applying this technique to the DVE-3 system in particular is that the time resolution of an FTIR is generally not fast enough to monitor a reaction that goes to completion in a few seconds.

A few preliminary scans were obtained to demonstrate the decrease in the C=C absorption bands with respect to the degree of cure (see *Figure 7-1*). This was done by curing a reactive sample of DVE-3, 10^{-2} wt% anthracene, and 1 wt% UV9310C initiator between two KCl salt plates. The reaction was slowed down due to the low intensity of 350 nm light reaching the sample though the KCl plate. An FTIR spectrum was obtained before reaction, after 9 minutes of curing under a lamp, and finally a spectrum was taken

24 hours in the dark after the lamp was removed. By comparing the height ratios of the 1635 cm^{-1} peak to the 1450 cm^{-1} internal standard peak for the unreacted sample and the sample after curing, it can be seen that there is a significant decrease in the concentration

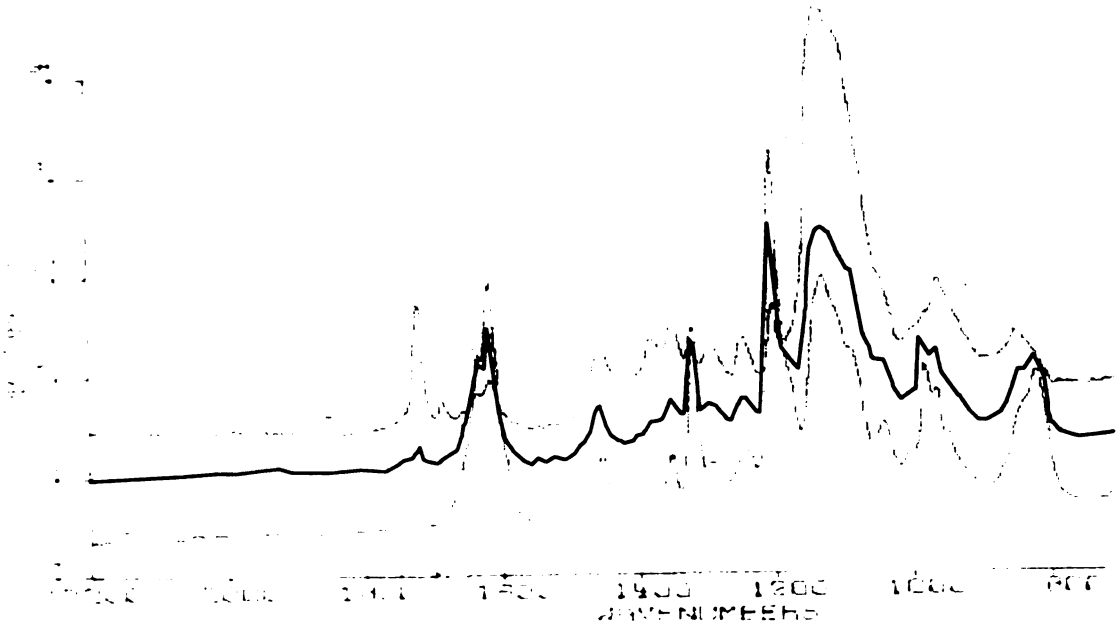

Figure 7-1. *An IR spectra of DVE-3 monomer and polymer at different times during the cure. The top curve is after the polymer was cured and then stored in the dark for 24 hours, the center curve is after curing under an initiating lamp for 9 minutes, the bottom curve is monomer.*

of vinyl bonds. In addition, the spectrum taken after 24 hours in the dark indicates that the polymer is continuing to cure even after the removal of the lamp.

An IR spectrum of DVE-3 monomer and a DVE-3 polymer film cured on a glass slide showed a large increase in absorption in the 3500 cm^{-1} -OH region. This indicates that water was absorbed into the polymer film after the polymer was formed.

7.3. References

1. Painter, P.C.; Coleman, M.M.; Koenig, J.L.; *The Theory of Vibrational Spectroscopy and its Applications to Polymeric Materials*, John Wiley & Sons: New York, NY, 1982.
2. Ishida, H. (Ed.); *Fourier Transform Infrared Characterization of Polymers*, Polymer Science and Technology; Plenum Press: New York, NY, **36**, 1987.
3. "Instrumentation '94"; *Chemical and Engineering News*, **72**, *11*, 32 (1994).
4. Siesler, H.W.; Holland-Moritz, K.; *Infrared and Raman Spectroscopy of Polymers*, Practical Spectroscopy Series, Marcel Dekker, Inc.: New York, NY, **4**, 1980.
5. "PittCon showcases real-world Raman spectroscopy, NEWSBREAKS"; *Laser Focus World*, **30**, *4*, 9 (1994).
6. Billmeyer, F. W.; *Textbook of Polymer Science*, 3rd ed., John Wiley & Sons, Inc.: New York, NY, 1984.
7. Tudor, A.M.; Melia, C.D.; Davies, M.C.; Hendra, P.J., Church, S.; Domb, A.J.; Langer, R., "The Application of Fourier Transform Raman Spectroscopy to the Analysis of Poly(anhydride) Homo- and Co-polymers," *Spectrochim. Acta.*, **47A**, 1335-1343 (1991).
8. Grasselli, J. G.; Snavely, M. K.; Bulkin, B. J., *Chemical Applications of Raman Spectroscopy*, John Wiley & Sons, Inc.; New York, NY, 1981.
9. Sperling, L.H., "Introduction to Physical Polymer Science," 2nd Edition, Wiley, New York, NY, 1992.
10. Rabek, J.F.; *Experimental Methods in Polymer Chemistry, Physical Principles and Applications*, John Wiley & Sons, Inc.: New York, NY, 1980.
11. Colthup, N.B.; Daly, L.H.; Wiberley, S.E.; *Introduction to Infrared and Raman Spectroscopy*, 2nd ed., Academic Press: New York, NY, 1975.
12. Hendra, P. J.; "Raman Spectroscopy"; In *Polymer Spectroscopy*; Hummel, D. O., Ed.; Verlag Chemie GmbH: Weinheim/Bergstr., 112-185, 1974.
13. Koenig, J. L.; *Spectroscopy of Polymers*; ACS Professional Reference Book; ACS: Washington, D.C., 1992.
14. Ingle, J. D.; Crouch, S. R.; *Spectrochemical Analysis*, Prentice Hall: Englewood Cliffs, New Jersey, 1988.
15 Fanconi, B.M., "Fourier Transform Infrared Spectroscopy of Polymers - Theory and Application," *J. of Test. Eval.*, **12**, 33-39 (1984).
16. Simon, U.; Tittel, F. K.; "Optical Parametric Device Serve as Sources for IR Spectroscopy"; *Laser Focus World*, **30:5**, 99 (1994).

17. Ciurczak, E. W.; "Detectors in Infrared Spectroscopy"; *Spectroscopy*, **8:8**, 12 (1993).

18. Brown, S. C.; Harvey, A. B.; "Polymers"; in *Infrared and Raman Spectroscopy, Part C*; Brame, E. G.; and Grasselli, J. G.; Eds.; Practical Spectroscopy Series; Marcel Dekker, Inc.: New York, NY, **1**, 873-932, 1977.

19. Polchlopek, S. E.; "Attenuated Total Reflectance"; In *Applied Infrared Spectroscopy*; Kendall, D. N., Eds.; Reinhold, New York, NY, 462, 1966.

20. Harris, R. L., Svoboda, G. R.; "Determination of Alkyd and Monomer-Modified Alkyd Resins by Attenuated Total Reflectance Infrared Spectrometry"; *Anal. Chem.*, **34:12**, 1655-1657, 1962.

21. Tompkins, H. G.; "Infrared Reflection - Absorption Spectroscopy"; In *Methods of Surface Analysis*; Czanderna, A. W., Eds.; Elsevier, Amsterdam , 447, 1974.

22. Gendreau, R.M.; Winters, S.; Leininger, R.I.; Fink, D.; Hassler, C.R.; Jakobsen, R.J.; "Fourier Transform Infrared Spectroscopy of Protein Adsorption from Whole Blood: *Ex Vivo* Dog Studies"; *Appl. Spectrosc.*, **35**, 353-357 (1981).

23. Hasirci, V.N.; "PVNO-DVB Hydrogels: Synthesis and Characterization"; *J. Appl. Polym. Sci.*, **27**, 33-41 (1982).

24. Allcock, H.R.; Kwon, S.; "Glyceryl Polyphosphazenes: Synthesis, Properties and Hydrolysis," *Macromolecules*, **21**, 1980-1985 (1988).

25. Gendreau, R.M.; Jakobsen, R.J.; "Fourier Transform Infrared Techniques for Studying Complex Biological Systems," *Appl. Spectrosc.*, **32**, 326-328 (1978).

26. Earhart, N.J.; Dimonie, V.L.; El-Aasser, M.S.; Vanderhoff, J.W.; "Infrared Studies on the Grafting Reactions of Poly(vinyl alcohol)"; In *Polymer Characterization: Physical Property Spectroscopic and Chromatographic Methods*; Craver, C.D; Provder, T., Eds.; American Chemical Society, **227**, 333-341, 1990.

27. Gulari, E.; McKeigue, K.; Ng, K.Y.S.; "Raman and FTIR Spectroscopy of Polymerization: Bulk Polymerization of Methyl Methacrylate and Styrene"; *Macromolecules*, **17**, 1822-1825 (1984).

28. Edwards, H.G.M.; Johnson, A.F.; Lewis, I.R.; "Applications of Raman Spectroscopy to the Study of Polymers and Polymerization Processes"; *J. Raman Spectrosc.*, **24**, 475- 483 (1993).

29. Edwards, H. G. M.; Johnson, A. F.; Lewis I. R.; Wheelwright, S. J.; "Raman and FTIR Spectroscopic Studies of Copolymers of Methylmethacrylate with Butadiene"; *Spectrochimica Acta*, **49A**, 457- 464 (1993).

30. Sain, G.; Leoni, A.; Simone, F.; "Solvent Effects in Radical Copolymerization III. Methacrylamide"; *Die Makromolekulare Chemie*, **147**, 213-218 (1971).

31. Chapiro, A.; Dulieu, J.; "Influence of Solvents on the Molecular Associations and on the Radiation Initiated Polymerization of Acrylic Acid"; *European Polymer Journal*, **13**, 563 - 577 (1977).

32. Makushka, R. Y.; Bayoras, G. I.; Shulskus, Y. K.; Bolotin, A. B.; Roganova, Z. A.; Smolyanskii, A. L.; "Effect of Complex Formation on Reactivity of Acrylic and Methacrylic Acids in Radical Polymerizations"; *Polymer Science U.S.S.R.*, **27:3**, 634 - 641 (**1985**).

33. Bajoras, G.; Makuška, R.; "Peculiarities of Radical Homo- and Copolymerizations of Acrylic, Methacrylic, and Itaconic Acids in Complexing Solutions"; *Polymer Journal*, **18:12**, 955 965 (1986).

34. Monti, P.; Simoni, R.; "The Role of Water in the Molecular Structure and Properties of Soft Contact Lenses and Surface Interactions"; *Journal of Molecular Structure*, **269**, 243-255 (1992).

35. Ward, I.M.; Wilding, M.A.; "Infra-red and Raman Spectra of Poly (*m*-Methylene Terephthalate) Polymers"; *Polymer*, **18**, 327-335 (1977).

36. Dybal, J.; Spevácek, J.; Schneider, B.; "Ordered Structures of Syndiotactic Poly(methyl Methacrylates) Studied by a Combination of Infrared, Raman, and NMR Spectroscopy"; *J. Polym. Sci.: Part B: Polym. Phys.*, **24**, 657-674 (1986).

37. Dybal, J.; Stokr, J.; Schneider, B.; "Vibrational Spectra and Structure of Stereoregular Poly(Methyl Methacrylates) and of the Stereocomplex"; *Polymer*, **24**, 971-980 (1983).

38. Dybal, J.; Krimm, S.; "Normal-Mode Analysis of Infrared and Raman Spectra of Crystalline Isotactic Poly(Methyl Methacrylate)"; *Macromolecules*, **23**, 1301-1308 (1990).

CHAPTER 8. COMPATIBILITY TESTS FOR CONSTRUCTION MATERIALS

8.1. Compatibility Tests for Construction Materials

Before the polymerization of DVE-3 can be fully utilized, the compatibility of the monomer with commonly used polymers must be characterized. As a result of the highly crosslinked network structure of the cured polymer this system has a number of desirable properties, such as chemical resistance. In addition, the low viscosity and vapor pressure of the monomer provide the advantages necessary for easy application in an ink or coating system. However, since these monomers are ethers there is serious potential for them to be solvents for other polymer systems, especially thermoplastics that are commonly used for containment and delivery systems. This study looks at the compatibility of two model vinyl ethers with a number of commonly used polymers. Since the monomer and initiator can be mixed in advance of their use it is important to know what types of polymers can be used for containment and delivery.

The first factor considered in this study was the degree of swelling experienced by a number of different polymers when submersed in the vinyl ether monomers for a sufficiently long period of time. The second factor was the extent to which these polymers were soluble in the monomers. Finally, changes in the physical characteristics of each polymer such as clarity and hardness were recorded. Conclusions were then drawn on the suitability of each type of polymer for use with the vinyl ether monomers.

8.1a. Experimental

Materials. The two vinyl ether monomers considered in this contribution were a divinyl ether, 3,6,9,12-tetraoxatetradeca-1,13-diene (DVE-3), sold by Aldrich Chemical Company under the name tri(ethylene glycol)divinyl ether (98%), and a monovinyl ether 2-methoxyethyl vinyl ether (2-MVE) (Polyscience, Inc.). Molecular sieves were added to the monomer in order to remove any trace amounts of water. The initiator for this system (UV9310C - GE Silicones) had an approximate composition of 5-10 wt% linear alkylate dodecylbenzene, ~50wt% 2-ethyl-1,3-hexanediol, and ~50 wt% bis(4-dodecylphenyl)-iodoniumhexafluoroantimonate. The anthracene photosensitizer was used as purchased from Aldrich Chemical Company (99%). The polymer samples that were considered were: polystyrene, polyethylene, polypropylene, nylon 6/6, Teflon, poly(ethylene terephthalate) (PET), poly(methyl methacrylate) (PMMA), polycarbonate, silicon foam rubber, and viton rubber.

Compatibility Experiments. The experimental setup for this study involved simply placing a carefully weighed sample of polymer in enough vinyl ether monomer to more than completely submerse the polymer. Before placing the polymer samples in the monomer they were cut into small pieces in order to increase the surface area in contact with the monomer. This was done to accelerate any swelling or dissolution that might take place and shorten the time required to reach equilibrium. The clarity, color, and texture of the polymer prior to exposure to the monomer was recorded along with the sample weight and the date. The polymers were then left in the monomer until they dissolved or up to three weeks to allow an equilibrium condition to be reached.

After this contact period, if the polymer had not completely dissolved it was removed from the monomer and the surface patted dry. The sample was then weighed to obtain a "wet" or swollen weight in order to determine the degree of swelling. The physical characteristics of the polymer were also observed and recorded. The polymer samples were then allowed to dry. They were periodically weighed over a period of several weeks until a stable weight was achieved. This final "dry" weight was used to determine the solubility of the polymer.

The degree of swelling was calculated and reported as the mass fraction of monomer in the polymer using the following equation:

$$Swollen\ \ Mass\ Fraction = \frac{(Equilibrium\ Swollen\ Mass - Initial\ Dry\ Mass)}{Equilibrium\ Swollen\ Mass}$$

Equation 8-1.

The degree to which the polymer samples were soluble in each monomer was calculated and reported as the soluble mass fraction according to the following equation:

$$Soluble\ Mass\ Fraction = \frac{(Initial\ Mass - Dried\ Mass)}{Initial\ Mass}$$

Equation 8-2.

The values obtained from these two equations were then plotted in bar charts in order to compare the relative compatibilities of each polymer in the two monomers.

Finally, the visible characteristics of each polymer, such as clarity, color, and texture were recorded. It was also noted, although not quantitatively, whether or not the monomer had resulted in a major weakening of the polymer's structure and flexibility.

8.1b. Results and Discussion

Swelling Results. The swelling characteristics of a polymer-solvent system is dependent on the thermodynamic behavior of the two species. The three major forces determining the swelling of a system are the entropy change caused by mixing polymer and solvent, the entropy change due the reduction in the number of possible conformations, and the enthalpy of mixing. The entropy of mixing is positive and therefore favors swelling while the entropy change due to conformations opposes swelling. The enthalpy of mixing can either favor or oppose swelling depending on the particular system, however, it normally slightly favors swelling.[1] Even if a polymer is insoluble in a solvent it will swell at least to some degree.

The effects of these two monomers on the degree of swelling of the polymers investigated varied greatly. The range of swelling extended from virtually no swelling for nylon to more than 40 wt% swelling of Teflon in DVE-3. *Figure 8-1* and *8-2* present the degree of swelling of various polymers in DVE-3 and 2-MVE monomers respectively.

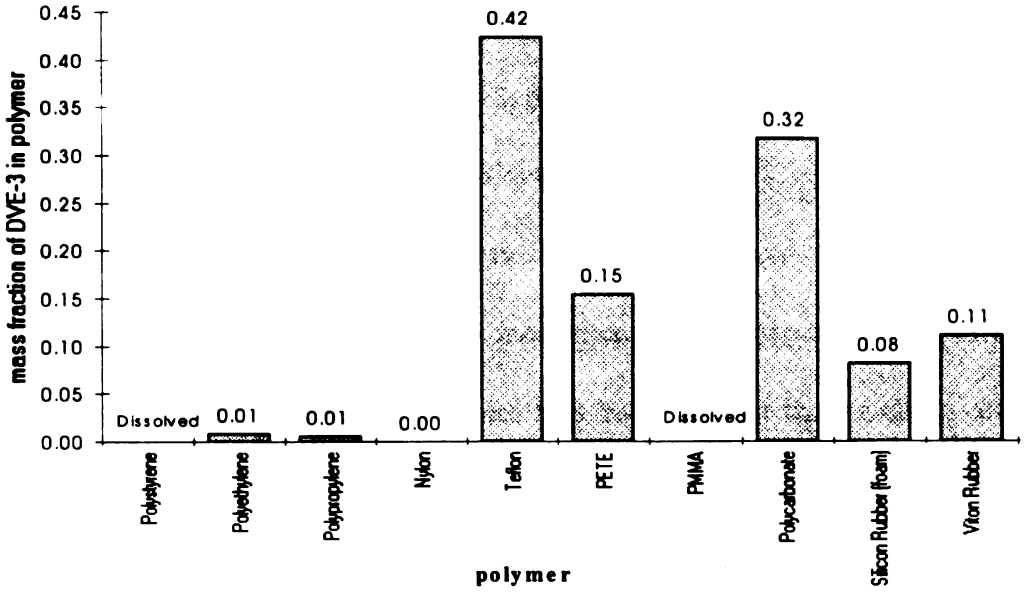

Figure 8-1. *Degree of swelling of polymers in DVE-3 monomer. The mass fraction of DVE-3 was determined by: (Eqm. swollen mass - Initial dry mass)/Eqm. swollen mass.*

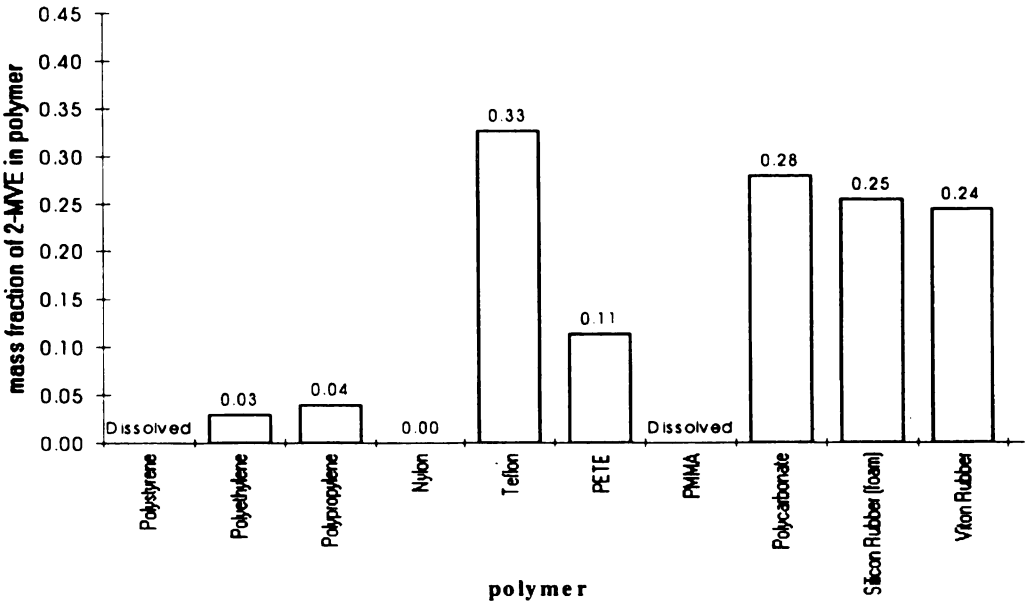

Figure 8-2. *The degree of swelling of polymers in 2-MVE monomer. The mass fraction of 2-MVE was determined by: (Eqm. swollen mass - Initial dry mass)/Eqm. swollen mass.*

Figure 8-1 and *Figure 8-2* show that nylon is the most resistant of the polymers considered to swelling in both monomers. Teflon, on the other hand, is the least resistant, absorbing more than 40 wt% in DVE-3 and over 30 wt% 2-MVE. Polycarbonate also has a high degree of swelling in both monomers. In 2-MVE (*Figure 8-2*) silicon rubber and viton rubber absorbed more than 20 wt% monomer. However, due to the difficulty of wiping off the surfaces of these two samples it is believed that this swelling result is an over-prediction of the actual value. The silicon sample was a foam and the viton sample was tubing so it was not possible to wipe the excess monomer off of the internal surface areas. Despite this, the results are still significant since there is more than twice as much swelling of these two polymers in the more volatile 2-MVE than in DVE-3. Since 2-MVE is much more volatile than DVE-3, more 2-MVE would have evaporated off of the internal surfaces of the polymer then DVE-3 before the samples were weighed. Therefore, the DVE-3 monomer should have appeared to have swelled more if the inability to wipe off the internal surface areas introduced a significant error.

Figure 8-3 illustrates that of the polymers that were investigated only polystyrene and PMMA were significantly soluble in the 2-MVE monomer. However, these two polymers were completely dissolved by 2-MVE. The only other two polymers to show any degree of solubility were polyethylene and nylon, although, in both cases the percent soluble was less than 1 wt%. Within the margin of error of the experiment, this represents a solubility of zero.

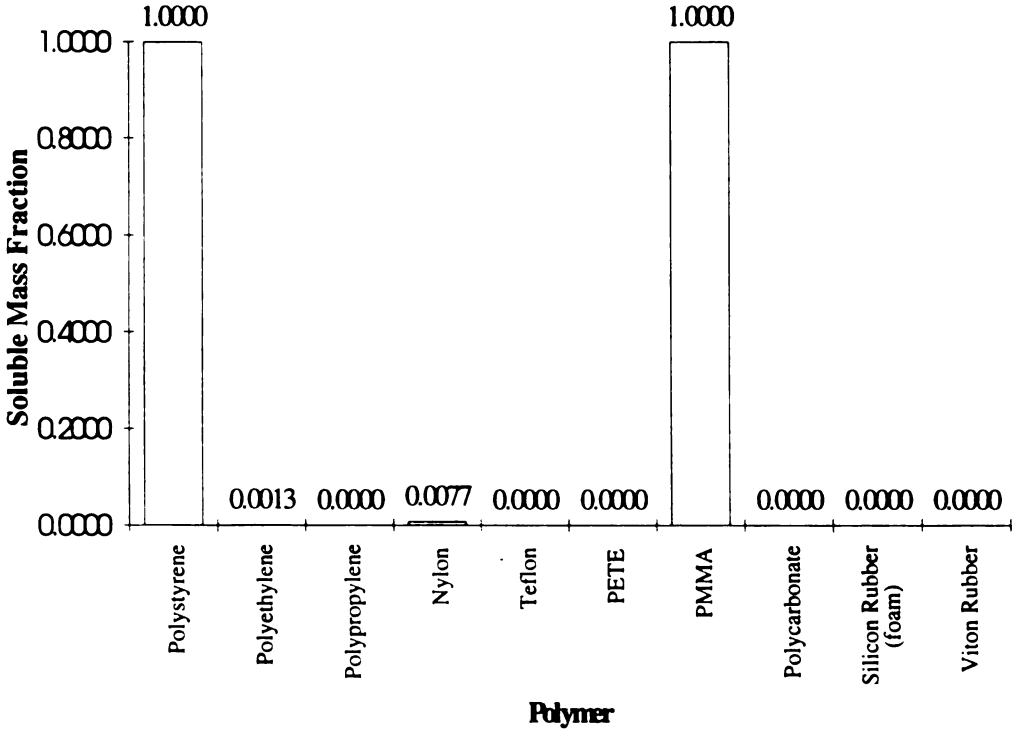

Figure 8-3. *The solubility of polymers in 2-MVE monomer. The mass sol fraction was determined by the equation (Initial Mass-Dried Mass)/Initial Mass.*

The solubility of various polymers in DVE-3 monomer is essentially the same as their solubility in 2-MVE. *Figure 8-4* shows that polystyrene and PMMA are again the two types of polymers that are completely soluble in this monomer. Nylon also demonstrated a slight solubility of less than 2 wt%.

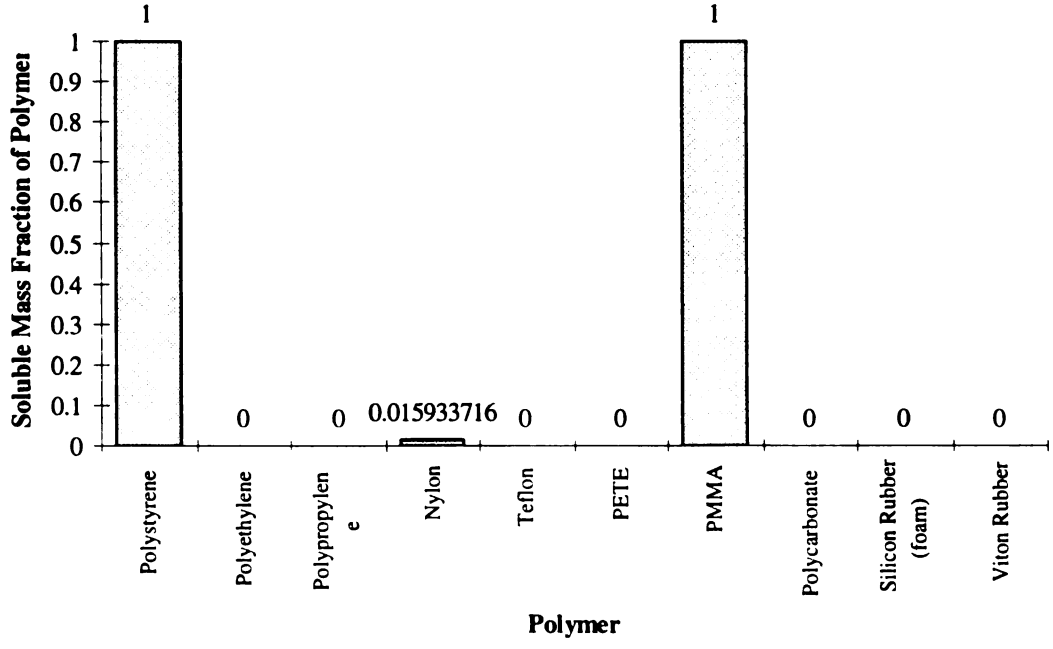

Figure 8-4. *Solubility of polymers in DVE-3 monomer. The mass sol fraction was determined by (initial mass - dried mass)/initial mass*

The overall swelling and solubility characteristics of the various polymers in DVE-3 and 2-MVE vinyl monomers that were presented in the previous figures are summarized in *Table 8-1.* This table characterizes the swellability of each specific polymer on an increase in weight percent basis.

Table 8-1. Swelling and Solubility of Polymers in DVE-3 and 2-MVE Monomers

Polymer Type	Polymers in DVE-3		Polymers in 2-MVE	
	Swelling (wt%)	Solubility (wt%)	Swelling (wt%)	Solubility (wt%)
Polystyrene	Infinite	Complete	Infinite	Complete
Polyethylene	v. Slight (0.81)	None	Slight (3.0)	v. Slight (0.13)
Polypropylene	v. Slight (0.62)	None	Slight (4.0)	None
Nylon	None	Slight (1.6)	None	Slight (0.77)
Teflon	High (42.4)	None	High (32.6)	None
PETE	Moderate (15.4)	None	Moderate (11.3)	None
PMMA	Infinite	Complete	Infinite	Complete
Polycarbonate	High (31.7)	None	High (27.9)	None
Silicon Rubber (foam)	Moderate (8.1)	None	High (25.4)	None
Viton Rubber	Moderate (11.1)	None	High (24.4)	None

Weight percent increases of less than 1.0% are characterized as very slight, between 1.0% and 5.0% as slight, between 5.0% and 15.0% as moderate. A weight percent increase greater than 15.0% is considered high. Polymers that dissolved in the monomer are listed as having an infinite swellability. *Table 8-1* also characterizes the solubility of the various polymers in the DVE-3 and 2-MVE monomer. Any decrease in the total weight of the dried polymer sample after exposure to the monomer is reported on

a weight percent decrease basis. A weight percent decrease below 0.5% is characterized as very slight and between 0.5% and 1.0% as slight.

8.2. Conclusions

In this chapter, the solubility and swellability of ten common types of polymers were characterized in two vinyl ether monomers (DVE-3 and 2-MVE). The following different types of polymers were considered: polystyrene, polyethylene, polypropylene, nylon, Teflon, PETE, PMMA, polycarbonate, silicon rubber, and viton rubber. This study reflects the fact since reaction systems based on these monomers have extended shelf lives if stored in the absence of light, it is important to identify materials suitable for containment. In addition since these monomers are ethers, there is considerable potential that many types of polymers may be soluble or significantly swelled in them.

In characterizing the solubility of these polymers in both DVE-3 and 2-MVE, two types of polymers, both of them thermoplastics, were found to be highly soluble in both monomers. The remaining eight different polymers were all found to be virtually insoluble in both monomers. Nylon indicated a slight solubility 1.6 wt% in DVE-3 and 0.8 wt% in 2-MVE, however this is within the estimated margin for error. The second consideration was the degree of swelling of each of these polymers in these two monomers.

In general, all of the polymers were found to swell at least slightly, however a degree of swelling less than 1 percent is not significant since this is within the margin of error. In general polymers are found to swell to some extent in any liquid. The degree of

this swelling is the important factor in determining the usefulness of the polymer in containing the liquid. From the results presented here, nylon demonstrated the highest degree of resistance to swelling in both DVE-3 and 2-MVE, followed closely by polypropylene and polyethylene. At the other end of the spectrum, polystyrene and PMMA, being soluble in these monomers, have an infinite degree of swelling. The remaining polymers Teflon, polycarbonate, PETE, silicon rubber, and viton rubber all demonstrated increases between 10 to 40 weight percent of polymer due to swelling, making them undesirable for use in contact with DVE-3 and 2-MVE monomers.

The combined solubility and swellability results for these polymers in either DVE-3 or 2-MVE indicate that polyethylene, polypropylene, and nylon are the only materials from those investigated that would be suitable for prolonged contact with these monomers.

8.3. References

1. Sperling, L.H., "Introduction to Physical Polymer Science," 2nd Edition, Wiley, New York, NY, 1992.

CHAPTER 9. SUMMARY AND RECOMMENDATIONS

9.1. Summary of the Background and Motivation for Research

This work is motivated by the fact that formulations of cationic photopolymerizations based upon multifunctional monomers lead to highly crosslinked polymers exhibiting unsurpassed adhesion, abrasion resistance, chemical resistance, and toughness. Cationic photopolymerizations are especially promising for the development of coatings and films because they exhibit rheological properties that are conducive to such cost-effective application techniques as rolling or spraying. The monomers exhibit low volatility, negligible toxicity and good rheological characteristics without the addition of diluting solvents providing a basis for a safe, low VOC coating.[1] Furthermore, the UV-initiated reactions proceed rapidly, but are remarkably stable in the absence of light with fully formulated systems exhibiting shelf lives of more than a year. These reactions may be carried out at normal atmospheric conditions, and proceed rapidly at room temperature to yield highly crosslinked polymer films. The combination of low VOC, low viscosity, rapid curing, and high durability presents the potential for excellent new coatings that meet environmental restrictions and consumers needs.

9.1a. Issues for the Development of Environmentally Benign Coatings

An important issue to consider with many traditional coating formulations is their contribution to atmospheric pollution. The emission of volatile organic components (VOCs) from the drying of finishes and coatings is a leading cause of atmospheric

pollution. Volatile organic solvents have traditionally been used to impart desirable viscosity and cure rate properties to coating formulations. In order to completely cover complex or intricate parts a coating formulation must be sufficiently fluid to penetrate inner recesses, but must cure rapidly to a protective film. However, meeting the coating formulation demands through the use of a rapidly evaporating organic solvent results in the formation of photochemical smog and other air pollutants. In light of increasingly stringent clean air regulations, there is substantial motivation for the inclusion of environmental concerns in the development of new high performance coatings. An important advantage of UV-cured, solvent-free systems is their cost-effective nature due to greatly reduced volumes and low energy requirements compared to traditional thermally cured solvent based coatings.[3] Commonly used coating systems require the use of low solids to achieve optical clarity, this necessitates the use of large volumes of expensive solvent and multiple coats which makes the application costs high.[2]

An improved, pollution-free formulation for coatings must meet several stringent requirements. The cured coating should exhibit excellent adhesion to the substrate, good clarity, abrasion resistance, and solvent (water) resistance. For applicability in a coating process the formulation should have a long shelf life[4] and should be stable during the application process, but should cure very rapidly when initiated by the energy source. For wood substrates the coating system must not cause swelling which distorts the wood grain.[2] An additional concern for the coating of polymer substrates is that the coating must be sufficiently elastic to expand or contract with the substrate. Coatings that are too rigid will crack under thermal expansion of the polymer substrate. Finally, to satisfy safety and environmental concerns, the formulations should be non-toxic, and should

emit no volatile organic components. The required abrasion resistance and chemical resistance can be readily provided by a highly crosslinked polymer network. For this reason many formulations, such as the alkyd/urea-formaldhyde (UF) varnishes, consist of pigments and volatile solvents dispersed in multifunctional oligomers that form highly crosslinked networks upon curing. The improved formulations could be based upon highly reactive monomers of low enough viscosity that no organic solvents are necessary. If the monomers used in 100% reactive systems also have a low vapor pressure, they will emit no organic vapors during cure.

The curing of a coating formulation to form a highly crosslinked polymer film could potentially be initiated by a variety of energy sources, including heat, electromagnetic radiation, and electron beam irradiation. Unfortunately, heat-initiated thermal systems typically require high temperatures to attain reasonable cure rates. The elevated temperatures not only lead to high energy costs, but can also result in significant distortions in substrate dimensions in many cases.[5] Furthermore, heat-initiated thermal systems may be unfeasible for coating applications involving large or preassembled parts. Finally, electron beam initiated systems are not only extremely expensive, but also lead to degradation of certain substrates. Light-induced photopolymerizations have many potential advantages for coating formulations including very high reaction rates at room temperature, low energy requirements, and versatility since a wide variety of monomers may be initiated photochemically.

9.1b. An Example of the Limitations of Current Coatings Systems

Although the development of environmentally benign furniture coatings is an area of active research, all of the formulations currently available have significant drawbacks and limitations. In addition to the nitrocellulose lacquer and alkyd/urea-formaldehyde coatings mentioned previously, a number of other types of coating formulations are either available or under development including water-based coatings, powder coatings and very recently supercritical application methods. In general, these developmental systems represent attempts to provide high quality furniture coatings with reduced VOC emissions. In addition, there have been several attempts to reduce the organic solvent fraction of traditional coating formulations. Although many of these coatings have significantly reduced emissions over the traditional lacquers, they generally fall far short of meeting the California emission requirement of 275g/L of VOC for wood or the EPA's baseline emission rate of 350g of VOC per liter of coating for metal furniture.[6] Additional other considerations such as high thermal energy requirements, the need for a nitrogen atmosphere, and long drying times, also make these coatings less than ideal.

Furniture coating formulations have traditionally used large solvent fractions and low solids to impart desirable flow, leveling and drying rates to the system. Therefore a large fraction of the formulations (the solvent) is essentially a process waste which enters the environment as a VOC. Furthermore multiple coats are often necessary which translates into high application costs.[2] A number of attempts have been made to produce formulations of higher solids content in order to both reduce emissions and application

costs. One widely used technique is a hot spray system. By applying the coating at an elevated temperature of 65°C, the nonvolatile weight (NVW) percent can be increased from 20 % to 28 %.[2] While this provides a definite reduction in VOCs it is not capable of meeting the expected increase in restrictions.[2]

Other attempts to achieve high solids coating have focused on replacing the nitrocellulose lacquer. The alkyd/urea-formaldehyde (UF) is the most successful of these efforts.[2] This is a thermosetting system with a typical solids content of 38% NVW.[2] This can be further increased by the use of hot spray. However, in both cases and especially with hot spray the pot life is limited. The disadvantages of this system include increased difficulty in making clear low-gloss coatings with good depth of appearance[2] Furthermore since the coating is a thermoset resin repair work is difficult. Possibly the most important drawback is that in order to achieve fast cure rates this system must be thermally cured at temperatures of 65-70°C for 20 to 25 minutes.[2] This requires significant energy costs especially for heating large pieces of furniture and also presents concern for the degradation of wood and plastic substrates at elevated temperatures.

An area that is receiving considerable interest is water-borne coatings. These coatings are being used to a very limited extent for both wood and metal. Typically, the nitrocellulose lacquer is emulsified in the water thereby reducing the volume of organic solvent required. While this technique is capable of providing a good finish with reduced emissions there are a number of significant problems. Direct application of water-borne coatings to wood substrates causes excessive gain raising, which results in an undesirable appearance to the wood.[2] For use on metal substrates the application equipment must be protected from rust, and the "Faraday effect" prevents uniform coverage for complex

shapes.[6] Additional problems with waterborne coatings include extended drying times, and the need for humidity control equipment.[6]

For metal substrates, powder coatings are experiencing rapid growth to achieve a high solids, low VOC coating.[2] These are usually an epoxy or polyester binder that is baked on to the metal surface at temperatures of 130-200°C. A major disadvantage of this system is that such high baking temperatures preclude its use with most wood or plastic substrates. Further problems include high capital costs for manufacturing and application equipment, high energy costs, "Faraday effect", and difficulty coating small numbers of parts.[6]

A relatively new method is to use as the solvent supercritical carbon dioxide. This method has shown potential for up to a 70 % reduction in solvent use. Since this approach still uses the same lacquer as the coating and merely uses CO_2 to replace traditional solvents, the finished coating has similar properties to traditional methods. A good deal of research is being conducted in this area but as of 1992 only a few production units where in use.[2] A major disadvantage of this system is the high cost of supercritical carbon dioxide and the processing equipment.

Finally, a limited number of UV cured coatings systems are in use, mostly in Europe and Japan where energy costs are higher.[2] However, these systems are free-radical based, not cationic, photopolymerizations. They have similar advantages to the proposed cationic system such as little or no VOC emissions, low energy costs, easy application, excellent solvent resistance and mechanical properties.[2] But since these are free-radical systems they have the disadvantage of requiring a nitrogen atmosphere to improve conversion. Furthermore, the free-radical mechanism will not continue to cure

in the absence of light due to radical-radical termination so coating of complex 3-D shapes is difficult. Unlike the proposed cationic systems using a divinyl ether or epoxy, the current UV curing systems generally use acrylates as the monomer. These monomers have been targeted as hazardous to human health and are ill-suited to metal substrates due to their poor adhesion to metal.

9.1c. UV-Initiated Photopolymerizations

Photopolymerizations initiated by ultraviolet (UV) light have gained prominence in recent years for the rapid, pollution-free curing of polymer films (for reviews, see references 3,7,8). These solventless polymerizations proceed very rapidly with a fraction of the energy requirements of thermally cured systems, and create films with excellent properties. Ultraviolet light is a convenient energy source for photopolymerization because a variety of readily available compounds will initiate chain polymerizations upon absorption of UV light.[3,7-12] UV-sensitive photoinitiators are currently available for free-radical or cationic polymerizations. These photoinitiators are typically effective for a variety of incident wavelengths.[3,7-12] This feature is useful for UV-curable coatings because commonly used pigments may be strong absorbers of light in the visible and ultraviolet wavelengths, and an initiator which will be effective at a wavelength outside this window must be chosen.

Free-radical photopolymerizations were first reported in the literature nearly fifty years ago,[11] and are currently receiving considerable attention (for reviews see references 2,3,7,8,11). For instance in Europe and Japan, UV curing of free-radical systems for

furniture coating is gaining prominence largely due to the higher cost of energy in these regions.[2] By far the most widely used classes of monomers for UV-initiated free-radical photopolymerizations are multifunctional acrylates and methacrylates. These monomers polymerize very rapidly, and are easily modified on the ester group, allowing materials with a variety of properties to be obtained.[7] However the acrylates are relatively volatile, and have an unpleasant odor.[7] Moreover, recently there has been growing concern over potential health hazards associated with the acrylates.[3,8,12] Several recent investigations have demonstrated that free-radical polymerizations of multifunctional acrylates and methacrylates exhibit unusual kinetic behavior, including immediate onset of autoacceleration causing the formation of heterogeneous polymers,[7,11-18] and the attainment of a maximum conversion significantly less than unity.[7,19-22] Finally, the free radical photopolymerizations are inhibited by oxygen and must be carried out under an inert atmosphere,[7,8,11] such as nitrogen increasing the application costs.

UV-initiated cationic photopolymerizations exhibit several advantages when compared with the free-radical photopolymerization discussed above. First, the cationic photopolymerizations are not inhibited by oxygen.[8,11,12,23] This feature provides an important practical advantage for the coating of large or complex parts since it is not necessary to blanket the system with nitrogen to achieve the rapid cure rates needed for quick application rates. Secondly, in contrast to the free-radical polymerizations which experience a rapid decrease in polymerization rate when the light source is removed (due to radical-radical termination reactions), the cationic polymerizations will proceed long after the irradiation has ceased, consuming nearly all of the monomer.[11,24] This is a key feature for the application of cationically photopolymerized coatings for complex shapes,

since light need not penetrate into all corners and crevasses of the substrate to achieve a completely cured coating. Finally, cationic photopolymerizations are a very versatile technique, and may be used to polymerize important classes of monomers, including epoxies and vinyl ethers.[12,23-26] These classes of monomers exhibit many desirable properties, including low volatility, good rheological properties and negligible toxicity.[8] Furthermore, the cured polymer films associated with these monomers exhibit excellent chemical resistance, adhesion, abrasion resistance, and clarity.[11,12]

9.2. Objectives of this Research on Cationic Photopolymerizations

Despite the promise of UV-initiated cationic photopolymerizations, these reactions have received only limited attention. This fact may be attributed primarily to the lack of suitable initiators until recent years. In fact, most of the work on cationic photopolymerizations reported in the literature focuses on the initiation step of the reaction (for reviews, see references 3,9,10,23-26). The development of thermally stable UV-sensitive cationic photoinitiators has lead to increased interest in the cationic photopolymerizations of epoxides and vinyl ethers in the last ten years,[24-26] however the field is significantly less developed than that of free-radical photopolymerizations. Not until recently have the detailed studies of the reaction been reported.[27] For example, Nelson *et al.*[27] reported a novel *in situ* laser-induced fluorescence technique for monitoring the initiation reaction in these high-speed polymerizations. Due to its extremely short intrinsic time scale, the fluorescence technique provided a means to characterize the kinetics of these polymerizations which proceed too rapidly to be monitored by traditional methods such as differential scanning calorimetry (DSC). These studies indicate that although the reactions are extremely rapid (the systems typically

react to completion in a few seconds), most of the conversion occurs in the last 100 milliseconds due to a dramatic increase in the reaction rate. Nelson *et al.*[27] attributed this characteristic reaction profile to thermal runaway resulting from the large amount of heat released by the rapidly polymerizing system. Similarly, the resulting highly crosslinked polymer networks have typically received only a cursory characterization by the pencil hardness test and solvent rub tests.

The research presented here deals with the characterization of the rate of photosensitization and the rate of propagation of a divinyl ether system as functions of concentrations of initiator and photosensitizers, light intensity, water, and temperature.[27,36-38,39] These studies indicate that high reaction rates can be achieved with standard light intensities and without a nitrogen blanket.

The first objective was to look at the polymerization kinetics this cationic photopolymerization using photo-differential scanning calorimetry. The second major objective was to identify and characterize the effects of humidity (water) on the reaction rate. A third objective was to look at the morphology of the divinyl ether polymer in order to identify the nature (homogeneous or heterogeneous) of the cured film with respect to degree of cure and cure conditions. The fourth objective was to characterize the chemical resistance of various polymers two different vinyl ether monomers. Finally, a fifth objective was to both gain familiarity with a variety of existing instrumental techniques as well as help develop new techniques necessary in meeting the previous objectives. The techniques encountered throughout this research include: photo-differential scanning calorimetry, transmission electron microscopy, Fourier transform infrared spectroscopy, fluorescence spectroscopy, UV-vis spectroscopy, and gel permeation chromatography.

9.3. Polymerization Kinetics from Photo-Differential Scanning Calorimetry

In this work, photo-differential scanning calorimetry (PDSC) was used to monitor cationic photopolymerizations of a divinyl ether. The PDSC method offers a direct method for evaluating the heat generated during a polymerization reaction. The heat of reaction profiles provided by PDSC were used to characterize the reaction kinetics and evaluate polymerization rate constants. However, the reaction system was extremely rapid and highly exothermic, making DSC measurements particularly challenging. To maintain isothermal reaction conditions, low light intensities and very small sample sizes (0.5 - 1.5 mg) were used to increase the reaction time for the divinyl ether photopolymerizations.

The PDSC experiments were used to determine kinetic constants for a series of unsteady-state divinyl ether polymerizations at different temperatures and light exposure times. Kinetic constants for propagation and termination were obtained from the PDSC experiments in conjunction with previously determined photosensitization rate constants. As expected, an increase in the initiating light intensity or an increase in the reaction temperature resulted in an increased reaction rate. This increase in reaction rate was found to result in higher final conversions as determined from the total heat of reaction.

To determine the termination rate constant, k_t, PDSC dark cure exotherms were fit with an exponential decay from the point at which the excitation source was removed (the exponential time constant was 17.3 $\pm$ 0.4 minutes). These results illustrate that the cationic centers exhibit a relatively long lifetime and relatively small termination rate constants compared to free radical systems, arising from the fact that cationic centers do not terminate by combination with themselves.

An apparent propagation rate constant that comprises all types of propagating centers (e.g. ion pairs, separated ions, etc.) with different reactivities was determined

from the PDSC reaction profiles. The apparent propagation constant, k_p, initially increases sharply and then levels off at a plateau value (as temperature is increased a higher value of k_p is observed). Finally, the value of k_p decreases as a limiting conversion is reached. This profile shape indicates that the apparent propagation rate constant k_p changes greatly as the reaction proceeds. The initial large increase in the apparent rate constant for propagation may be explained by a change in the reactivity of the carbocation species due to the proximity of the counterion. During the polymerization, the counterion experiences a decrease in the mobility of the large hexafluoroantimonate counterion as the viscosity of the system increases. However, the active carbocation retains diffusional mobility by reacting with vinyl bonds and may lead to separation of the two species. Since separated ions are orders of magnitude more reactive than ion pairs,[42] the apparent value of k_p increases dramatically during the early stages of the reaction. The final decrease in k_p arises from active center trapping during these highly crosslinked polymerizations. Therefore, a limiting conversion at which the reaction ceases is observed despite the presence of active centers.

The PDSC profiles for the propagation and termination rate constants as functions of conversion provide important insight into the nature of these high-speed cationic photopolymerizations. Understanding the kinetics of these cationic photopolymerizations is important due to the increasing number of applications for rapid, solvent-free curing of polymer films.

9.4. Effect of Water on Polymerization Reaction

In this chapter, a time-resolved fluorescence monitoring scheme is used to investigate the effect of small concentrations of water on the polymerization kinetics. These studies are important because monomers will absorb water in humid environments, which may inhibit cationic polymerizations. In addition, a photo-differential scanning calorimeter is used to verify how water causes the effects observed in the fluorescence monitoring experiments.

In conclusion, Nelson *et al.* have previously shown that anthracene effectively photosensitizes the cationic polymerization of divinyl ethers initiated with iodonium salts for wavelengths in the 350 nm range.[27,39,38,43,36] An anthracene fluorescence intensity decay, which was attributed to consumption of the photosensitizer, can be used to monitor the reaction progress.[43] The reaction of "dry" solutions of DVE-3 proceed to completion in under 2.0 seconds, while the presence of no more than a few weight percent of water in the monomer substantially slows the reaction. A sharp reduction in fluorescence intensity was attributed to large temperature increases arising from the heat of polymerization. It was found that increasing the anthracene concentration partially offset the effect of the water in the monomer.

In addition photo-differential scanning calorimetry (PDSC) was used determine the mechanism by which the presence of water slows down the reaction of the cationic photopolymerization of DVE-3. The PDSC method offers a direct way to evaluate the heat generated during a polymerization reaction. The heat of reaction profiles provided

by the PDSC were used to monitor the isothermal reaction for samples containing different concentrations of water. However, the reaction system was extremely rapid and highly exothermic, which made DSC measurements particularly challenging. To maintain isothermal reaction conditions, low light intensities and very small sample sizes (0.5 - 1.5 mg) had to be used to increase the reaction time for the divinyl ether photopolymerizations. These results indicated that under isothermal conditions the addition of water did not effect the rate of reaction. This suggests that during the initial part of the reaction even small concentrations of water are absorbing significant amounts of the heat generated by the polymerization probably through chain transfer reactions with the propagating cations. PDSC measurements of heat capacity showed that water is not simply increasing the heat capacity of the solution. As long as the water is capable of absorbing heat from the reaction solution the sharp decrease in fluorescence attributed to thermal runaway is prevented resulting in a slower reaction rate.

9.5. Temperature-Dependent Luminescence Probes

The temperature-dependent luminescence of tris(β-diketone) chelates of europium was used for in situ temperature measurements during cationic photopolymerizations of vinyl ethers. These molecular-level luminescent probes provided a real-time, noninvasive method for monitoring temperature during these high-speed polymerizations. For temperature monitoring during photopolymerizations of vinyl ethers, two β-diketone tris chelates of europium [tris(1,1,1,5,5,5-hexafluoroacetylacetone) europium, $Eu(hfa)_3$ and tris(benzoyl-1,1,1-trifluoroacetone) europium, $Eu(btfa)_3$] were found to meet several

stringent requirements. These probes exhibit a reproducible temperature dependence over a wide temperature range and, in the case of $Eu(hfa)_3$, may provide a detector-insensitive calibration. Calibration curves of luminescence intensity versus temperature were generated for the temperature range of interest (between 20 and 90 °C). In addition, these probes meet specific spectral requirements, such as excitation in the 350 nm range and emission above 500 nm. Finally, the luminescence response of these probes was found to be independent of viscosity.

My temperature profiles for cationic photopolymerizations verified the importance of thermal effects in these high-speed polymerizations. The luminescence from the europium probe indicated that the temperature increased gradually from ~25 to ~55 °C, then increased dramatically in a period of a few hundred milliseconds. These results confirm that a thermal runaway effect is responsible for the large increase in polymerization rate, as previously postulated by Nelson *et al.*[27]. While the temperature-sensitive probes appear to accurately monitor the temperature prior to thermal runaway, they are unable to determine the maximum reaction temperature due to detector dynamic range limitations and problems associated with the sample losing optical clarity. Furthermore, the luminescence of the probes was found to be sensitive to sample components (solvent, initiators, and water) and seemed to degrade at long times. However, this can be overcome with the use of system specific calibration curves and the use of fresh samples.

These studies have demonstrated the utility of the temperature-dependent luminescence of tris(β-diketone) europium chelates for characterizing the temperature during high-speed photopolymerizations that cannot be monitored using conventional

techniques. However the applicability of these probes is not limited to this reaction system. These probes could find application in any system in which an *in situ*, non-intrusive measurement of temperature is desired. For example, due to their temperature dependence and viscosity insensitivity, the probes are appropriate for systems in which a change in phase occurs. The broader applicability of these probes was illustrated by our studies of the HEA free radical polymerizations. Finally, a host of other lanthanide compounds could possibly be used as temperature sensitive fluorescent probes. For example, commercially available probes worthy of further study include tris(6,6,7,7,8,8,8-heptafluoro-2,2-dimethyl-3,5-octanedionato) europium and tris(2,2,6,6-tetramethyl-3,5-heptanedionato) europium.

9.6. Polymer Morphology

In meeting this objective, transmission electron microscopy was used to characterize the morphology in the homopolymer of a cationically polymerized divinyl ether. There has been significant interest in the characterization of these ethers due to their tremendous potential for development as high-performance films, and coatings which emit no volatile organic components. A procedure was developed for preparing sections of soft, brittle divinyl ether polymers for transmission electron microscopy. Cryo-ultramicrotomy was used to section DVE-3 with thicknesses on the order of 100 nm. In addition, osmium tetroxide was found to be a suitable stain for selectively increasing the contrast (electron density) of vinyl bonds in the polymer structure. Finally, a Gatan cold stage maintained at -150 °C was found to successfully prevent radiation

damage of the DVE-3 sections while exposed to an electron beam accelerated by 100 keV. This technique offers the ability to characterize the morphology of polymers of divinyl ethers with resolutions down to several nanometers.

Our electron microscopy results indicate that heterogeneities are present in the polymer morphology due to unpolymerized vinyl bonds in the cationically photopolymerized divinyl ether. Two different types of inhomogeneous regions were identified. The first type of inhomogeneity (dark regions on the micrograph) is suspected to be a result of trapped pockets of unreacted double bonds. The second type (light regions on the micrograph) suggests the presence of microgels of highly crosslinked polymer. In DVE-3 we identified heterogeneities ranging in size from 5 nm to 100 nm.

9.7. Material Compatiblity

In chapter 8, the solubility and swellability of ten common types of polymers were characterized in two vinyl ether monomers (DVE-3 and 2-MVE). The following different types of polymers were considered: polystyrene, polyethylene, polypropylene, nylon, Teflon, PETE, PMMA, polycarbonate, silicon rubber, and viton rubber. This study reflects the fact since reaction systems based on these monomers have extended shelf lives if stored in the absence of light, it is important to identify materials suitable for containment. In addition since these monomers are ethers, there is considerable potential that many types polymers may be soluble or significantly swelled in them.

In characterizing the solubility of these polymers in both DVE-3 and 2-MVE, two types of polymers, both of them thermoplastics, were found to be highly soluble in both

monomers. The remaining eight different polymers were all found to be virtually insoluble in both monomers. Nylon indicated a slight solubility 1.6 wt % in DVE-3 and 0.8 wt % in 2-MVE, however this is within the estimated margin for error. The second consideration was the degree of swelling of each of these polymers in these two monomers.

In general, all of the polymers were found to swell to at least slightly, however a degree of swelling less than 1 percent is not significant since this is within the margin of error. In general polymers are found to swell to some extent in any liquid. The degree of this swelling is an important factor in determining the usefulness of the polymer in containing the liquid. From the results presented here, nylon demonstrated the highest degree of resistance to swelling in both DVE-3 and 2-MVE, followed closely by polypropylene and polyethylene. At the other end of the spectrum, polystyrene and PMMA, being soluble in these monomers, have an infinite degree of swelling. The remaining polymers Teflon, polycarbonate, PETE, silicon rubber, and viton rubber all demonstrated increases between 10 to 40 weight percent of polymer due to swelling.

The combined solubility and swellability results for these polymers in either DVE-3 or 2-MVE indicate that polyethylene, polypropylene, and nylon are the only materials from those investigated that would be suitable for prolonged contact with these monomers.

9.8. Recommendations and Future Work

The research presented in this thesis has provided important information about the kinetics, structure, and properties of the polymer films formed by cationic photopolymerizations. A novel time-resolved fluorescence monitoring scheme provided previously inaccessible information about the effect of water on the rates of polymerization. Careful photo-differential scanning calorimetry directly provided specific information on the reaction kinetics for the propagation and termination reactions. Development of a cryogenic transmission electron microscope technique suitable for the preparation the DVE-3 polymer provided information on the polymer morphology. Based on these techniques and results, a major future objective should be to look at the now reasonably broad variety of commercially-available cationic monomers and initiators. This will allow the selection of optimum formulations for different coating and inking applications. Once specific formulations have been identified, complete thermal, mechanical, and structural characterization of the crosslinked polymer films can be carried out.

An example for which this type of future work would be useful is to characterize and develop these systems for the specific application of environmentally benign protective furniture top coatings and particle board fillers. Rigorous testing of these polymers as protective coatings on wood, polymer, and metal substrates needs to be done. These results would identify which of this class of monomers best meets the requirements for a protective top coat, and details on its durability such as adhesion, crack resistance, and thermal stability. Furthermore, a cost-effective spray or roll type application system

for this particular type of light-induced polymerization needs to be developed. Important issues such as the ideal light intensity and source, monomer viscosity, process speed, and cure rate also need to be addressed.

9.9. References

1. Ansell,J.M., "Safety Assessment of a New Reactive Diluent: Triethylene Glycol Divinyl Ether," RadTech '90 North America Conference Proceedings, 1990.
2. Wicks, Z. W. Jr.; Jones, F. N.; Pappas, S. P., *Organic Coatings Science and Technology*, Vol. 2: Applications, Properties, and Performance, Wiley, New York, 1994.
3. Pappas, S.P., "UV Curing, Science and Technology," Technology Marketing Corporation, Norwalk, CT, **2**, 1985.
4. Chalsma, J.K., *Machine Design*, **65**, *1*, 64 (1993).
5. Graminski, E.L., in "Fundamental Chemical and Engineering Issues in Paper Currency Production," National Science Foundation, Washington D.C., 1 (1991).
6. "Surface Coating of Metal Furniture: Background Information for Proposed Standards," U.S. Environmental Protection Agency, Office of Air, Noise, and Radiation, Office of Air Quality Planning and Standards, Springfield, Va. (1980).
7. Kloosterboer, J.G., *Adv. Polym. Sci.*, **84**, 1 (1988).
8. Roffey, C.G., "Photopolymerization of Surface Coatings," Wiley, New York, (1981).
9. Ledwith, A.; Al-Kass, S.; Hulme-Lowe, A., in "Cationic Polymerization and Related Processes," edited by E.J. Goethals, International Union of Pure and Applied Chemistry, Oxford, UK, 275, 1984.
10. Crivello, J.V., in "Cationic Polymerization and Related Processes," edited by E.J. Goethals, International Union of Pure and Applied Chemistry, Oxford, UK, 289, 1984.
11. Reiser, A., "Photoreactive Polymers," Wiley, New York, NY, 1989.
12. Lapin, S.P., in "Radiation Curing of Polymeric Materials," edited by C.E. Hoyle and J.F. Kinstle, *ACS Symposium Series*, Vol. 417, American Chemical Society, Washington D.C., 363, 1989.
13. Boots, H.M.J.; Kloosterboer, J.G.; van de Hei, G., *Brit. Polym. J.*, **17**, 219 (1985).
14. Galina, H.; Kolarz, B.; Wieczorek, P.; Wojczynska, M.; *Brit. Polym. J.*, **17**, 215 (1985).
15. Funke, W., *Brit. Polym. J.*, **21**, 107 (1989).
16. Bastide, J.; Leibler, L., *Macromolecules*, **21**, 2649 (1988).
17. Matsumoto, A.; Matsuo, H.; Ando, H.; Oiwa, M., *Eur. Polym. J.*, **25**, 237 (1989).
18. Baselga, J.; Llorente, M.; Hernandez-Ruentes, I.; Pierola, I., *Eur. Polym. J*, **25**, 471 (1989).

19. Turner, D.; Haque, Z.; Kalachandra, S.; Wilson, T., *Polym. Mater. Sci. Eng. Proceed,* **56**, 769 (1987).

20. Simon, G.P.; Allen, P.E.M.; Bennett, D.J.; Williams, D.R.G.; Williams, E.H., *Macromolecules*, **22**, 3555 (1989).

21. Kloosterboer, J.G.; Lijten, G.F.C.M.; Zegers, C.P.G., *Polym. Mater. Sci. Eng. Proceed.*, **60**, 122 (1989).

22. Allen, P.E.M.; Bennett, D.J.; Hagias, S.; Hounslow, A.; Ross, G.; Simon, G.P.; Williams, D.G.R.; Williams, E.H., *Eur. Polym. J.*, **25**, 785 (1989).

23. Crivello, J.V.; Lam, J.H.W., in "Epoxy Resin Chemistry," edited by R.S. Bauer, *ACS Symposium Series*, Vol. 114, American Chemical Society, Washington D.C., 1, 1979.

24. Watt, W.R., in "Epoxy Resin Chemistry," edited by R.S. Bauer, *ACS Symposium Series*, Vol. 114, American Chemical Society, Washington D.C., 17, 1979.

25. Pappas, S.P., *Prog. Org. Coat,* **13**, 35 (1985).

26. Crivello, J.V., in "Organic Coatings, Science and Technology," Vol. 5 edited by G.D. Parfitt and A.V. Patsis, Marcel Dekker, Inc., New York, NY, 35, 1983.

27. Nelson, E.W.; Carter, T.P.; Scranton, A.B., "Fluorescence Monitoring of Cationic Photopolymerizations: Divinyl Ethers Photosensitized by Anthracene Derivatives," *Macromolecules,* **27**, 1013-1019 (1994).

28. Odian, G., "Principles of Polymerization," 2nd Edition, Wiley, New York, NY, 1981.

29. Plesch, P.H., in "Cationic Polymerization and Related Processes," edited by E.J. Goethals, International Union of Pure and Applied Chemistry, Oxford, UK, 1, 1984.

30. Dunn, D.J., in "Developments in Polymerization," edited by R.N. Haward, Applied Science Publishers, London, **1**, 45, 1979.

31. Pelgrims, J., *Pigm. Resin Technol.*, **16**, 4 (1987).

32. Crivello, J.V.; Conlon, D.A.; Olson, D.R.; Webb, K.K.; "The Effects of Polyols As Chain Transfer Agents And Flexibilizers In Photoinitiated Cationic Polymerization," J. Rad. Cur., 13, 3 (1986).

33. Crivello, J.V.; Conlon, D.A.; Olson, D.R.; Webb, K.K., "Accelerators In UV Cationic Polymerization," *Polym. Paint Colour J.*, **178**, 696, (1988).

34. Ledwith, A., *Macromol. Chem.Suppl.*, **3**, 348 (1979).

35. Eckberg, R.P.; Riding, K.D., in "Radiation Curing of Polymeric Materials," edited by C.E. Hoyle and J.F. Kinstle, *ACS Symposium Series*, Vol. 417, American Chemical Society, Washington D.C., 382, 1989.

36. Nelson, E.W.; Carter, T.P.; Scranton, A.B., "The Role of the Triplet State in the Photosensitization of Cationic Polymerizations by Anthracene," *J. Polym. Sci., Polym. Chem.*, **33**, 247 - 256 (1995).

37. Crofcheck, C.L.; Nelson, E.W.; Jacobs, J.L.; Scranton, A.B., "Temperature-Sensitive Luminescence of Tris(β-diketone) Europium Chelates for Monitoring High-Speed Cationic Photopolymerizations," *J. Polym. Sci; Part A: Polym. Chem.*, in press.

38. Nelson, E.W.; Jacobs, J.L.; Scranton, A.B.; Anseth, K.S.; Bowman, C.N., "Photo-differential Scanning Calorimetery Studies of Cationic Polymerizations of Divinyl Ethers," *Polymer*, in press.

39. Jacobs, J.L.; Nelson, E.W.; Scranton, A.B., "Use of Fluorescence to Monitor Temperature and Observe the Water Effects of Cationic Photopolymerization of Divinyl Ethers Photosensitized by Anthreacene," *Proc. ACS Polym. Mat. Sci. and Eng.*, **70**, 74 (1994).

40. Dougherty, J.A.; Vara, F.J., RadTech '90 North American Conference Proceedings, RadTech International North America, 1990.

41. Radak, W., *Chemical Business*, October, 1990.

42. Kennedy, J. P.; Marechal, E., "Carbocationic Polymerization," John Wiley & Son, New York, 1982.

43. Nelson, E.W.; Carter, T.P.; Scranton, A.B., "Fluorescence Monitoring of Cationic Photopolymerization of Divinyl Ethers Photosensitized by Anthracene," *Polymer Preprints - ACS Division of Polymer Chemistry*, **34**, 779 (1993).